Emulsion Polymerization Kinetics with Crosslinking

By

HUA GUO, B.Eng., M.Sc.

A Thesis
Submitted to the School of Graduate Studies
in Partial Fulfillment of the Requirements
for the Degree
Doctor of Philosophy

McMaster University

© Copyright by Hua Guo, December, 1995

DOCTOR OF PHILOSOPHY (1995) McMASTER UNIVERSITY

(Chemical Engineering) Hamilton, Ontario

TITLE: Emulsion Polymerization Kinetics with Crosslinking

AUTHOR: Hua Guo, B.Eng., M.Sc.

(Nanjing Institute of Chemical Technology, China)

SUPERVISORS: Professor A. E. Hamielec

Professor S. Zhu

NUMBER OF PAGES: 252

Emulsion Polymerization Kinetics with Crosslinking

To my wife, Xiaoming

and my son, Hao

ABSTRACT

Emulsion polymerization of vinyl/divinyl monomers may result in crosslinked polymers and lead to peculiar characteristics for the kinetics and network structure. Herein is provided a comprehensive study including both extensive experimentation and computer modeling with the aim of elucidating the effects of crosslinking on emulsion polymerization kinetics.

The model monomer system chosen for the present study was methyl methacrylate (MMA) and ethylene glycol dimethacrylate (EGDMA) as the comonomer and crosslinker. The polymerization temperature was 50^{O}C. Potassium persulfate (KPS) was the initiator. Sodium dodecyl sulphate (SDS) as emulsifier was used below and above the critical micelle concentration(CMC).

The monomer conversion, polymer particle number and size development, swellability of crosslinked polymer particles, pendant double bond (PDB) conversion, the glass transition temperature (Tg) and the internal heterogeneity in polymer particles were measured as a function of time in a batch reactor. It has been found that EGDMA level in the monomer feed and the initiator concentration have a pronounced effect on the behavior of the polymerization process. The experimental responses were very different when polymerizations were done below and above the critical micelle concentration.

ESR was used to measure the dramatic radical concentration increase which is particularly great at higher levels of crosslinking. Time profiles of propagating radical concentrations have two regions. A relatively constant radical concentration region coupled with high rates of monomer conversion and polymer particle generation and a dramatic radical concentration increase coupled with a level off in monomer conversion and polymer particle concentration. These observations suggest that a trapping of radicals within the crosslinked polymer network occurs during emulsion polymerization and this is further confirmed by ESR testing of solid polymer samples coupled with DSC testing of residual PDB in the same samples.

The second part of this study features kinetic modeling and the simulation of the kinetic equations by the Monte-Carlo method. An existing kinetic model for crosslinking density distribution has been revised to account for the shielding effect on pendant double bond reactivity. In addition, a stochastic Monte-Carlo simulation algorithm for emulsion polymerization has been developed. After basic testing, the program has been applied to emulsion homopolymerization with long chain branching and copolymerization with or without branching/crosslinking. Calculated results clearly reflect the kinetic phenomena when crosslinking is relevant. In the present study, Monte-Carlo simulation has been used to simulate kinetic behavior in stage II where polymer particle concentration is constant. However, the algorithm can readily be extended to include the nucleation period (stage I) and the finishing stage (stage III) and to consider a host of kinetic event combinations provided that the proper kinetic expressions, constraints and criteria conditions are available.

ACKNOWLEDGMENTS

I wish to express my sincere gratitude and appreciation to those people who gave their support during the course of this thesis. In particular, I am indebted to:

Professor **A.E. Hamielec**, my supervisor, for his guidance, encouragement, inspiration, enthusiasm and patience. Your insight and high standards are truly unforgettable. You shall definitely continue to be a source of motivation for my future work.

Professor **S. Zhu**, my supervisor. Your encouragement, friendship, valuable advice and continuous help are greatly appreciated.

Professors **R.B. Pelton** and **H.D.H. Stöver**, members of my supervisory committee, for their excellent service and advice. Your chemistry/polymer expertise will be remembered forever.

Drs. **Y. Deng**, **L.K. Kostanski**, for their friendship and helpful discussions.

D. Keller, L. Morrine, George Timmins for their assistance, collaboration and all convenience to access research facilities.

Sara Gallo-O'Toole, Barb Owen, Sharin Ciraolo and Paul Gatt, for their help through many years.

McMaster Institute for Polymer Production Technology, Department of Chemical Engineering, Canadian International Development Agency (CIDA) McMaster University, Ontario Center for Materials Research for their financial support.

My great thanks are extended to Professors **Jun Shi, Zuren Pan** for encouraging me and recommending study abroad, specifically to my deceased M.Sc. supervisor, Professor **Qida Ji** for introducing me to polymer science and engineering.

Last, but certainly not least, my everlasting love goes to my wife, Xiaoming Wang; my son Hao; my parents, Yushan Guo and Xian Yang for their patience, understanding, confidence and moral support throughout these years. A special debt of gratitude is due to my wife, Xiaoming, and son, Hao, my aim could not have been realized without their sacrifices.

TABLE OF CONTENTS

TABLE OF CONTENT (continued)

TABLE OF CONTENT (continued)

Page

TABLE OF CONTENT (continued)

CHAPTER 3: ELECTRON SPIN RESONANCE (ESR) MEASUREMENT OF FREE RADICAL CONCENTRATION IN CROSSLINKED POLYMER PARTICLES 74

TABLE OF CONTENT (continued)

CHAPTER 4: KINETIC MODELING OF VINYL / DIVINYL MONOMER EMULSION POLYMERIZATION 114

TABLE OF CONTENT (continued)

CHAPTER 5: MONTE-CARLO SIMULATION OF EMULSION POLYMERIZATION KINETICS WITH CROSSLINKING 161

TABLE OF CONTENT (continued)

LIST OF FIGURES

LIST OF FIGURES (continued)

LIST OF FIGURES (continued)

LIST OF FIGURES (continued)

LIST OF FIGURES (continued)

LIST OF FIGURES (continued)

LIST OF FIGURES (continued)

LIST OF FIGURES (continued)

CHAPTER 1

INTRODUCTION

1.0 Introduction

Polymer latices and emulsion polymerization are commercially important with applications in the manufacture of adhesives, protective coatings, synthetic rubbers engineering thermoplastics and substrates for biochemical and medical technology. A polymer latex could be defined as a thermodynamically or mechanically stable or sub-stable dispersion of polymer particles in a liquid medium (normally it is water).

In addition to the solids content, pH and ionic strength, the applications of polymer latices are mainly dominated by the polymer and polymer particle properties, such as particle size distribution, molecular weight distribution, long chain branching and crosslinking density. Polymer particle size distribution is an important property. It influences the latex dispersion stability, the relationship between suspension viscosity and particle concentration, shear rate and coagulated film properties(particle packing density, mechanical and optical properties).

As for the polymer chain properties, the molecular weight distribution, chain composition, chain structure characteristics such as linear, short/long chain branching and crosslinking are relevant. These affect film properties which include in addition to film mechanical and optical properties, adhesion and cohesion.

Fundamental understanding of the synthesis mechanisms and critical parameters that affect the above mentioned polymer and polymer particle properties will lead to improved design and control of latex manufacturing processes and to superior polymer product properties. In this investigation, the focus is on the kinetics of emulsion polymerization with crosslinking.

To date, a comprehensive investigation of the effects of crosslinking on emulsion polymerization kinetics has not been done. In this study, both computer modeling and extensive experimentation have been done with the aim of elucidating the effects of crosslinking on emulsion polymerization kinetics. The model monomer system chosen for this study was methyl methacrylate (MMA) and ethylene glycol dimethacrylate (EGDMA) as the comonomer and crosslinker.

1.1 Characteristics of Emulsion Polymerization that Crosslinking Might Influence

Emulsion polymerization is done using free radical polymerization and therefore crosslinking via free radical mechanisms is of concern in this study and is now discussed.

There are two possible mechanisms which can cause crosslinking during free radical polymerization. To experience gelation, the formation of a network or gel molecule with weight average molecular weight approaching infinity (Flory's criterion for gelation) tetrafunctional long chain branching must occur. There are two mechanisms of synthesizing tetra functional branches via free -radical chemistry.

When there are labile hydrogen atoms in monomer units in polymer chains, chain transfer to polymer will produce backbone radical centers. When two backbone radical centers mutually terminate via combination termination there will result a chemical bond between them to form one tetrafunctional long chain branch.

The most direct method of tetrabranching formation is to incorporate reactive pendant carbon-carbon double bonds into the polymer chains using a divinyl comonomer as crosslinker in the polymerization. When a propagating radical adds to a pendant double bond, a tetrafunctional long chain branch will form upon further propagation. The successive formation of tetra-branched nodes will ultimately lead to a three dimensional polymer network and gel formation.

One or both of these tetrafunctional branch formation mechanisms might be operative in emulsion polymerization. The generation rate of tetrafunctional long chain branches via pendant double bonds is proportional to the mass of polymer chain per unit volume. When a polymer particle is nucleated, from its very time of birth, it contains a high concentration of polymer and therefore crosslinking reactions can occur over the total lifetime of the polymer particle.

This is not so for a bulk or solution polymerization, when at time zero, the polymer concentration is zero and it builds gradually over the polymerization period. Free radical polymerization with long chain ranching or crosslinking is therefore conveniently carried out in emulsion polymerization

From the point of view of crosslinking kinetics, the micro-environment for emulsion polymerization with and without crosslinking is different. For example, crosslinking can reduce equilibrium swelling of a polymer particle by monomer. This can reduce the rate of surface area growth rate in stage I and thereby increase the micellar nucleation rate of polymer particles.

High levels of crosslinking in polymer particles may cause a significant increase in the average number of radicals per particle. Crosslinking may also retard the diffusion rate of monomer into and within the particle causing significant monomer concentration gradients. At the same time, the existence of divinyl monomer in the aqueous phase will alter the structure of oligomer radicals. This may cause a change in the nucleation mechanism which might change the major particle nucleation path and the suspension system stability.

These effects which have little been studied may give rise to significantly altered kinetic phenomena in the emulsion polymerization process. So it is clear that the importance of having a detailed understanding of the characteristics of emulsion polymerization with crosslinking can not be overstated. This understanding would likely permit one to develop advanced latex manufacturing processes with a significant technological impact.

Comprehensive studies of the interrelation of fundamental emulsion polymerization processes and the kinetics of crosslinking in free radical polymerization have not been reported to date.

1.2 Objectives and Scope of this Study

The main objectives of this research are first to elaborate the mechanisms and kinetics involved in crosslinking emulsion polymerization of vinyl and divinyl monomers using methyl methacrylate (MMA) and ethylene glycol dimethacrylate (EGDMA) as a model monomer system and to use this knowledge to identify how to control polymer network properties.

Secondly, to develop a dynamic model which includes a stochastic Monte-Carlo simulation algorithm of emulsion polymerization with crosslinking to calculate crosslinking density, molecular weight in addition to other standard latex properties.

1.2.1 Dynamical modeling

The objective of this work is to develop a kinetic mathematical model for emulsion polymerization of vinyl and divinyl monomers considering the mass balances, diffusion control of termination and propagation, different concentrations of polymeric radicals in the three polymerization stages. The present model is to be a generalization of a dynamic model for SBR production[1].

The reaction mechanisms include initiation of free radicals in the water phase and formation of polymer particles via micellar nucleation. As for the reaction steps within the polymer particle, propagation with monomers and with pendant double bonds (PDB), chain transfer to monomers, to chain transfer agent (CTA) and to polymer, and primary and secondary cyclizations are to be accounted for.

The derivation is based on the following assumptions: propagating radicals are statistically distributed among all particles; monomers consumed in the water phase for oligomer radical formation will be neglected in total monomer balances; radical desorption and termination in the water phase will be neglected. The model derived should calculate the following quantities: monomer and PDB conversion; number and size of latex particles; polymer molecular weight averages, polymer composition and crosslinking density.

1.2.2 Monte-Carlo simulation

A general stochastic Monte Carlo simulation algorithm is to be developed for the emulsion polymerization process. It should account for all elementary reaction steps which occur in stage II when the polymer particle nucleation process is completed (the model could be extrapolated to include the particle nucleation process or stage I when proper criteria are set up). No assumptions about molecular weight distribution of starting polymer chain in the particles needs to be made.

The simulation is based on the distribution of time interval between two adjacent free radicals entering polymer particles, the time interval distribution between two adjacent reaction steps within one radical entering and the probability for a specific reaction to happen in this step. This general algorithm can be easily modified to predict the number of polymer chains in a particle, particle volume growth rate, copolymer molecular weight distribution, copolymer composition, long chain branching frequency and crosslinking density.

1.2.3 Emulsion polymerization experiments and latex characterization

The experimental polymerizations to be done are to be carried out in a batch polymerization reactor. The following data are to be collected:

1) total monomer conversion versus polymerization time

2) monomer volume fraction in the polymer particles versus time
3) polymer particle size and number versus time
4) conversion of pendant double bonds versus time
5) free radical concentration in the polymer latex versus time
6) glass transition temperature (Tg) and internal heterogeneity of polymer particle free of monomers

The polymerization conditions such as monomer feed composition, levels of emulsifier (sodium dodecyl sulfate) and concentration of initiator ($K_2S_2O_8$ / KPS) are considered important factors to examine. In this experimental investigation, the polymerization temperature is set at 50^{0}C. It is based on the consideration that for ESR measurement we would like to reduce the number of radical types, so it was decided not to use a redox initiation system. The temperature of 50^{0}C is the typical "Hot Rubber" polymerization temperature for commercial SBR manufacture based on KPS as the initiator.

1.3 Outline of Thesis

Following an introduction, the whole thesis is divided into four chapters. Each chapter begins with an introduction in which a critical literature review is given and the basic theoretical principles and objectives of each subsection are stated. After presenting details of the model calculations and/or experimental measurements in each chapter, a discussion section is given. In this section the major results and conclusions are presented. A concise review of the thesis and a summary of contributions can be found in the summary section at the end of each chapter. Also suggested in this section are potential paths for future research investigations on each major topic.

Chapter 2 includes a report of the major part of the experimental results. The effects of crosslinking on the following are given:

(1) total monomer conversion history and polymerization rate,

(2) particle nucleation mechanisms,

(3) particle number and size distribution development

(4) particle swellability

Also in this chapter, pendant double bond conversion measurements by DSC are reported and also reported are DSC measurements used to detect phase separation in polymer particles.

In the present research, free radical concentrations in the polymer particles with crosslinking were measured for the first time. In Chapter 3, experimental results on measurement accuracy and radical concentration versus total monomer conversion are discussed. The kinetic analysis for investigation of free radical trapping and the effect of oxygen on radical concentration in emulsion polymerization are discussed.

In Chapter 4, the kinetic modeling of vinyl and divinyl monomer emulsion copolymerization is presented. It begins with the description of mechanisms in the emulsion polymerization process and kinetics of network formation in polymer particles. Later kinetic modeling using the method of moments is illustrated. The shielding effect on pendant double bond reactivity was investigated in detail. After parameter estimation, an investigation of the shielding effect on crosslinking density distribution was done using the model. In addition, the basic criteria for the Monte Carlo simulation are introduced.

In Chapter 5 is presented a stochastic simulation algorithm of the emulsion polymerization kinetics. This general algorithm design consists of four major parts: the time interval distribution for radicals entering a particle; the radical desorption from the polymer particle; the time interval distribution for the adjacent reaction in the particle and the criteria in the adjacent reaction type determination. The model was first tested using the basic testing procedure to confirm each component in the program. Later the long chain branching, copolymer composition and the crosslinking and network formation were calculated by this model.

1.4 References

1 Broadhead, T. O., Hamielec, A. E. and MacGregor, J. F. *Makromol. Chem. Suppl.* 1985, **10/11**, 105

CHAPTER 2

PREPARATION AND CHARACTERIZATION OF CROSSLINKED POLYMER PARTICLES

2.1 Literature Review

2.1.1 Effect of divinyl monomer type and concentration on kinetics of polymerization

Investigations of the kinetics of vinyl/divinyl monomer polymerization and in particular diffusion-controlled reactions, gel-point-conversion and density of crosslinking, and procedures for fitting experiment data to obtain rate parameters have been reported by several workers [1-5]. Li *et al* [6] reported extensive experimental data on the kinetics of MMA/EGDMA bulk polymerization covering wide ranges of divinyl/vinyl monomer ratio, effect of chain transfer agent concentration on the gel-point conversion. The temperature control in ampoule reactors; radical concentration and radical trapping, radical decay, diffusion control of rate parameter have been reported by Zhu *et al*[7].

Salovey *et al*[8-11] published procedures for the synthesis and characterization of crosslinked monodispersed polymer beads and micro-beads for application as fillers for polymer composites by emulsion polymerization in the absence of emulsifiers. For the styrene/divinyl benzene (St/DVB) monomer system they found that DVB reacts more rapidly than styrene at low monomer conversion. In batch polymerization the crosslinking density as well as Tg of the polymer decreased with increase in conversion.

An interesting result is observed when one compares methyl methacrylate/5% wt allyl methacrylate (MMA/AM) with methyl methacrylate/5%wt ethylene glycol dimethacrylate (MMA/EGDMA), the rate of polymerization is slightly faster for MMA/EGDMA than that for (MMA/AM). For ethylene methacrylate/allyl methacrylate (EMA/AM), it was observed that the polymerization rate increased in the following sequence[9]:

(EMA/10% wt AM) > (EMA/5%wt AM) 3 ≥ (EMA/20%wt AM) > EMA.

However, it was not clear when the AM concentration was increased to 20 %wt, why the polymerization rate decreased falling in-between those of (EMA/5%wt AM) and EMA. This was possibly due to chain transfer to AM[10].

Capek [12] published experimental data on the effects of divinyl monomer structure on the emulsion polymerization of ethyl acrylate. Generally it is expected that if the distance between two double bonds in the divinyl monomer is greater and the connection more flexible, a looser gel structure would form. Small species such as monomer and initiator radicals could diffuse more easily within this network, the polymerization rate would be similar to that without crosslinking (at least in the early stage of the gelation period). Comparing ethyl acrylate, ethyl acrylate/4.9wt% divinyl benzene, and ethyl acrylate/4.9wt% 1,6-hexamethylene diacrylate, they found that divinyl benzene decreased both the polymerization rate and the mean polymer particle size, (increase particle number) while 1,6-hexamethylene diacrylate slightly increased both the reaction rate and the size of polymer particles.

Considering the high solubility of 1,6-hexamethylene diacrylate in water (50mM), Capek [13,14] concluded that for the ethyl acrylate/1,6-hexamethylene diacrylate system the hydrophilic microgel separated from the hydrophobic reaction medium in the particle. This more compacted microgel might thus have had more opportunity to undergo intramolecular propagation (primary cyclization) reducing the number of elastically effective crosslinks per pendant double bond consumed. As for the ethyl acrylate/divinyl benzene system they attributed the observed effect on the reaction rate and tighter network to radical trapping in the microgel. The polymerization rate in

Stage II was found to be proportional to the 0.37, 0.23 and 0.5 power of the emulsifier concentration for the system of pure EMA, EMA with DVB and EMA with HMDA.

2.1.2 Particle nucleation and particle number and size development

The development of particle morphology in emulsion polymerization is an important area to consider. For vinyl and divinyl monomer systems, crosslinked polymer latex particles with different internal structure can be prepared by the seeded process [15], the emulsifier free process [8-11], and the micelle nucleation process [13,14].

Nomura *et al* [16] studied particle nucleation in the copolymerization of divinyl monomers. They first clarified the nature of particle formation for the styrene/divinyl benzene (St/DVB), and St/EGDMA monomer system. They found that for a particular monomer recipe, the final particle number increased sharply at the CMC of the emulsifier used (SDS: 0.75 g/liter at the ionic strength used). This means that above the CMC particles are almost all formed via micellar nucleation.

This was confirmed in their experiments [16] by changing the EGDMA monomer fraction in the St/EGDMA monomer feed. Their results showed that for up to 70%wt EGDMA, polymer particle number increased with increase in EGDMA fraction. Also, polymer particle number remained constant for most of the monomer conversion range (from about 20%wt to about 95%wt total monomer conversion). It was found that the effects of initiator and emulsifier levels on particle number are the same for both systems.

The most meaningful result is that when the fraction of divinyl monomer in their recipe increased, the number of polymer particles increased, while the polymerization rate per particle decreased. They, unlike Capek, explained this as due to a reduction in the monomer concentration in the polymer particle because of elastically effective crosslinking in the particles and this is in agreement with Flory's swelling theory.

2.1.3 Pendant double bond conversion and phase separation

In the polymerization of vinyl/divinyl monomers the network formed is swellable but not soluble in the monomer medium, so that some micro phase separation may occur and this will cause phase heterogeneity in the polymer particle. Very recently, Vasi *et al*[17] verified that in the bulk polymerization of MMA/EGDMA there were microscopic segregation processes and build up of localized heterogeneity in the gel structure. This phenomenon was observed when the EGDMA fraction in the monomer mixture is greater than 3% by weight ($f2 = 0.015$). In emulsion polymerization this microscopic segregation will produce partitioning of monomer between sol/gel polymer domains within the particle.

Vanderhoff *et al* [18,19] noticed this phenomenon even on a macro scale. Using it they produced uniform non-spherical latex by seeded emulsion polymerization of styrene on to crosslinked monodispersed styrene latex particles. At first they found that there was a critical DVB concentration (0.03% wt) required to give a crosslinked network. Increasing crosslinking density of St/DVB seed will increase the degree of phase separation and the number of phase domains of final polymer particles.

The phase separation occurred after monomer swelling but before polymerization and was enhanced with increasing conversion. This means that the separation in the swollen seeds came from relaxation of polymer chains aided by temperature and swelling time. They developed a thermodynamic model considering the free energy of monomer-polymer mixing (promoting particle expansion) relative to those of polymer elastic retractive (crosslinking) and interfacial energies. The over all result of this energy balance is the monomer transfer driving force for phase separation. This is sometimes referred to as synerysis.

2.2 Experimental

2.2.1 Experimental design

The concentration of emulsifier, initiator; EGDMA ratio in the monomer feed were chosen as the important changes to make. The basic experimental conditions selected in the present study are as follows:

Recipes		**Reactor**
Water:	650 g	1 Liter (H/D=1.6)
Monomer:	100 g (EGDMA 0-25%wt)	300-350 rpm (Agitation)
SDS:	$(3.5\text{-}10)\times10^{-3}$ (mol/liter-H_2O)	50±0.2°C
$K_2S_2O_8$:	$(2.2\text{-}8.8)\times10^{-3}$(mol/liter-$H_2O$)	Vacuum sample outlet

A typical recipe for an emulsion polymerization in the present investigation includes 650g water, 100g monomer. The monomer and water ratio is not very high in order to isolate the crosslinking effect from other external influence such as agitation. Most part of experiments were in the low to middle EGDMA concentration range (from 0 to 25%wt). While two experiments were done with pure EGDMA monomer feeds, at low and high SDS concentration separately to explore the limiting conditions. Initiator, potassium persulphate (KPS) concentrations used were about $(2.2\text{-}8.8)\times10^{-3}$ mol/liter-H_2O and this covered a fairly wide concentration range. Sodium dodecyl sulphate (SDS) concentration used was at both below and above its CMC, $(3.5\text{-}10)\times10^{-3}$ mol/liter-H_2O.

2.2.2 Materials

MMA and crosslinking agent EGDMA (Aldrich Chemical Co.) were purified by vacuum distillation. Potassium persulphate (KPS) (Fisher Chemical, certified) and sodium dodecyl sulphate SDS (BDH Chemicals, analytic reagent) were used without further purification.

2.2.3 Polymerization and polymer and polymer particle characterization

Polymerization

Polymerizations were conducted in a 1 liter glass reactor having height to diameter ratio of about 1.6 and with a stainless steel four-bladed flat paddle type stirrer of diameter 65 mm. The reactor was fitted with a nitrogen inlet, a water-cooled condenser with wash-bottle trap filled with oil to prevent back-contamination by air. A vacuum sample outlet was also fitted at the dished bottom of the reactor.

After the desired level of water, monomers and emulsifier were added to the reactor a small amount of sodium hydroxide solution was added to adjust the pH to about 7. Several drops of pH=7 buffer solution was also added at this time. Then dissolved oxygen and oxygen in the head space of the reactor were removed by bubbling nitrogen gas (UHP grade) for more than 30 min. The nitrogen bubbling was carried out at room temperature in order to reduce the loss of monomers by evaporation.

The polymerization was started by injecting about 30 ml aqueous KPS solution that had also been de-oxygenated by bubbling nitrogen gas through it. At this time, the nitrogen gas was switched to another inlet above the liquid surface. The nitrogen gas flow rate was monitored by the bubbling extent in the wash-bottle trap to just keep a nitrogen gas blanket. The polymerization temperature was kept at 50±0.2°C for all runs. The agitation speed was set to 300-350 rpm for all runs.

Polymer and polymer particle characterization

2.2.3.1 Monomer conversion and rate of polymerization

Total monomer conversion (polymer production)-time history was determined by gravimetry using methanol as precipitant for the polymer. The sampling time interval was about 10 min. Ice-water bath was used to quench the polymerization in each sample. The vacuum oven temperature was kept at 30 ^{0}C.

2.2.3.2 Particle size determination by dynamic light scattering (DLS)

Polymer particle size distribution was measured by "Semimicro Particle Sizer -Model 370" with version 5.0 Nicomp software. The measurement error of the instrument was estimated by using two monodispersed polystyrene latex particle standards obtained from "Polysciences Inc. USA":

CAT#00876: (110 ± 3nm)

CAT#08691: (60 ± 2nm).

Particle number concentrations were estimated by using the measured particle size distribution data and polymer concentration.

2.2.3.3 Equilibrium swellability of particles

The equilibrium swellability of polymer particles was also measured by the DLS method. Polymer particles sampled at different polymerization conversions were washed and centrifuged several times. The particle size was then measured. Then the concentrated samples at the bottom of the centrifuge tube were diluted with the solvent. In the present study, acetone and MMA monomer were used as swelling agents. The swelling process was carried out at 25 °C for 72 hours. The sample was stirred during the swelling process with a magnetic stirrer. The size of the equilibrium swollen polymer particles was measured again by DLS to get the equilibrium volume increase of the polymer particles.

2.2.2.4 DSC measurement of pendant double bond conversion

Conversion of PDB and glass transition temperature (Tg) were determined using "910 Differential Scanning Calorimeter" with a Thermal Analysis 2000 System. The heating rate used was 10°C/min for all tests. The sample taken at different times was washed and dried before DSC testing. The conversion of PDB was calculated by the exothermic peak in the first heating process. After the sample was cooled down, it was heated again. No further exothermic reaction peak was detected in the second run that reflected the consumption of PDB in the sample tested.

2.3 Results and Discussion

2.3.1 Monomer conversion and rate of polymerization

The experimental investigation part of this study was aimed at making clear the influences of crosslinking on emulsion polymerization kinetics and the difference in kinetics between bulk and emulsion polymerization. Experiments were done using batch operation.

2.3.1.1 Effect of EGDMA level in monomer feed

Figure 2.1 shows the total monomer conversion histories with different EGDMA levels in the monomer feeds. The SDS concentration was $3.47\text{x}10^{-3}$ mol/ liter-H_2O that is below the critical micelle concentration (c.a. $CMC_{SDS,\ @\ 20^oC} \approx 8.0\text{x}10^{-3}$ mol/liter-H_2O [32]). The initiator (KPS) concentration was $2.2\text{x}10^{-3}$ mol/liter-H_2O. **Figure 2.2** shows the total monomer conversion histories with different EGDMA levels in the monomer feeds. In this case, the SDS concentration was $10\text{x}10^{-3}$ mol/liter-H_2O that is above CMC.

It can be seen in **Figure 2.1** that when the SDS concentration was below the critical micelle concentration CMC, there was not much difference in the polymerization rate for the systems with different EGDMA levels (from zero to 10%wt).

The reason can be that under this condition, because of its very low water solubility, EGDMA did not copolymerize with MMA to form oligomer chains for the homogenous particle nucleation. The newly formed primary particles mainly contain MMA repeat units in oligomer chains. EGDMA started to play a role in polymerization only in the later stages by diffusing into those stabilized primary particles.

So that it can be understood that in this case, the low EGDMA solubility in water makes its effect on particle nucleation negligible. This can be further verified by observing the pure EGDMA conversion data. The polymerization rate is extremely slow and the particle suspension is not stable. The reason is that those precipitated primary particles can not coalescence together to increase the surface charge density to stabilize themselves because they are glassy particles.

On the other hand, in **Figure 2.2**, one can see that when polymerization was carried out with SDS concentration above its CMC, there is a very clear effect of EGDMA or crosslinking level on polymerization rate. In the present experiments, the polymerization rate increased with increasing of EGDMA level to about 10%wt. Then the polymerization rate for 25%wt EGDMA is slower than that for 10%wt and decreases with further increase in EGDMA concentration.

These conversion-time histories are very different from those observed in a bulk polymerization of MMA/EGDMA. In the bulk polymerization, all the rate data showed that the polymerization rate was a monotonous increasing function of EGDMA concentration in the monomer feed[6.]

In emulsion polymerization with crosslinking, a change in divinyl monomer concentration can have two opposite effects on the polymerization rate. On one hand, increasing EGDMA concentration in the monomer feed will produce more crosslinking and this will cause an increase in polymer particle viscosity and a decrease in the termination rate. This will increase the number of free radicals per particle and so increase polymerization rate.

On the other hand, high crosslinking of polymer particles will lower their free volume. From the mass transfer rate and swelling equilibrium point of view, the higher the EGDMA level, thc lower will be the monomer concentration in the polymer particle. This will, in turn, reduce the polymerization rate per polymer particle .

This reduction in polymerization rate (especially in stage I) will lower the surface area increase rate of the formed polymer particles. Thus more micelles will be consumed to form new polymer particles than to cover growing surface area.

Therefore more micelles will be available to generate a higher concentration of polymer particles and this leads to a higher polymerization rate.

Experimental studies on the bulk polymerization kinetics of MMA and alkyl glycol dimethacrylate have been reported [20-22]. It was found that gelation occurred at low conversions with increase in (-CH2-)n units in the ester group beyond two ($n > 2$). This result was attributed to the suppression of intermolecular termination between the growing polymer radicals having loop structure due to intramolecular cyclization.

Comprehensive research on bulk polymerization of MMA/EGDMA[6] has shown that the polymerization rate is a monotonous increasing function of EGDMA monomer concentration in the polymerization feed. The major difference between bulk and emulsion polymerization process is the compartmentalized loci of polymerization and the monomer supply mechanism. In the emulsion polymerization process, a change in divinyl monomer concentration will affect the polymerization rate by changing these two phenomena.

At first, increasing EGDMA concentration in monomer feed will produce a more crosslinked internal micro-environment, diffusion controlled bimolecular termination should be similar to that observed in a bulk polymerization process. While, at the same time, highly crosslinked internal structure of the polymer particles will reduce the monomer diffusion rate in the polymer particle.

From the free volume theory, the higher the EGDMA level, the tighter will the network structure in the polymer particles be, giving a smaller monomer concentration in the particles. This will, in turn, cause a reduction in the polymerization rate per polymer particle. This reduction in polymerization rate (especially in stage I) will decrease the consumption of micelles due to growing polymer particle surface area. Therefore, more micelles will be available to generate polymer particles and thus a higher concentration of polymer particles results.

Crosslinking should also reduce the rate constant for radical-radical termination, however, for the very small polymer particles found in stage I, the termination is nevertheless instantaneous and thus two radicals can not coexist in a particle in this early stage of the emulsion polymerization.

2.3.1.2 Effect of initiator concentration

Figure 2.3 shows the effect of initiator concentration on the conversion-time history. EGDMA is 10%wt and SDS is $10\text{x}10^{-3}$ mol/liter-H_2O. It can be seen that initiator concentration affects the initial time period of polymerization. The final total monomer conversion, a similar limiting conversion in both cases, was reached after about 35 min. This is the result of the glassy effect. The final particle size and particle number were also reached about this time as expected. The SDS concentration is above the CMC and the nucleation process is micellar [16]. The higher the initiator concentration, the more rapid is the nucleation rate. The conversion rate (slope in the linear range in both profiles) is about 2.4 and 5.8 for low and high initiator concentrations respectively.

2.3.1.3 Effect of emulsifier concentration

Figure 2.4 shows the effect of SDS concentration on the polymerization rate. The A1 and B1 lines show the system with low SDS concentration 3.47×10^{-3} mol/liter-H_2O. A2 and B2 lines, the system with high SDS concentration 10×10^{-3} mol/liter-H_2O, above CMC. Group A lines are for the 10%wt EGDMA while group B lines, pure EGDMA. A faster polymerization rate specially in the early stage can be seen in high SDS concentration case (comparing A1 and A2) with A1 having a very earlier auto-acceleration effect.

The reason is that the particle nucleation process is different. MMA has a moderate water solubility (50°C, 1.43 ± 0.08 g/100g H_2O). When the SDS concentration is below the CMC, the nucleation process is homogenous. When the

SDS concentration is above the CMC the nucleation process is micellar. The micellar nucleation generates polymer particles at a faster rate than homogenous nucleation.

Another reason is that EGDMA has a very low water solubility and before the start of polymerization, the micelles will have a strong solubilization effect on the EGDMA monomer (considering the total amount of monomer dissolved in the water phase--outside the monomer droplets). EGDMA is a fast monomer, so that in the early stage, polymerization rate will increase and large and small size particles with a high EGDMA content per polymer chain will be formed.

However, this micelle solubilization effect on EGDMA monomer is based on the preliminary condition that the internal crosslinking of polymer particle is not very high. Otherwise, the very low monomer swellability of highly crosslinked polymer particles because of the extremely high crosslinker concentration in monomer feed will counteract this micelle solubilization effect. This can be clearly seen observing the B2 conversion / time history in **Figure 2.4.**

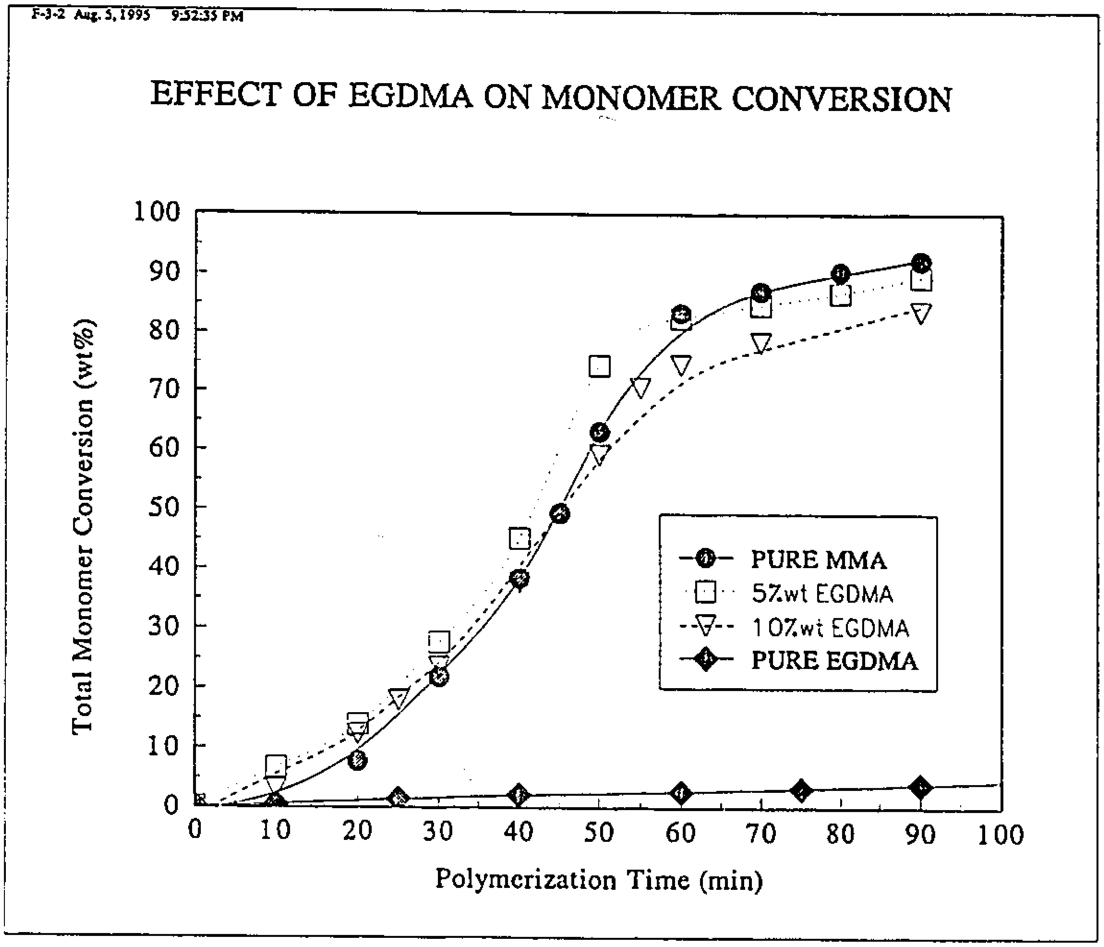

Figure 2.1 Experimental results showing the effect of EGDMA monomer level on total monomer conversion vs time in MMA/EGDMA emulsion polymerization at low emulsifier concentration. SDS: 3.47×10^{-3} mol/ liter-H_2O (below CMC), KPS: 2.2×10^{-3} mol/liter, T=50°C.

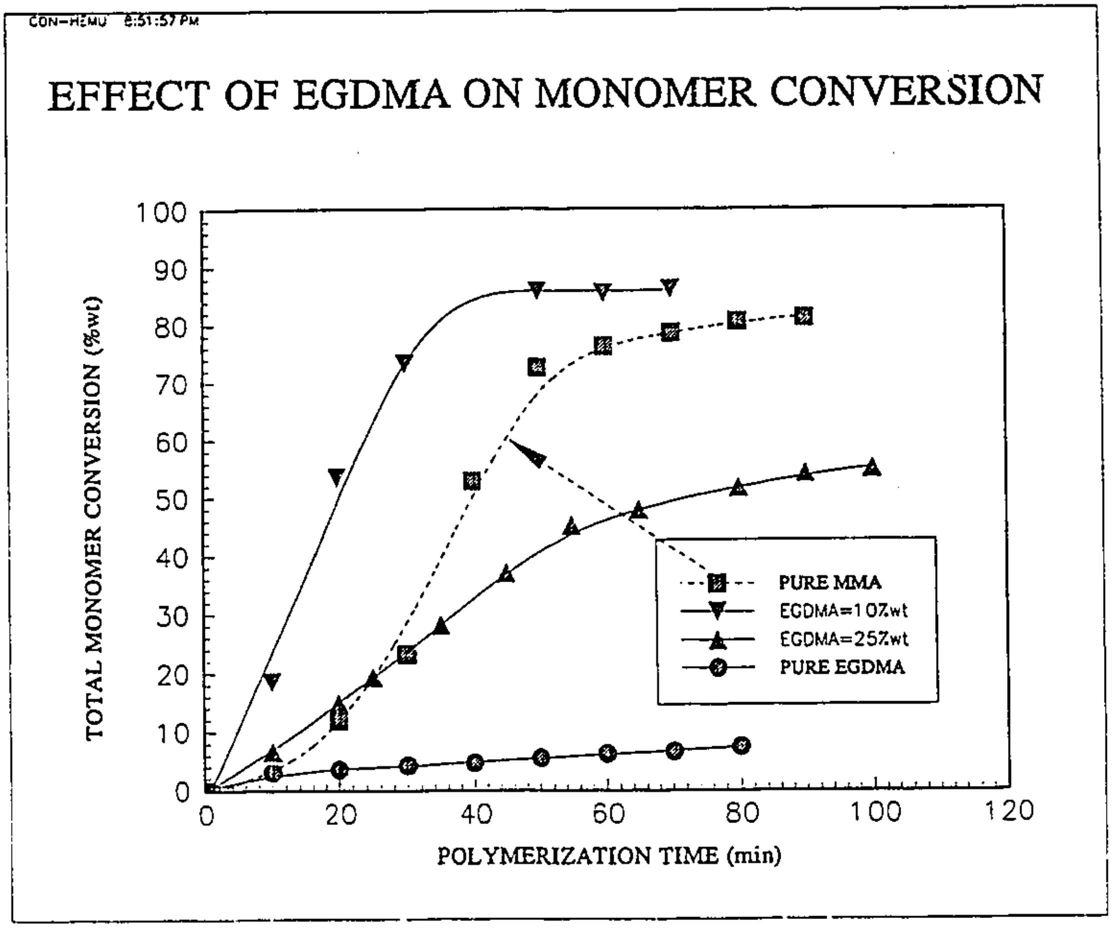

Figure 2.2 Experimental results showing the effect of EGDMA monomer level on total monomer conversion vs time in MMA/EGDMA emulsion polymerization at high emulsifier concentration. SDS: 10×10^{-3} mol/ liter-H_2O (above CMC), KPS: 2.2×10^{-3} mol/liter, T=50°C.

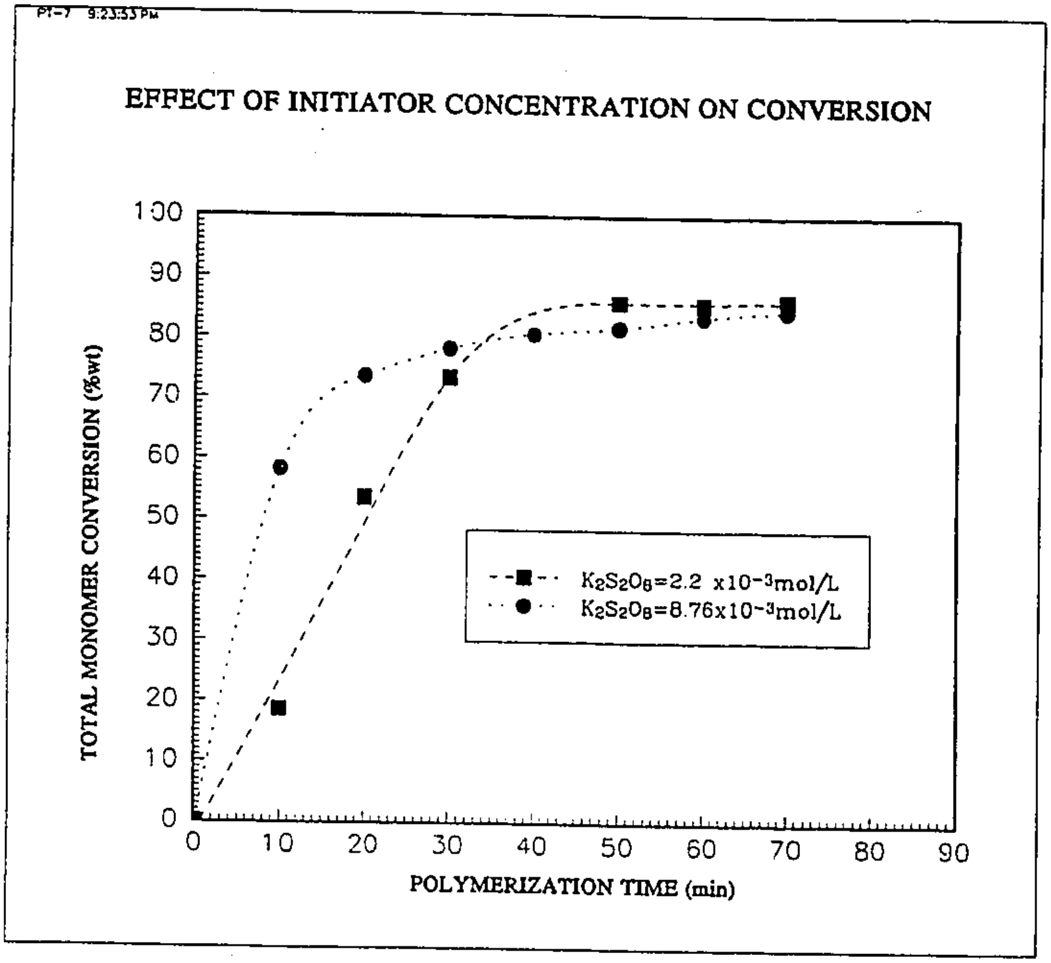

Figure 2.3 Experimental results showing the effect of KPS concentration on total monomer conversion vs time in MMA/EGDMA emulsion polymerization. EGDMA: 10%wt, SDS: 10×10^{-3} mol/ liter-H_2O, T=50°C.

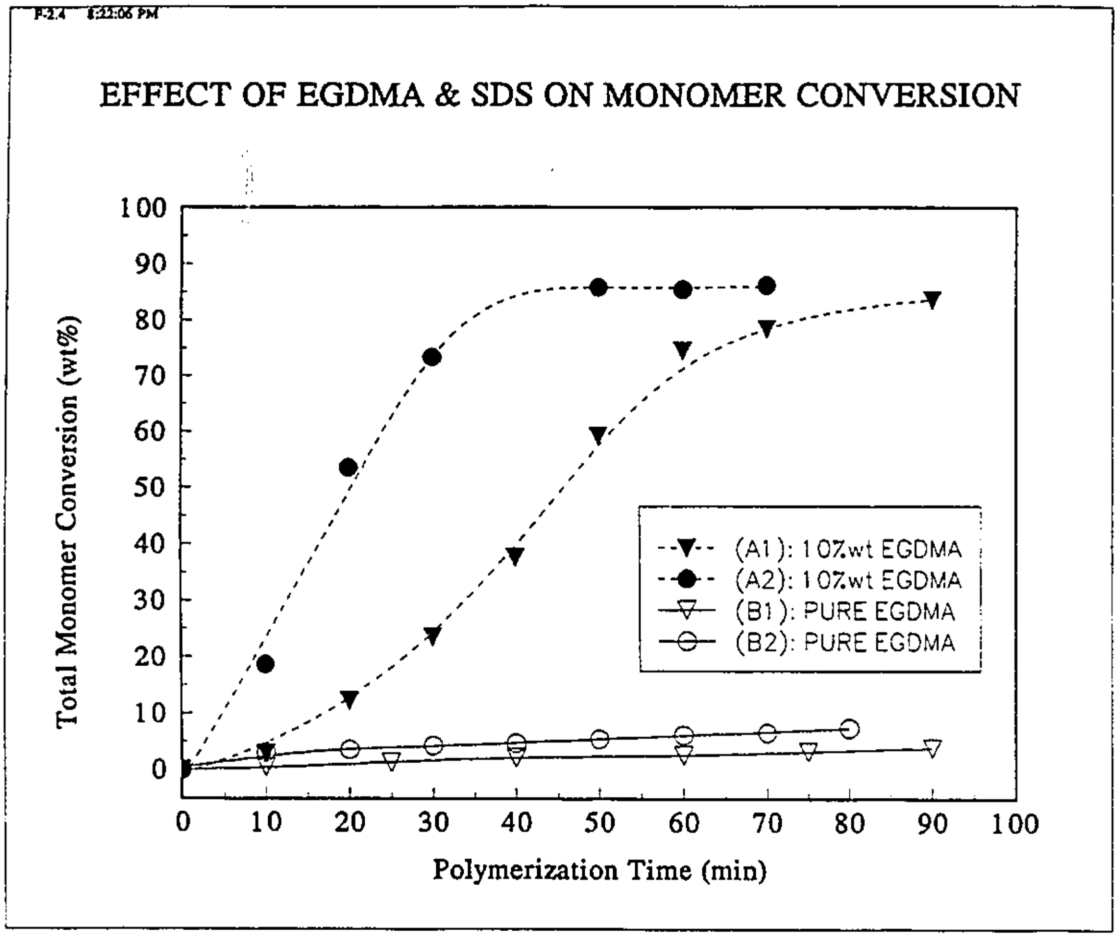

Figure 2.4 Experimental results showing the effect of SDS concentrations on total monomer conversion vs time in MMA/EGDMA emulsion polymerization. KPS: 2.2x10^{-3} mol/ liter-H_2O, T=50°C.
(A1, B1: SDS = 3.47x10^{-3} mol/ liter-H_2O)
(A2, B2: SDS = 10x10^{-3} mol/ liter-H_2O.

2.3.2 Polymer particle nucleation and polymer particle number and size development

2.3.2.1 Micellar and homogeneous nucleation

Particle nucleation is the first step in emulsion polymerization. The emulsifier concentration plays a critical role. So that, in the present study, particle nucleation mechanism was clarified by employing SDS concentrations above and below the CMC.

Figures 2.5 shows the effect of SDS concentration on the particle number change with polymerization time for the system containing 10%wt EGDMA. As a reference, also shown in this figure are the total monomer conversion at each related polymerization time. In this figure, the two solid symbols with solid lines show the total monomer conversion, and the two open symbols show the polymer particle concentrations. SDS concentration for the two triangle symbols (both solid and open) is above the CMC. While SDS concentration for the two circle symbols (both solid and open) is below the CMC. Other conditions were kept constant. A conclusion that can be made is that with high SDS, polymerization is fast initially with a large number of polymer particles produced.

EGDMA has a very low water solubility. Before the start of polymerization, the solubilization of monomer by micelles will have an more obvious effect on EGDMA monomer (considering the total MMA molecules dissolved in the water phase). EGDMA is the faster monomer in polymerization therefore particles formed in the nucleation stage will have a higher EGDMA content per polymer chain.

When there is no crosslinking (no crosslinker), the higher the SDS concentration, the greater the number of polymer particles nucleated and therefore the polymer particles are smaller for the same initial charge of monomer and same total conversion. For the situation of high SDS concentration, in the presence of crosslinker, crosslinking in the polymer particles will reduce monomer swelling of primary polymer particles formed in the nucleation stage giving a slower surface area growth rate. A large number of solubilized micelles will therefore be nucleated instead of being consumed by covering freshly formed surface or growing polymer particles.

For this reason, the polymerization carried out at a high SDS concentration (above CMC) will have smaller particle size with more particles than that carried out under low SDS condition. It is also evident that polymer particles produced at the high SDS concentration are more stable because no particle coagulation trend can be seen in this **Figure 2.5**. The total number of polymer particles reaches a plateau and remains constant with time.

2.3.2.2 Effect of initiator concentration

The micelle nucleation mechanism was further studied by checking the effect of initiator concentration. A system with 10%wt EGDMA and $10x10^{-3}$ mol/liter-H_2O SDS was considered.

Figure 2.6 shows the particle size and particle number change with time at two different initiator levels. The solid lines with solid symbols represent the particle diameters. The short dash lines with open symbols show the particle concentrations. Circular symbols (both solid and open) are for the low initiator concentration case.

It can be seen that the initiator concentration affects the early stage of polymerization (initial 35 min). When the initiator concentration was increased by about four times, the particle diameter was reduced by about one time, while the particle concentration was increased by about four times.

An interesting observation is that the final diameter of particles prepared with the higher initiator concentration ($8.76x10^{-3}$ mol/liter-H_2O) is just a little larger than the diameter of monomer solubilized micelles. It is likely, therefore, that the majority of monomer swollen micelles were stung to nucleate polymer particles and that the particles did not undergo a significant growth in size during the whole polymerization.

This clearly suggests that a high level of crosslinking existed in the particles giving a very low monomer concentration in the particles and as a consequence a very slow volume and surface area growth rate for newly formed polymer particles occurs. This, in turn, reveals a micellar nucleation domain that can be confirmed by recalling the results shown in **Figure 2.3.**

2.3.2.3 Effect of divinyl monomer concentration

Because of the effect of different SDS levels on the polymer particle size and number mentioned in the above section, two experiments have been done at low and high SDS concentrations in order to isolate the effect of EGDMA.

Polymerization at low SDS concentration

Initially, the particles were produced at SDS concentrations below its CMC. **Figure 2.7** shows the effect of EGDMA level on the change in particle number with polymerization time at the same initiator concentration. The open square symbols with a solid line is for the pure MMA monomer. The number near these symbols is the related polymer particle diameter in nm for pure MMA polymerization under the same conditions. This result is used as the base case (i.e. no crosslinking).

For the pure MMA system, both particle size and number continually increase up to 60min, then they remain essentially constant thereafter. This indicates a long nucleation stage (about 60 min).

However, for the system having 10%wt EGDMA monomer, there is sharp increase in particle number in the initial stage of polymerization up to 30 min. After this point, polymer particle number remains constant until about 60 min corresponding to the final polymerization conversion about 75%wt. This is a typical stable particle growth period.

The reason is that for a homogenous nucleation process, the existence of EGDMA in the water phase will produce oligomeric chains with some degree of branching. These primary chains will therefore have less ionic initiator end groups per chain. Because of the low water solubility of EGDMA, these very short oligomeric chains will readily precipitate out of the aqueous phase giving more primary particles with less surface charge density compared with the pure MMA system. By adsorbing emulsifier molecules from the water phase, a stable suspension can be obtained.

With this recipe, the SDS concentration is below the CMC and after a certain time, with continuous growth of polymer particle surface area, the surface charge density will not be large enough to stabilize the whole suspension system so that modest levels of particle agglomeration occurs. It should be understood that at this conversion the particles are solid at the polymerization temperature used, so that this aggregation is not a coalescence process but more like a loose flocculation.

Polymerization at high SDS concentration

In section 2.3.1.1 we have mentioned that when polymerization was carried out at the high SDS concentration, increase in the EGDMA monomer level in the monomer feed lowers the surface area growth rate of the freshly formed polymer particle. Thus more micelles will be consumed by particle nucleation leading to higher particle concentrations. In other words, a greater fraction of micelles forms polymer particles. The highest concentration of particles results when every micelle forms a particle.

The present experimental data confirm the above explanation. **Figure 2.8** shows the effect of EGDMA concentration on the change of polymer particle diameter and number versus polymerization time for higher levels of crosslinker. In this figure, the two solid lines with solid symbols are for polymer particle diameter. While the two dot lines with open symbols are for particle number. Square symbols (both solid and open) are for the highest EGDMA concentration level (25%wt). Triangle symbols (both solid and open) are for the low EGDMA level (10%wt).

First, one can see that for 25%wt EGDMA, particle size is about one half that for 10%wt EGDMA, while particle concentration is two times higher than for 10%wt EGDMA. Secondly, after the nucleation stage, particle number remains constant for both EGDMA monomer levels. This suggests that at these SDS concentration, the latex is a stable dispersion. With sufficient emulsifier molecules adsorbed on the surface to stabilize them electrostatically. Also, for the 25%wt EGDMA level, particle size increases only slightly. This recipe should give polymer particles with a very tight internal structure.

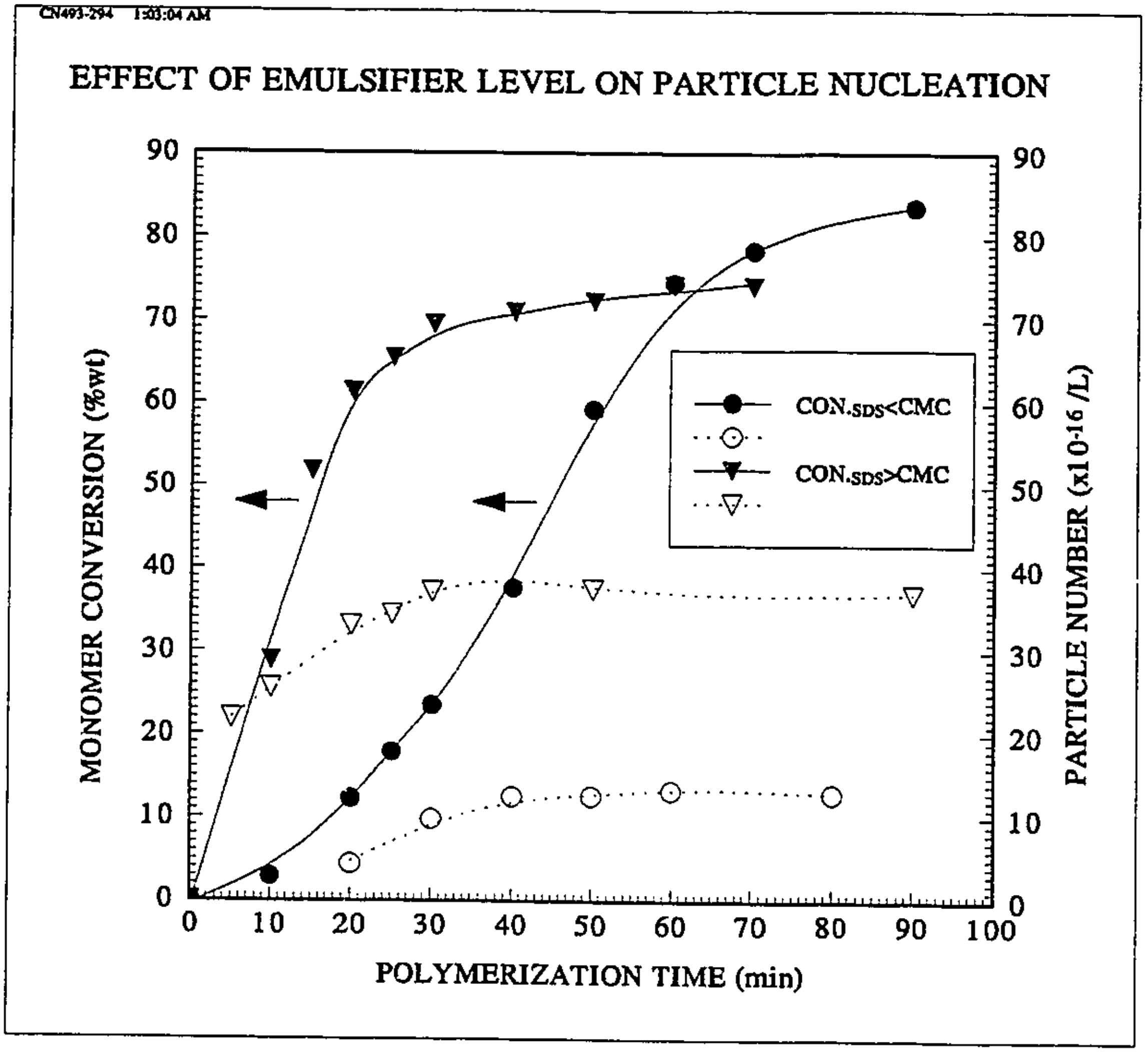

Figure 2.5 Effect of SDS concentration on polymer particle nucleation. EGDMA: 10%wt, KPS: 2.2x10^{-3} mol/liter-H_2O, T=50°C, SDS : 3.47x10^{-3} mol/ liter-H_2O and 10x10^{-3} mol/ liter-H_2O.

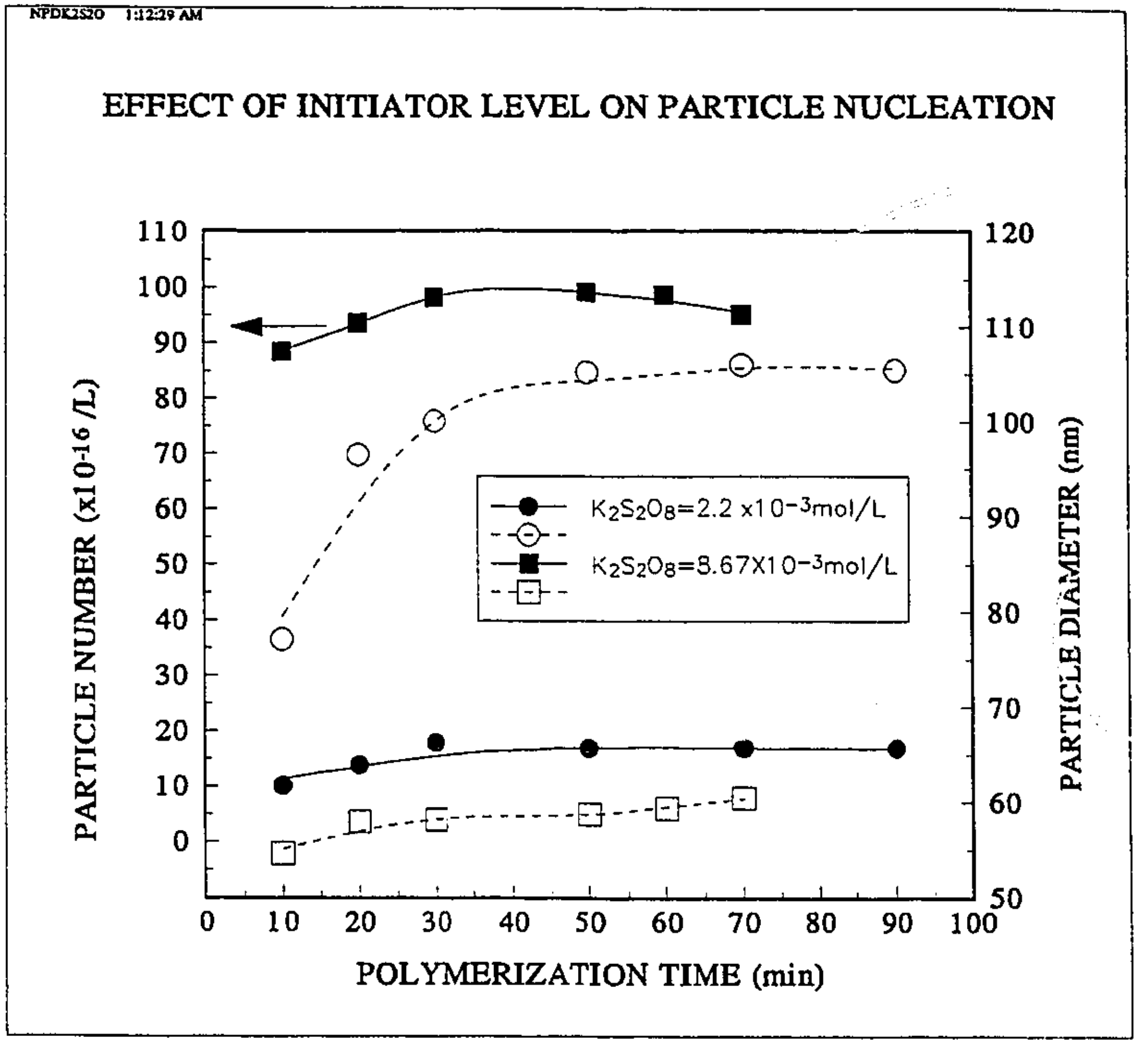

Figure 2.6 Effect of initiator (KPS) concentration on polymer latex particle diameter and number vs polymerization time. EGDMA: 10%wt, SDS: 10×10^{-3} mol/liter-H_2O, T=50°C.

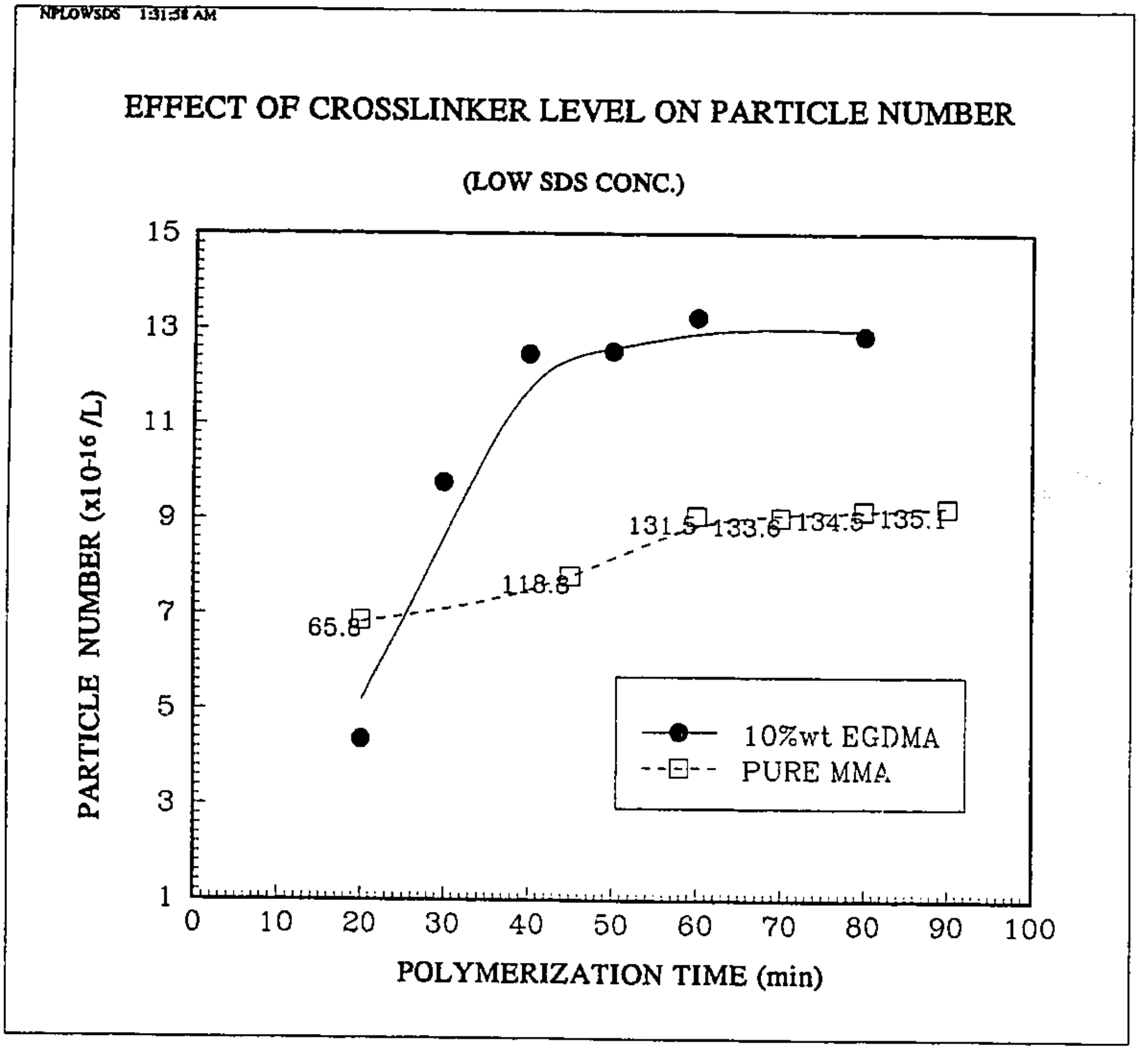

Figure 2.7 Effect of EGDMA monomer level on polymer latex particle diameter vs polymerization time. SDS: 3.5×10^{-3} mol/liter-H_2O(below CMC), KPS: 2.2×10^{-3} mol/liter-H_2O, T=50°C.

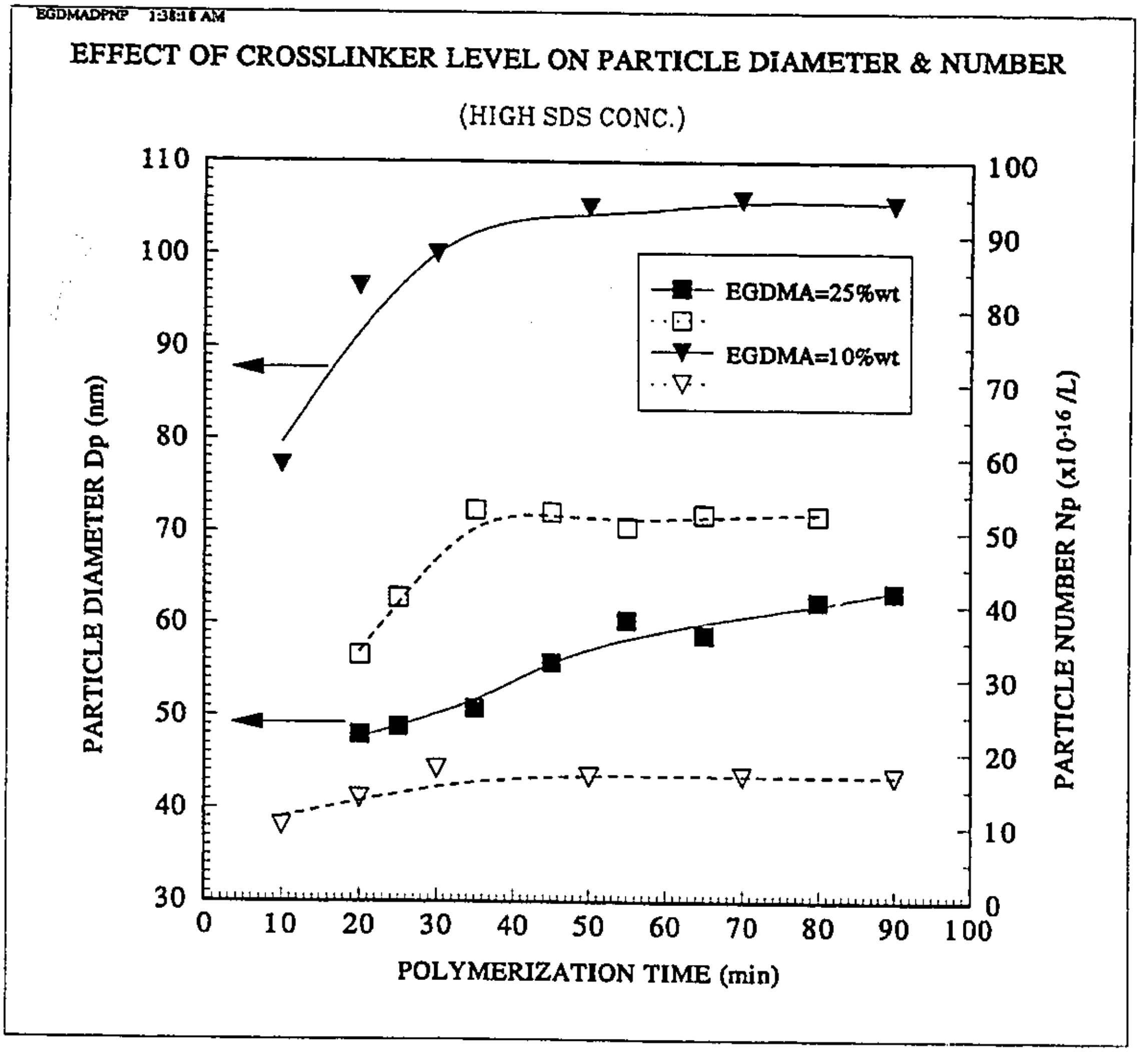

Figure 2.8 Effect of EGDMA monomer level on polymer latex particle number and diameter vs polymerization time. SDS: 10x10^{-3} mol/liter-H_2O (above CMC), KPS: 2.2x10^{-3} mol/liter-H_2O, T=50°C.

2.3.3 Swellability of crosslinked polymer particles

The swelling ratio is defined here as the ratio of particle diameter before and after equilibrium swelling using an inert swelling solvent which is a good solvent for the linear chains. One of the characteristics of emulsion polymerization is that at least three phases exist in the reactor. Chemical species must transfer from one phase through an interface into another to maintain the polymerization.

As for monomers, they can be in the water phase, monomer droplets (in stages I and II) and polymer particles and for gaseous monomers a significant amount in the reactor headspace. It is accepted that the mass transfer of monomer is not the rate controlling step in emulsion polymerization, in fact, instantaneous equilibrium regarding monomer transfer is invariably assumed. The very large interfacial areas justify this. An interesting phenomenon occurred in stage two where the volumetric fraction of monomer in the polymer particles is essentially constant (for pure MMA with no crosslinking this is about 0.7) due to rapid diffusion of monomer from the monomer droplets to the polymer particles.

As mentioned earlier, some workers [12-14] attributed the low polymerization rate with vinyl/divinyl monomers to the low monomer concentration in the polymer particles. This change in the polymer swellability reflects the crosslinking density change of polymer in the particles. For the MMA/EGDMA system, Tobita [23] reported that in stage II the volume fraction of monomer in polymer particles is 0.62 for an EGDMA level of 5%wt and 0.56 at a higher 10%wt level.

2.3.3.1 Effect of initiator concentration on swellability

Figure 2.9 shows the present results for equilibrium swelling ratio versus total monomer conversion for particles produced with different initiator concentrations. Acetone was used as the swelling solvent. It is clear that at both levels of initiator swelling ratio is a monotonous decreasing function of monomer conversion, but at different rates. Particles prepared with a low initiator concentration have higher swelling ratio. Higher initiator levels clearly give higher crosslinking densities for the polymer chains in the particle.

The rate of change of swelling ratio with monomer conversion is greater at high conversion levels with evidence of a possible transition point which may be a result of some structural change in the polymer particles. The higher the level of initiator, the earlier is the transition point.

Figure 2.10 shows the change of liquid volume fraction in polymer particles with total monomer conversion calculated from above swelling ratio data. In this figure, open symbols (square and circle) are for the swelling condition with acetone as a solvent. Solid square is the case wherein MMA monomer was used as the swelling agent. Square symbols (both solid and open) show the swelling with polymer samples produced using high initiator concentration.

Again it is clear that the solvent volume fraction has a similar pattern as that of swelling ratio based on particle diameter ratio. The liquid volume fraction in polymer particles initially remains a stable value to certain monomer conversion and decreases abruptly thereafter. The lower the initiator concentration used in the preparation of polymer particle samples, the higher is the stable value and the later does this transition point appear. It is understandable that the swellability reflects the crosslinking density and internal structure of polymer particles. It has been mentioned in section 2.3.2.2 that the initiator concentration has a clear effect on the development of size and number of polymer particles

Recall results shown in **Figure 2.6** and the interesting observation that the final diameter of particles decreases with increase in initiator concentration (from 2.2 to 8.76x10^{-3} mol/liter-H_2O). It is likely, therefore, that with the increase of initiator concentration more and more monomer swollen micelles were stung to nucleate polymer particles.

As a result, with increase of initiator concentration, the particles will undergo a less significant volume growth during the whole polymerization. This clearly suggests that a high level of crosslinking existed in the particles with a low monomer concentration with the higher initiator concentration. The swelling experimental results confirm this conclusion.

2.3.3.2 Effect of solvent type on swellability

In **Figure 2.10** is also shown the effect of solvent type on the change of solvent volume fraction in polymer particles versus total monomer conversion. Acetone and pure MMA were used as swelling solvents for the polymer sample produced at the same initiator concentration (c.a. 4.4×10^{-3} mol/liter-H_2O). It can be seen that for this polymer sample, the solvent and/or monomer volume fraction in the polymer particles keep a relative constant value **0.48** up to about 35%wt total monomer conversion. The swelling ratios reported in this study are smaller than those reported by Tobita [23].

The reason for this may have been that in these experiments a higher initiator concentration was used. This dependence on initiator concentration was shown in **Figure 10.** For conversions up to about 40%wt, the solvent volume fraction remains almost at about **0.48** for particles prepared at the higher initiator concentration

(4.4×10^{-3} mol/liter-H_2O) and about **0.58** for particle prepared using the lower initiator concentration (2.2×10^{-3} mol/liter-H_2O). Tobita [23] reported a value of **0.56** using 2.3×10^{-3} mol/liter-H_2O, respectively.

As is mentioned above, not only this initial liquid volume fraction but also the transition point is strongly influenced by the initiator concentration in the emulsion polymerization among the other thing. This clearly reflects an effect of increased crosslinking density in these polymer particles.

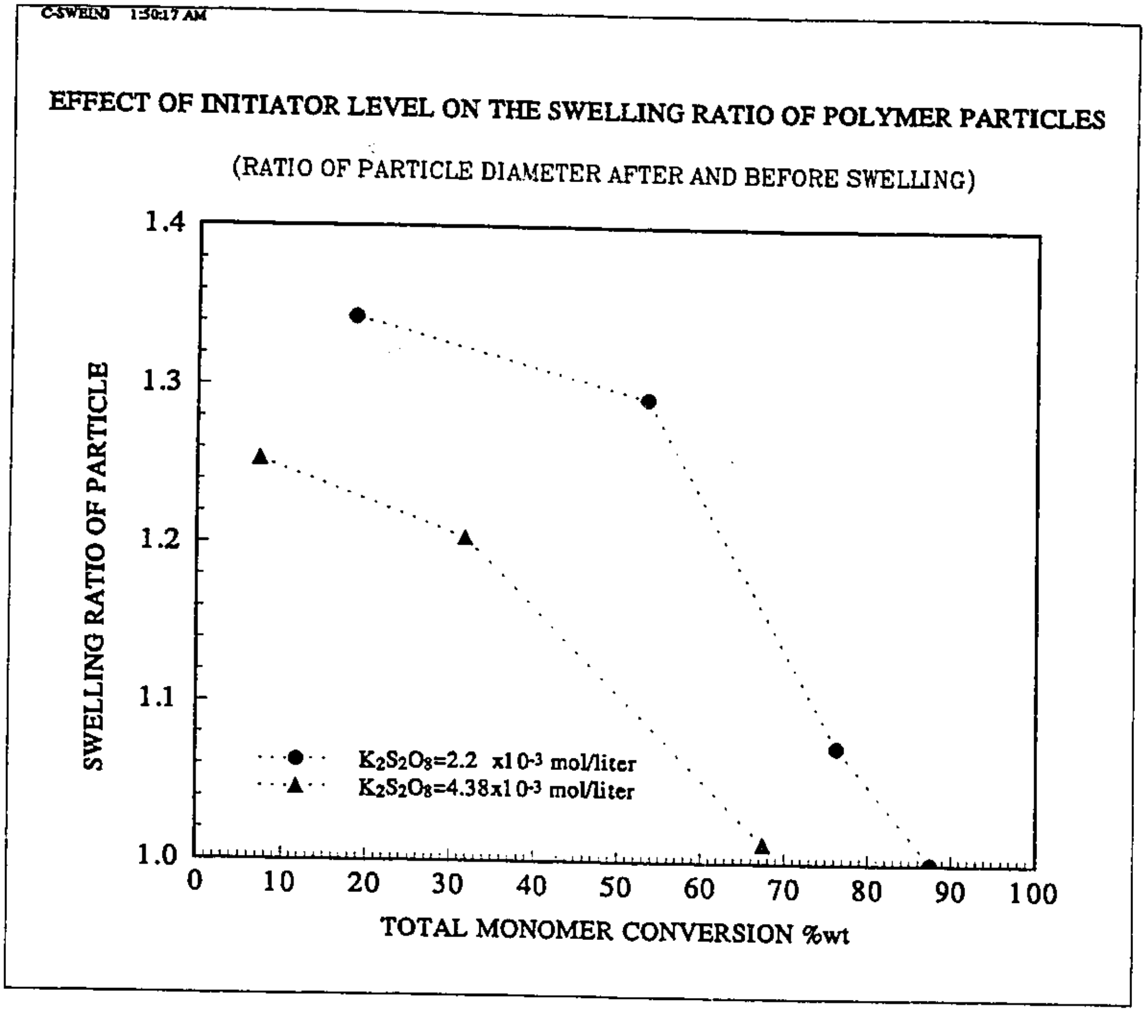

Figure 2.9 Effect of KPS concentration on swelling ratio of polymer particles. Polymerization conditions: EGDMA: 10%wt, SDS: 10×10^{-3} mol/liter-H_2O, T=50°C. Swelling conditions: solvent: acetone, at 25°C for 72 hours.

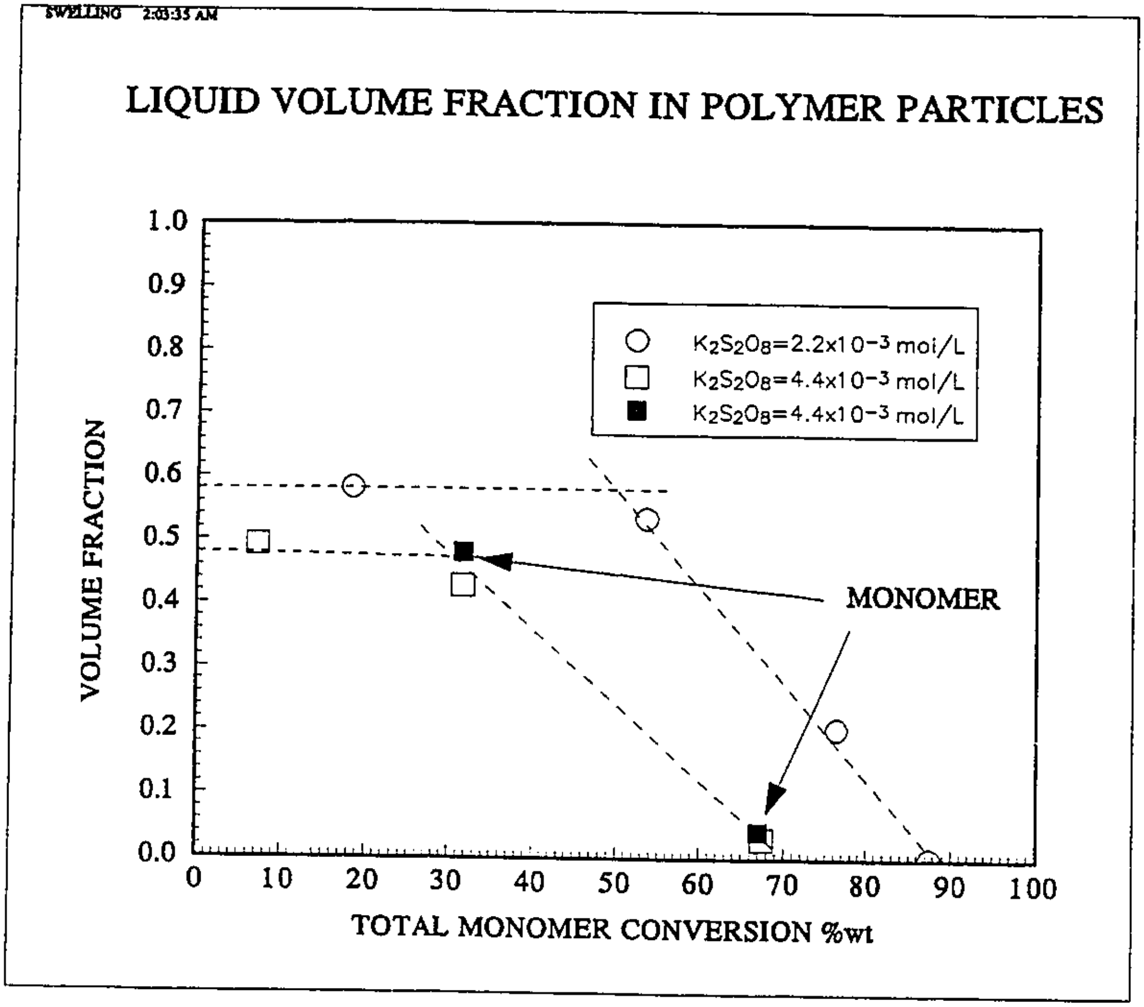

Figure 2.10 Swelling of polymer particles made at different initiator levels with two solvent types. Polymerization conditions: EGDMA: 10%wt, SDS: $10x10^{-3}$ mol/liter-H_2O, T=50°C. Swelling conditions: swelling at 25°C for 72 hours (swelling solvents: pure acetone and MMA monomer).

2.3.4 Pendant double bond (PDB) conversion and glass transition temperature (Tg)

To reveal the effect of shielding if any on the reactivity of pendant double bonds one needs to measure PDB concentration with time. Besides the normal chemical analysis methods, Raman [24], NMR [25-30] are extensively applied for this purpose. For conversions before the gelation point, ^{1}H NMR is normally used [15, 25-27].

Macosko *et al* [15] reported that by extrapolating a plot of PDB conversion versus monomer conversion to zero conversion primary cyclization levels can be estimated. The micro-environment of PDB in pre and post gelation periods is not the same and one needs to test the PDB conversion in both total monomer conversion ranges to evaluate the primary cyclization effects.

The method often used to measure PDB conversion in the post gelation range is ^{13}C solid-state NMR. In 1986, Price *et al* [28] applied this method to the polymerization of MMA with 8 different kinds of dimethacrylate crosslinkers. They found that the concentration of unreacted PDB in solid samples increased with increasing length of chain between ester groups in the crosslinker. Allen *et al* [29] used this method to follow the network formation for MMA/EGDMA in bulk polymerization. The positions of chemical shift of different carbon atoms have been reported for this system.

St⬀ver *et al* [30] used NMR to characterize crosslinked polystyrene gels. These gels exemplified a large group of polymeric materials that undergo rapid but anisotropic reorientation on the molecular scale. They confirmed that the direct polarization magic angle spinning (DP/MAS) NMR was ideally suited for the characterization of these solvent-swollen crosslinked polystyrene gels. The line broadening due to the residual dipolar coupling (^{1}H NMR) or chemical shift anisotropy (^{13}C NMR) in swollen gels could be removed by moderate-rate magic angle spinning to give highly resolved spectra.

They found that the application of those methods permitted full characterization of polystyrene gels including well-resolved signals attributed to the crosslink junctions. The complementary nature of this technology has a potential application to directly monitor crosslinking polymerization kinetics around the gel point.

2.3.4.1 DSC measurements of PDB

In the present research, DSC was used to measure the content of residual double bonds in polymer samples. **Figure 2.11** shows DSC spectra of MMA/EGDMA polymer samples prepared by emulsion polymerization. Every DSC measurement was repeated once. The reproducibility is very good. The figure shows that at different monomer conversions, the heat flow profile for residual double bonds has only one peak. The relationship between total monomer conversion and integrated total heat flow for residual or unreacted double bonds in these sample is a monotonous decreasing function of total monomer conversion. In the present experiment, the sample was washed and dried to remove unreacted monomers before DSC measurement. The heat flow profiles for polymer samples can be used to estimate residual PDB. In the present study the DSC testing began, after the testing sample was cooled to room temperature whereupon it was heated. No other reaction peaks were detected.

2.3.4.2 Calibration of DSC

To convert the total area of heat flow to that of residual PDB content in the polymer network, the following calibration process was used. First the bulk polymerization of pure EGDMA monomer with AIBN initiator in a DSC sample cell was done. The temperature range was from 40 to 200^0C. The upper temperature limit was set to 200 °C in order not to cause thermal degradation of the polymer. The heating rate chosen was 10 ^{0}C/min. After the sample was cooled to room temperature, the sample was heated a second time and no additional exothermic peaks were found and that confirmed the complete consumption of total double bonds during the first DSC scan.

Figure 2.12 shows the DSC spectrum of pure EGDMA synthesized by bulk polymerization. The total heat released during the polymerization (area of the peak) is 358.0 (J/g). The estimated heat of polymerization is about 35.45 kJ/(mol. double bonds).

Then the bulk polymerization of MMA/EGDMA monomer mixture with 10%wt EGDMA using the same DSC method was done. **Figure 2.13** shows the results. The total heat released during bulk copolymerization (area of the peaks) are 552.8 and 502.1 (J/g). The calculated average heat of copolymerization per mole is around 52.61 kJ/ (mol. double bond). The relative error based on this average value is 9.9%.

The second step in calibration is to convert total heat released measured by DSC to the enthalpy change based on the same thermodynamic state. **Figure 2.14** shows the scheme of the thermodynamic path designed to calculate residual double bond content at constant pressure. In this figure:

Ts,b is the starting temperature of heat flow peak in spectrum of bulk polymerization

Te,b is the end temperature of heat flow peak in spectrum of bulk polymerization

Ts,l is the starting temperature of heat flow peak for polymer sample taken from latex

Te,l is the end temperature of heat flow peak for polymer sample taken from latex

$\Delta H_{DSC,b}$ is the total heat peak area in spectrum for bulk polymerization

$\Delta H_{DSC,l}$ is the total heat peak area in spectrum for polymer sample taken from latex

State A is the state of pure monomer at 50^0C

State B is the state of polymer without residual double bonds from bulk process at 50^0C

State C is the state of polymer with residual double bonds from latex at 500C

State D is the state of pure monomer at Ts,b

State E is the state of polymer without residual double bonds from bulk process at Te,b

State F is the state of polymer with residual double bonds from latex at Ts,l

State G is the state of polymer without residual double bonds from latex at Te,l

Process A⇒B is the total enthalpy change from pure monomer to polymer without residual trapped double bonds in the bulk polymerization at reference temperature 50^0C and constant pressure ($\Delta H_{p,50,AB}$). Process A⇒C is enthalpy change from pure monomer to polymer with residual trapped double bonds in emulsion polymerization at reference temperature 50^0C and constant pressure. Process C⇒B is the enthalpy change from pure polymer with residual trapped double bonds to that of without it in DSC cell at reference temperature 50^0C and constant pressure ($\Delta H_{p,50,CB}$). The follow ratio was defined as conversion of residual double bonds CPDB:

$$C_{PDB} = \frac{\Delta H_{p,50,AC}}{\Delta H_{p,50,AB}} = \frac{\Delta H_{p,50,AB} - \Delta H_{p,50,CB}}{\Delta H_{p,50,AB}}$$

Enthalpy change is a thermodynamic process. It is independent of the process path. One can get ($\Delta H_{p,50,AB}$) from DSC result $\Delta H_{DSC,b}$ according to path A⇒D⇒E⇒B by equation:

$$\Delta H_{p,50,AB} = C_{p,m}(T_{s.b} - 50) + \Delta H_{DSC,b} + C_{p,p}(50 - T_{e.b})$$

Designing path C⇒F⇒G⇒B, one can get the ($\Delta H_{p,50,CB}$) from DSC date $\Delta H_{DSC,e}$ by equation:

$$\Delta H_{p,50,CB} = C_{p,m}(T_{s.l} - 50) + \Delta H_{DSC,l} + C_{p,p}(50 - T_{e.l})$$

In the above equations, $C_{p,m}$ is the average heat capacity of monomers and $C_{p,p}$ is the average heat capacity of polymer. From the definition of CPDB one can understand that this value represents the extent of double bond conversion in the solid polymer sample based on the data for bulk polymerization in which all double bond have been consumed at complete monomer conversion. This implicitly reveals that the composition of polymer sample from latex at different monomer conversions is the same in the above thermodynamic path design.

2.3.4.3 Pendant double bonds (PDB) conversion

Figure 2.15 is the profile of pendant double bond conversion and glass transition temperature (Tg) versus total monomer conversion. In this figure, open symbols represent Tg. Solid symbols show PDB conversion. Triangle symbols (both solid and open) are for polymerization conditions with low SDS concentration.

Regarding the PDB conversion it can be seen that under both high and low SDS concentrations, the plots are monotonous increasing functions with total monomer conversion. A sharp change in slope is observed and this may reflect a change in micro structure of polymer network.

For the system having the higher SDS level, PDB conversion levels are higher. It has been shown in section 2.3.2.1 that for emulsion polymerization at a high SDS concentration, micelle nucleation gives smaller particles with a lower monomer concentration. So that high EGDMA content might be expected in both free monomer and copolymer chains. These conditions favor a higher rate of PDB conversion.

Considering the data for pendant double bond conversion mentioned above one can understand that the crosslinking density of the these polymers would vary differently with conversion. This phenomenon is an outcome of the different characteristics in emulsion polymerization mentioned above. Smaller particles have lower monomer concentration, and when one considers an active free radical in the particle, the competition between propagation with monomer and reaction with PDB is clear, however, in this case reaction with PDB is more favorable and thus crosslinking in smaller polymer particles occurs at a higher level than that for large particles.

A second explanation might be that for the system at high SDS concentration and above the CMC polymer chains formed at earlier time have more EGDMA units. Glass transition temperature measurements for these samples further confirmed that this explanation is also possible. In the absence of micelles, copolymer chains produced in the water phase would be lean in EGDMA because of its very low water solubility

2.3.4.4 Glass transition temperature (Tg)

In the present study, glass transition temperature is defined as the on-set-point of glass transition. In **Figure 2.15,** the glass transition temperatures of those two polymer samples are shown as a function of monomer conversion. The only difference in the synthesis of these two samples is the SDS concentration used in the polymerization process. This figure shows that SDS concentration in the emulsion polymerization does have an effect on the polymer Tg. It is clear that samples prepared at higher SDS concentration have a higher Tg than those prepared at low SDS level. For samples prepared at higher SDS concentration, initially Tg is closer to that of a pure EGDMA polymer[31] then decreases with conversion.

For samples prepared at low SDS, at low conversion, Tg has values typical of polymers prepared by bulk polymerization with 0% and 25% EGDMA in the monomer feed[31.] Then it increases a little with conversion. The difference of Tg between these two samples narrows with conversion as chains with higher MMA levels are produced later in the polymerization when synthesized above the CMC.

As mentioned in section 2.3.1.3, when SDS concentration is above its CMC, the solubilization of micelles will have a significant effect on the availability of EGDMA monomer for polymerization. Polymers formed in the early stage of polymerization will have more EGDMA monomer units and higher crosslinking density. They also have higher double bond conversion and a higher glass transition temperature.

When SDS concentration is below the CMC, there are no micelles in the polymerization system. The homogeneous particle nucleation process makes larger particles. Chains precipitating out of the water phase to form particles are much richer in MMA. The larger particles are simply agglomerates of primary particles and hence EGDMA levels in the chains are smaller giving lower crosslinking levels and Tg values.

2.3.4.5 Evidence of internal heterogeneity in polymer particles

Recalling the result in section 2.3.1.1 that under high SDS concentration, the polymerization rate with 25% EGDMA is lower than that with 10% EGDMA and effect of initiator concentration on the swellability of polymer particles in section 2.3.3.1, attention was directed to the micro-internal heterogeneity of polymer particles. This directly reflects the crosslinking effect on micro-environment in polymerization. In the present study, DSC was used to study this phenomenon.

Figure 2.16 shows the DSC spectra for polymers produced at the higher SDS concentration (10×10^{-3} mol/liter-H_2O), 10%wt EGDMA in monomer feed and KPS (4.4×10^{-3} mol/liter-H_2O). One can see that the polymer formed in the early stage shows two reaction peaks overlapping in the DSC spectra. That suggests that the polymer formed in the early stage of polymerization experiences micro-phase separation. This phase separation effect gradually reduces in intensity. These measurements reveal that the internal structure changes with conversion and reveal the shielding effect on trapped pendant double bonds might also change in intensity with conversion.

Figure 2.17 shows the DSC spectra for polymers produced at SDS concentration (10×10^{-3} mol/liter-H_2O), 25%wt EGDMA in monomer feed and KPS (2.2×10^{-3} mol/liter-H_2O). Phase separation occurs again. At the higher EGDMA level, micro-phase-separation situation showed more intensity and lasted longer. The effect of crosslinking on monomer swelling is more pronounced, PDB conversion slows and free radical trapping and diffusion control of propagation become distinct possibilities. This phase separation effect gradually decays with total monomer conversion as the system approaches the glassy state.

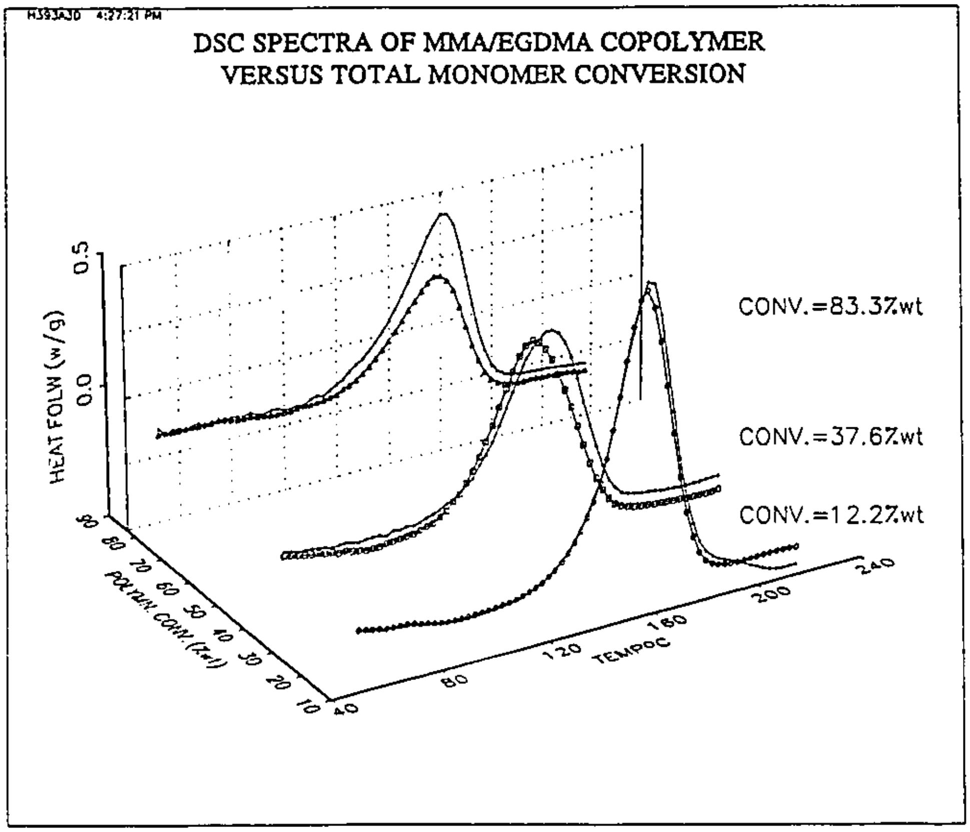

Figure 2.11 **3-D** Experimental results of DSC spectra for MMA/EGDMA copolymer recovered from the latex. Polymerization conditions: EGDMA: 10%wt, KPS 2.2×10^{-3} mol/liter-H_2O, SDS: 3.47×10^{-3} mol/liter-H_2O, T=50°C.

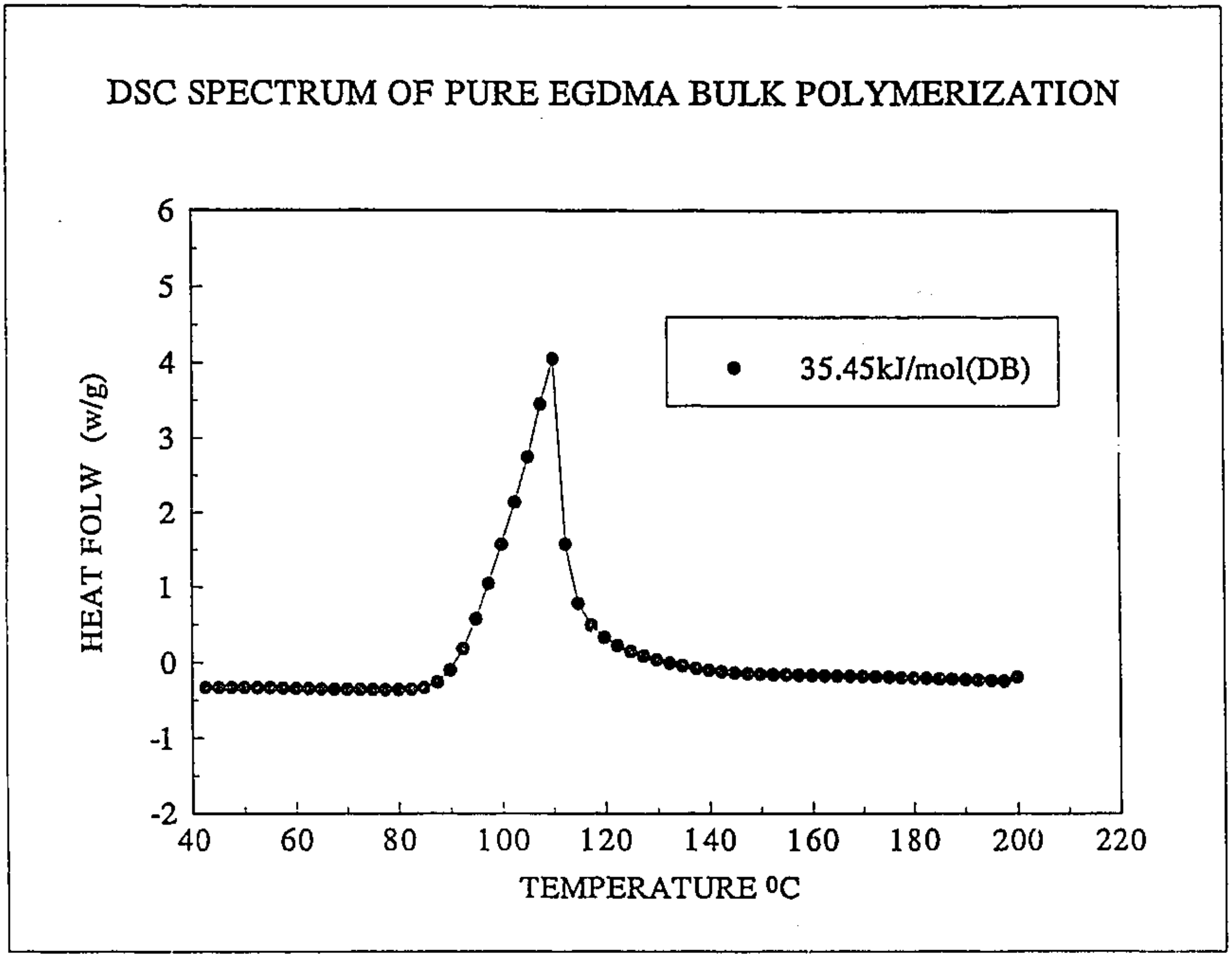

Figure 2.12 DSC spectrum for pure EGDMA in bulk polymerization. AIBN: 0.353%wt.

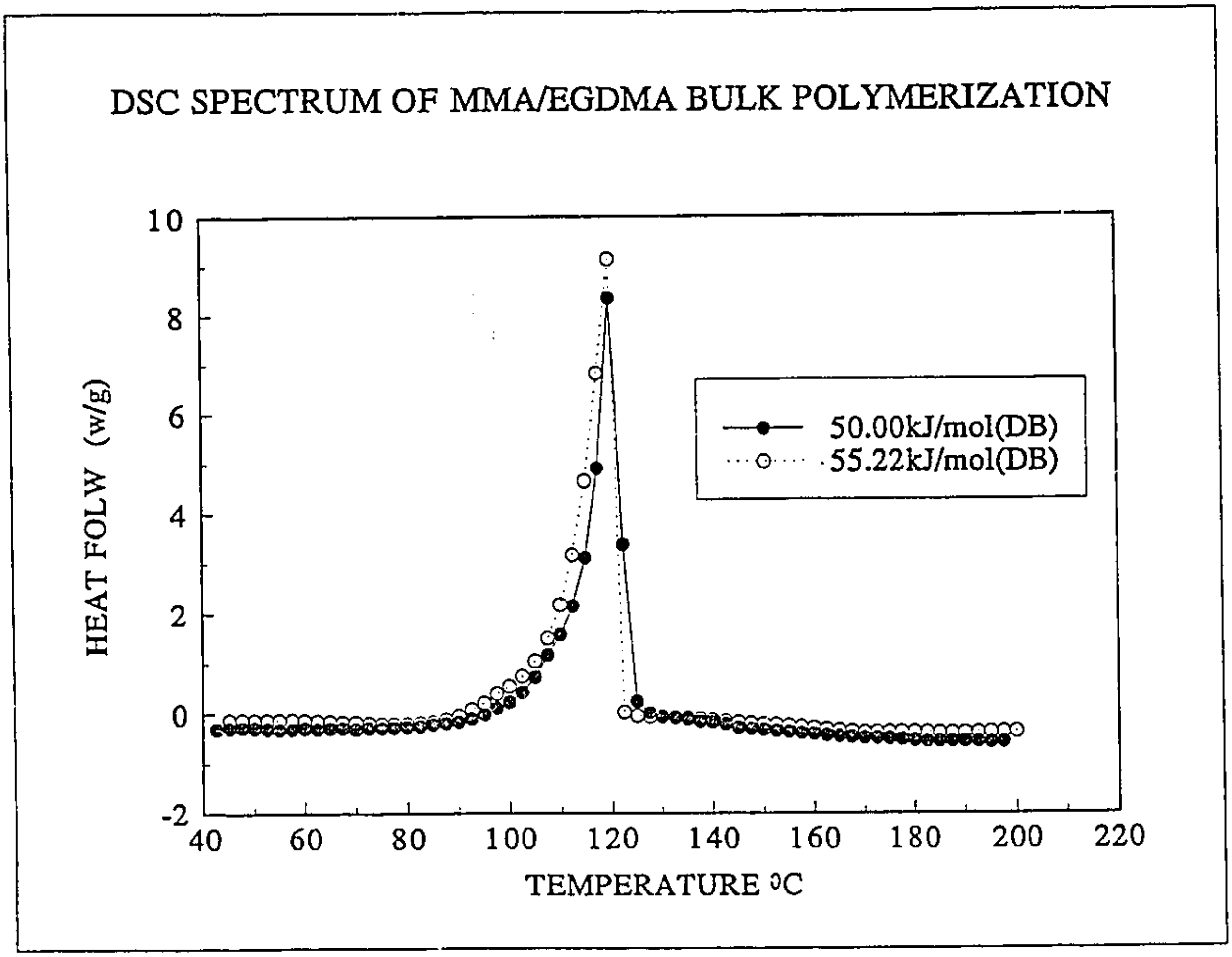

Figure 2.13 DSC spectra for MMA/EGDMA bulk polymerization. EGDMA: 10%wt, AIBN: 0.653%wt.

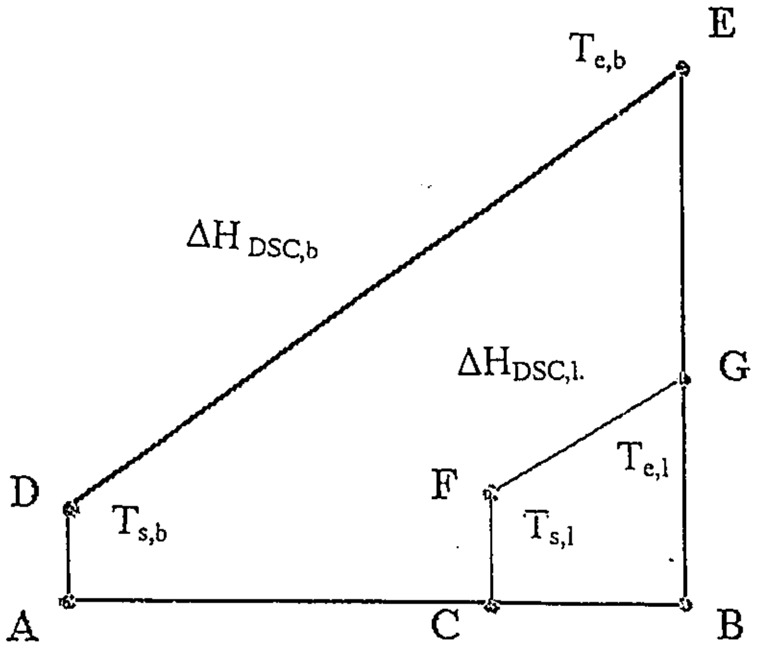

Figure 2.14 Schematic drawing of thermodynamic path for converting DSC data to residual double bond content in MMA/EGDMA copolymer recovered from the latex. Each point represents one thermodynamic state at constant pressure.

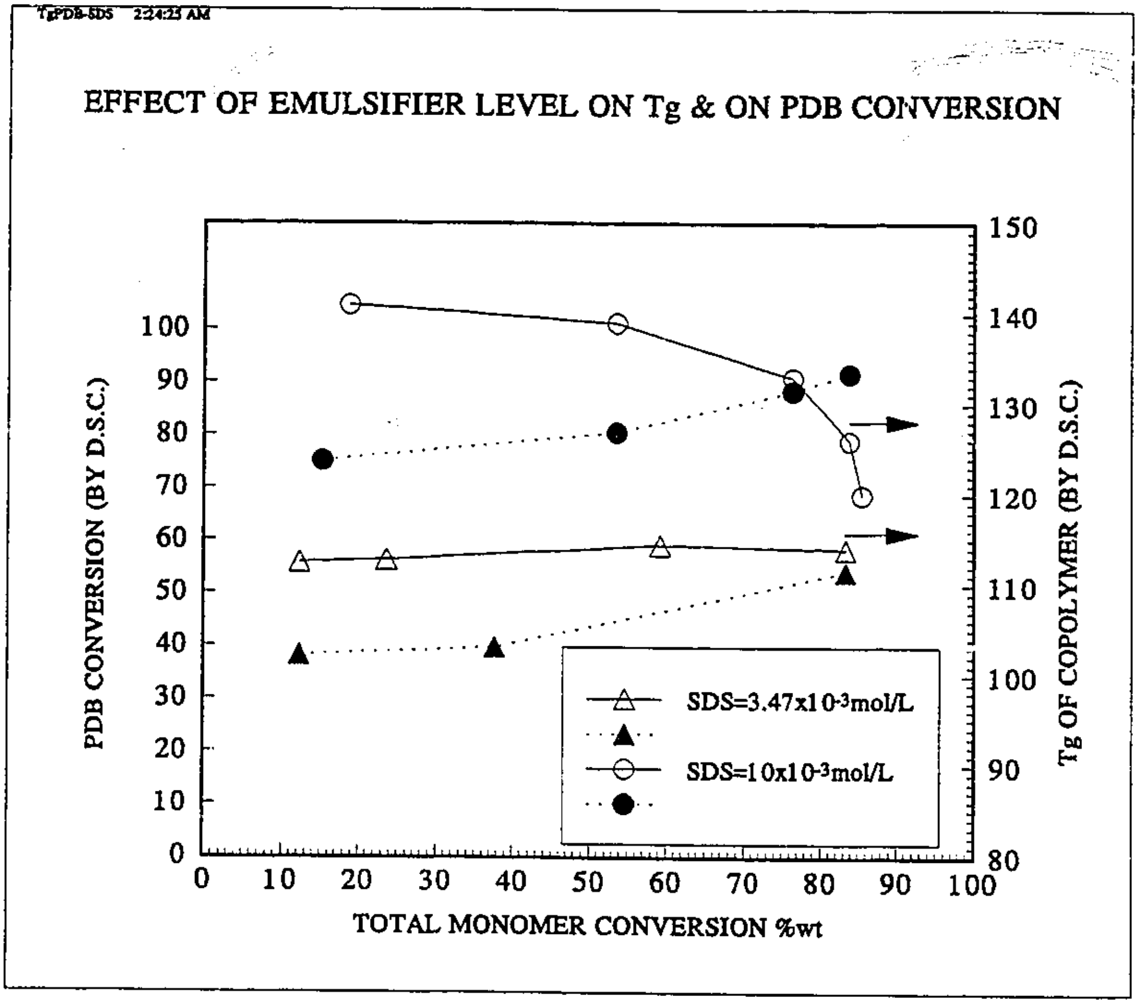

Figure 2.15 Effect of SDS concentration on residual double bond content and glass transition temperature in MMA/EGDMA copolymer recovered from the latex. Polymerization conditions: EGDMA: 10%wt, KPS 2.2×10^{-3} mol/liter-H_2O, T=50°C (Tg ≡ open symbols, PDB ≡ solid symbols).

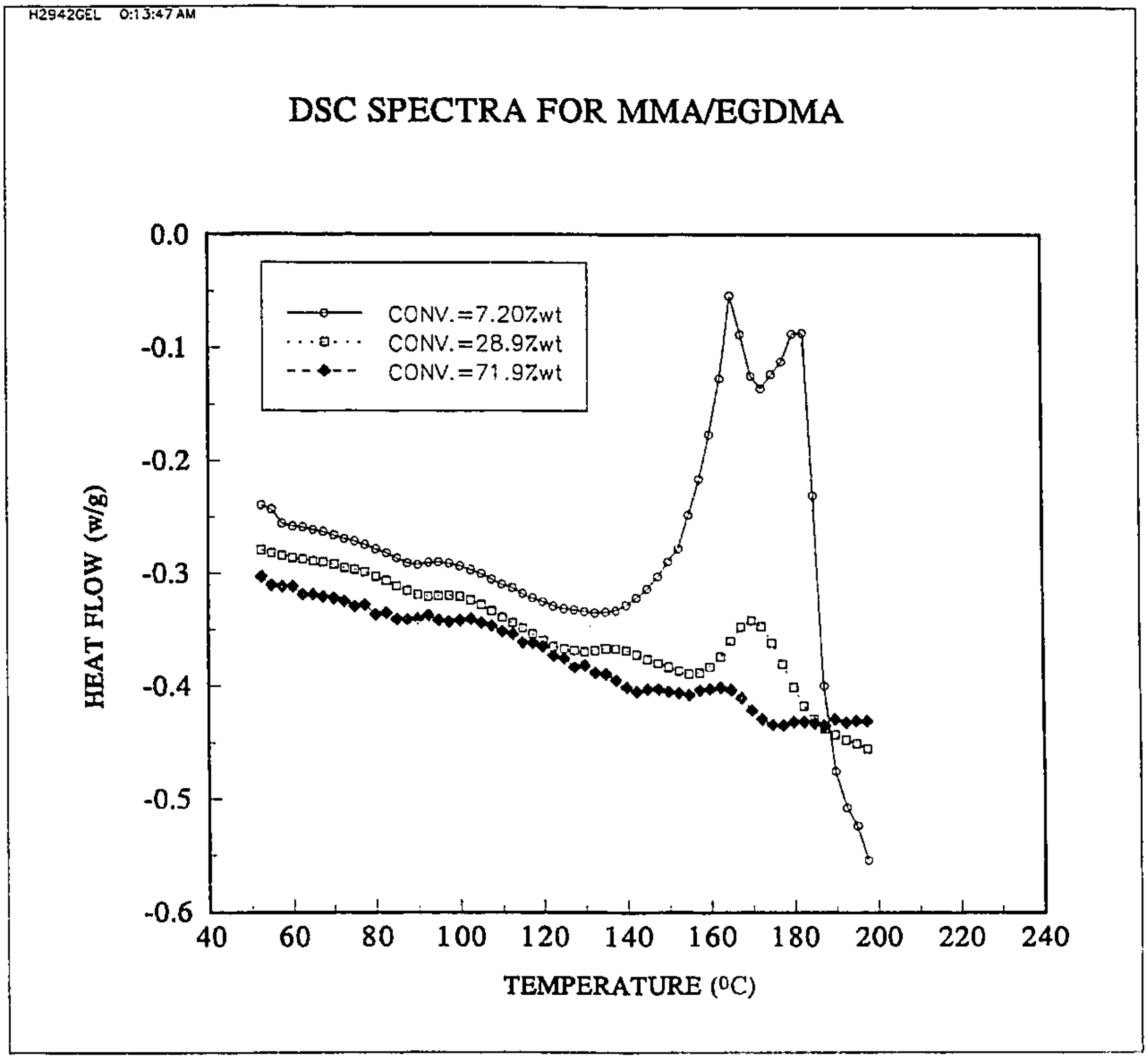

Figure 2.16 DSC spectra showing internal phase heterogeneity in MMA/EGDMA copolymer recovered from the latex. Polymerization conditions: EGDMA: 10%wt, KPS: 4.4×10^{-3} mol/liter-H_2O, SDS: 10×10^{-3} mol/liter-H_2O, T=50°C.

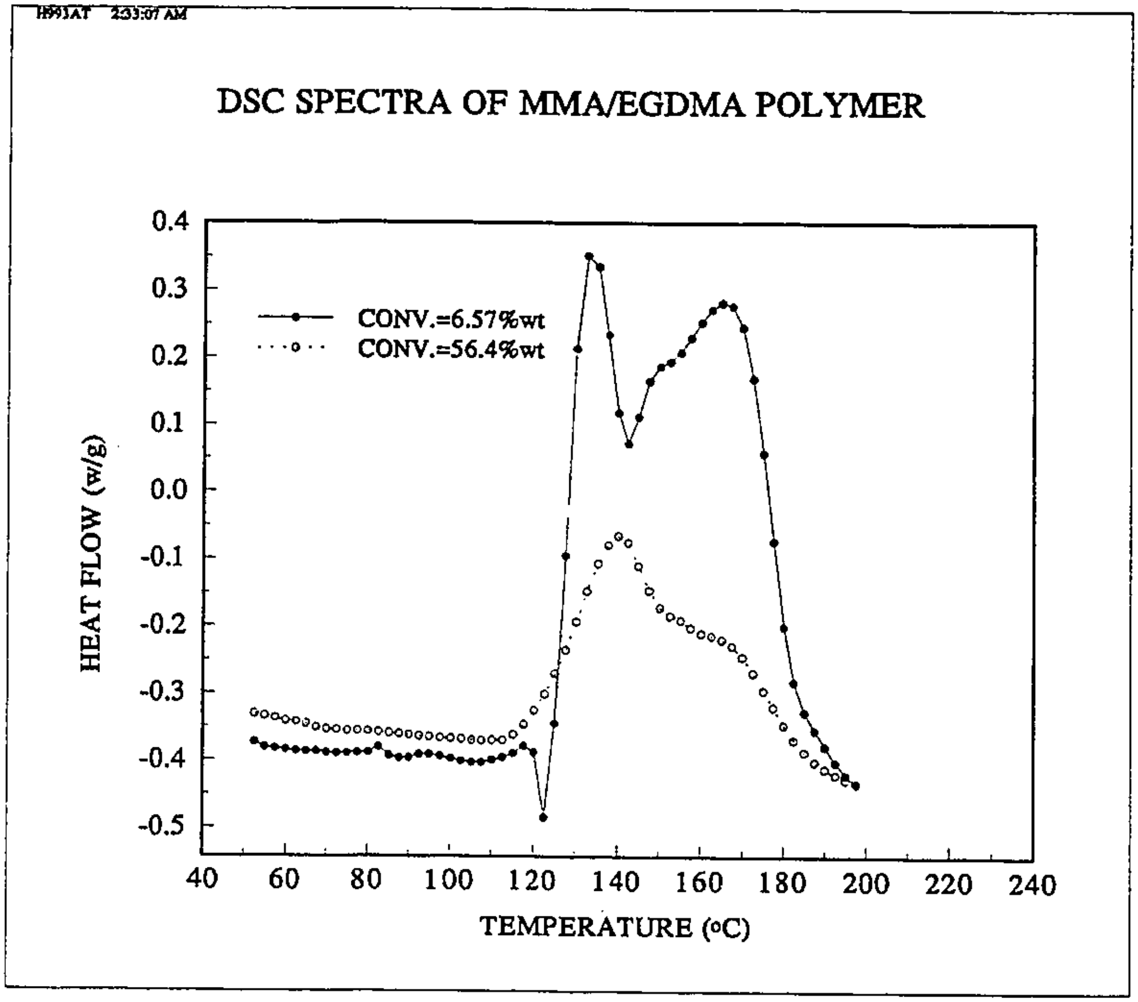

Figure 2.17 DSC spectra showing internal phase heterogeneity in MMA/EGDMA copolymer covered from latex. Polymerization conditions: EGDMA: 25%wt, KPS: 2.2x10^{-3} mol/liter-H_2O, SDS: 10x10^{-3} mol/liter-H_2O, T=50°C

2.4 Summary

In this chapter, the results of a comprehensive experimental study are reported. Polymerization conversion and rate, polymer particle nucleation and polymer particle number and size development, the swellability of crosslinked polymer particles, pendant double bond (PDB) conversion, increase in the glass transition temperature (Tg) and the development of internal heterogeneity in polymer particles were observed.

Micellar and homogeneous nucleations processes were studied. In the micellar nucleation domain case, solubilization by micelles caused a fast initial polymerization rate, a higher polymer particle concentration and a smaller polymer particle size with higher initial PDB conversion and Tg.

When polymerization was carried out at higher emulsifier concentration (above the CMC), EGDMA level in the monomer feed caused a very obvious crosslinking effect on the kinetics of emulsion polymerization. The polymerization rate increased with increase in EGDMA content to about 10%wt. However, the polymerization rate at 25%wt EGDMA level was lower than that at 10%wt. This is a result of two opposing effects, the lower monomer concentration and the smaller polymer particles, the negative effect, and the higher free radical concentration in the polymer particles, the positive effect.

Internal heterogeneity was detected by DSC in polymer particles prepared at higher initiator concentration and higher EGDMA monomer levels. This complex micro-environment for polymerization suggests that the shielding effect of pendant double bonds in the polymer particles is a most complex phenomenon which is likely most difficult to model.

2.5 References

1. Batch, G. L. and Macosko, C. W. *J. Appl. Polym. Sci.* 1992, **44**, 1711

2. Okay, O. and Gürün, C. *J. Appl. Polym. Sci.* 1992, **46**, 401, 421

3. Fink, J. K. et al *J. Polym. Sci., Part A: Polym. Chem.* 1990, **18**, 195

4. Chern, C. S. *Polym.-Plast. Tech. Eng.* 1990, **29**, 577

5. Mikos, A. G. and Peppas, N. A. *Macromolecules* 1986, **19**, 2174

6. Li, W-H., Hamielec, A. E. and Crowe, C. M. *Polymer* 1989, **30**, 1513, 1518

7. Zhu, S. *"Advances in Free Radical Polymerization Kinetics"*, Ph.D. Thesis, McMaster University, Canada,(1990)

8. Zou, D., Derlich, V., Gandhi, K., Park, M., Sun, L., Kriz, D., Lee, Y. D., Kim, G., Aklonis, J. J. and Salovey, R. *J. Polym. Sci., Polym. Chem.* 1990, **28,** 1909

9. Zou, D., Ma, S., Guan, R., Park, M., Sun, L., Aklonis, J. J. and Salovey, R. *J. Polym. Sci., Polym. Chem.* 1992, **30,** 137, 2443

10. Ding, Z. Y., Aklonis, J. J. and Salovey, R. *J. Polym. Sci., Polym. Phys.* 1991, **29,** 1035

11. Ding, Z. Y., Ma, S., Kriz, D., Aklonis, J. J. and Salovey, R. *J. Polym. Sci., Polym. Phys.* 1992, **30**, 1189

12. Capek, I., Kostrubovà,J. and BartoñJ *Makromol. Chem., Macromol. Symp.* 1990, **31**, 213

13. Capek, I. and Potisk, P. *Polymer J. (Japan)* 1992, **24**, 1037

14. Capek, I. *Makromol. Chem.* 1992, **193,** 1423

15. Landin, D. T. and Macosko, C. W., *Macromolecules* 1988, **21**, 846

16. Nomura, M. and Fujita, K in "*Internal. Symp. on Polym. Microsphere, Fukui, Japan, 1990*"

17. Mallamace, F., Micali, N., Vasi, C., Bansil, R., Pajevic, S. and Sciortino, F. *Progr. Colloid Polym. Sci.* 1992, **88**, 77

18. Sheu, H. R., El-Aasser, M. S. and Vanderhoff, J. W. *Polym. Mater. Sci. Eng.* 1988, **59**, 1185

19. Sheu, H. R., El-Aasser, M. S. and Vanderhoff, J. W. *J. Polym. Sci., Polym. Chem.* 1990, **28**, 629, 653

20. Matsumoto, A., Yonezawa, S and Oisa, M. *Eur. Polym. J.* 1988, **24**, 703

21. Matsumoto, A., Matsuo, H. and Oisa, M. *J. Polym. Sci., Polym. Letter* 1988, **26**, 287

22. Matsumoto, A., Matsuo, H., Ando, H. and Oisa, M. *Eur. Polym. J.* 1989, **25**, 237

23. Tobita, H., Kimura, K., Fujita, K. and Nomura, M. *Polymer* 1993, **34,** 2569

24. Moran, M. B. *Polym. Pre. print,* 1983, **24,** 141

25. Pavel, K., *J. Polym. Sci., Polym. Phys.*, 1981, **19**, 1675

26. Watter, B., *Makromol. Chem.*, 1980, **181**, 869

27. Shevelve, V. A., *Polym. Sci. USSR.*, 1986, **28**, 27

28. Price, C. A., *J. Applied Polym. Sci.*, 1986, **32**, 5337

29. Allen, P. E. M., *Eur. Polym. J.*, 1986, **22**, 549, 1989, **25**, 785

30. Stöver, H.D.H. and Fréchet, J. M. J. *Macromolecules*, 1991, **24**, 883

31. Li, D., Zhu, S. and Hamielec, A. E. *Polymer,* 1993, **34**, 1383

32 Binana-Limbele, W. and Zana, R. *Colloids Surfaces* 1986, **21**, 483

CHAPTER 3

ELECTRON SPIN RESONANCE (ESR) MEASUREMENT OF FREE RADICAL CONCENTRATION IN CROSSLINKED POLYMER PARTICLES

3.1 Introduction

Information on radical concentration development during polymerization is most useful for any kinetic study on free radical polymerization including emulsion polymerization. In a typical oil-in-water emulsion polymerization process, the thermal decomposition of the initiator (e.g. KPS) generates primary radicals (e.g. sulfate radical anions) in the water phase which propagate in the water phase to give oligomeric radicals that then transfer from the water phase across the phase boundary into the polymer particle phase wherein the polymerization occurs at a rapid rate. It is an important mass transfer process which occurs in emulsion polymerization. In emulsion polymerization with crosslinking the kinetic characteristics of these radicals in the polymer phase are responsible for the unusual kinetic behavior of the system as a whole.

3.1.1 Preparation of crosslinked polymer particles

Polymer chains may occur in many different forms. A simple way to group them is according to their general structure. Four categories might exist: (1) linear macromolecules, (2) macromolecules with long and/or short branches, (3) microgels and (4) macroscopic networks [1].

Microgels are crosslinked polymer in a small polymer particle. The molecular weight of crosslinked polymer is limited by the size of the particle. They intermediate between branched and macroscopically crosslinked system [1]. The overall dimensions of microgels are comparable with high molecular weight linear polymers (around 10^6 g/mol). However, their internal structure resembles a typical network. Microgels can dissolve or swell in suitable solvents with a finite limit depending on the crosslinking degree of their 'sponge-like' structure. Therefore, the definition has been extended from the "sub-microscopic particles in the size range 1-100 nm" [2] to "colloidal dispersions of crosslinked polymer particles" [1].

Funke *et al* [2-4] have published on the preparation and characterization of "reactive microgels" formed in emulsion polymerization of DVB. Not all carbon-carbon double bonds of multi-functional monomers can participate in network formation for steric reasons. Residual reactive groups (e.g. pendant double bonds and trapped polymeric radicals) are available at their surface and interior for further reaction [3].

Unlike the usual emulsion polymerization, the preparation of these microgel particles requires that monomer droplets not be present in the system. Thus, the microgel particles have a higher concentration and smaller size than that of particles formed via micellar nucleation. For DVB monomer, the number of microgel particles is about 6 ~ 9 times higher than that for a standard styrene emulsion polymerization [3].

They also found that the ratio of vinyl/divinyl monomer played a very important part in emulsion polymerization [2]. Low crosslinker levels produce macrogel and very high crosslinker levels will produce both microgel and agglomerates. The pendant double bond on the surface of the microgel can be changed to other functional groups such as carboxyl, hydroxyl, sulphate, amino or halogen. They might also further react with various monomers to get network structures of desired heterogeneity.

Since the early 1980's, poly N-isopropyl acrylamide (Poly(NIPAM)) has become a very active subject in the research on hydrogel microspheres (microgel). The reason is that, for poly(NIPAM), there exists a lower critical solution temperature (LCST) in water (approx. 32^0C). Below this LCST, this micorgel is water-swollen and the surface is sufficiently hydrophilic. Above this temperature, the microgel shrinks and the surface becomes hydrophobic.

In this research area, the important research done by Pelton *et al* [5-8] following up on the pioneering work of Guillet [9] should be noted. In a recently published book "Colloidal Polymer Particles" [10], the work of Pelton and co-workers is reviewed.

3.1.2 Free radicals in emulsion polymerization

Emulsion polymerization is a most effective method for the preparation of crosslinked colloidal polymer particles. The process of the initiation itself is not a simple one. It is normally accepted that the primary initiator radicals such as the sulfate radical anions, because of their negative charge, are unlikely to transfer into polymer particles which have hydrophobic interiors and negatively charged surfaces.

Priest [11] first suggested the concept that the addition of several monomer units to a primary radical would be required before the transfer becomes possible. The accumulation of the hydrophobic part in the primary radical by propagation with monomer will increase the disperse force between polymer particles and an oligomeric radical then can overcome the electrostatic repulsion force between them. It was suggested that the rate-determining step for radical entry is the water phase propagation to the appropriate critical size.

The role of aqueous-phase kinetics in emulsion polymerization was investigated by Gilbert *et al* [12-13] systematically. The entry of free radical into latex particle in emulsion polymerization was modeled and fitted to their seeded styrene polymerization data. Considering the "diffusion capture", the "surfactant displacement" and the "colloidal entry" assumptions, the "aqueous-phase propagation to a critical chain length of polymerization" was claimed to be the rate-determining step for the radical entry. The capture or irreversible absorption of the resulting oligomeric free radical by a particle is essentially instantaneous. This critical chain length was suggested to be about 2-5 monomer units based on their styrene emulsion polymerization data.

This explanation was supported by the accelerating effect of the use of the intermediate molecular weight chain transfer agent (e.g. $C_{12}H_{25}SH$) on emulsion polymerization rate [14]. The transfer radical which rapidly forms can readily enter the polymer particle and promote polymerization.

The fate of a free radical once it enters a polymer particle plays a key role in the kinetics. Once entry of an initiating radical into a polymer particle has been achieved, polymerization proceeds. Thus, the latex particles are generated in a state swollen by the monomers that are continually replenished by fresh monomer molecules from the monomer droplets until these droplets disappear at the end of stage II and the beginning of stage III.

Other kinetic opportunities for this radical also exist that include desorption from the polymer particle, transfer to monomer molecules, transfer to chain transfer agent molecules, transfer to some repeat units on polymer chains, propagation with terminal and/or pendant double bonds and radical/radical termination.

Termination is a complicated process, particularly with the presence of crosslinked chains. Based on the diffusion controlled mechanism in dilute solution, two radical coils meet each other by translation diffusion. With latex particles polymer concentrations are high and polymer self diffusion with many chain entanglement points is operative. Radicals on polymer network can move only by propagation.

Under these circumstances, instantaneous termination will not be valid and many radicals per particle will be the result. Some free radical centers will become so occluded within dead polymer chains entangled together that these radical centers would be isolated from the radical/radical termination. Under these conditions, it has been suggested that radical centers may only wander and terminate by "residual termination" or "propagation diffusion". At high levels of crosslinking, this slow termination process will cause radical content to increase and sometimes dramatically.

ESR provides one with the opportunity to follow these changes in radical concentration and perhaps this knowledge may permit one to follow environmental changes in the polymer particles during emulsion polymerization.

3.1.3 ESR application in free radical polymerization

The advent of modern electron spin resonance (ESR) has provided a powerful direct method for measurement of radical type and concentration. For bulk polymerization, Bresler *et al*[15] used ESR to study the homogeneous polymerization of MMA and vinyl acetate and, to some extent, solved the problems of how to detect rapid changes in free radical concentration during the pre- and post- gel-effect periods.

In the late 1980's, the application of ESR techniques has been improved to cover a broad range of studies of bulk polymerization kinetics. Kamachi *et al*[16, 17] reported the results on ESR observation of propagating radicals of vinyl acetate in stationary state and of conformation of propagating radicals of triphenymethyl methacrylate. Shen *et al*[18] used ESR to study the propagation rate constant and radical concentration for bulk polymerization of MMA.

Most recently, a comprehensive study using in-situ ESR technology for bulk polymerization has been done by Zhu *et al*[19]. The radical trapping and termination in free radical polymerization of MMA, the radical concentration in free radical copolymerization of MMA/EGDMA, the termination of trapped radicals at elevated temperatures during copolymerization of MMA/EGDMA and the conformation, environment and reactivity of radicals in copolymerization of MMA/EGDMA have been covered. The importance of this investigation is that the corresponding conversion measurements have been coupled so that a deep understanding of the mechanism and a better estimation of kinetic parameters involved have been achieved.

3.1.4 ESR application in emulsion polymerization

Although free radical byproducts detected by ESR in emulsion polymerization has been previously reported in 1970 [20], the propagating radicals apparently have not been directly observed until the late 1980's. The failure of direct application of ESR to the emulsion polymerization process presumably results from the low radical concentrations in normal oil-in-water systems and from the heterogeneous nature of them. The other point that should be mentioned is that the dielectric constant of water at polymerization temperature is unfavorable, however, at liquid nitrogen temperature this is favorable.

The direct observation of propagating free radical ESR spectra is useful in understanding the polymerization process. The quantitative measurement coupled with concomitant measurement of polymerization rate enables the deduction of mechanism and kinetic rate constants.

The advent of commercial ESR spectrometers with enhanced sensitivity, field stability and computerized data collecting and processing makes possible the acquisition of accumulated multi-scan data. That opens the possibility of detecting free radicals in the emulsion polymerization system.

For emulsion polymerization without crosslinking, Smith-Eward case II kinetics may apply. That is, the average number radical per polymer particle ($\bar{n} = 0.5$). It could be calculated that under this condition, the total free radical concentration [R*] is 10^{-9} and 10^{-8} (mol/liter) for total particle concentration (Np) of 10^{15} and 10^{16} (particle / liter) separately.

For a typical ESR spectrometer, the detection limit is about 10^{-7} (mol/liter). So that it should be possible to measure the presence of polymeric radicals, providing there are about 10^{17} (particle/liter). For these systems, much higher radical concentrations would be expected during the course of polymerization, particularly during the period of auto-acceleration in rate.

The heterogeneous nature of an emulsion polymerization renders difficult the direct application of in situ ESR technology (rapid flow technology). The presence of liquid water always places a severe restriction on the ESR sample size, because its dielectric properties tend to reduce the quality factor of ESR cavity and therefore to weak ESR. signal intensity to a practicably inappropriate low value. This makes it difficult to directly measure radicals by doing emulsion polymerization in the cavity of ESR.

Similar to the application of ESR to bulk polymerization, spectra are most readily obtained in the emulsion polymerization system by sample removal. The influence of liquid water on the intensity of the ESR. signal can be overcome by using the freeze-quench technique before ESR measurement. Freezing permits a much larger sample size to be placed in the ESR cavity because solid ice has a significantly lower dielectric constant than liquid water that is the major constituent in most emulsion polymerizations (around 50%wt to 90%wt). The ESR. signal/noise ratio is inadequate to give reliable measurements at radical concentration levels of 10^{-8} mole/liter or smaller.

There are only a few publications on the use of ESR. to measure radical concentration in emulsion polymerization [21-26]. All these publications covered the emulsion polymerization in batch and semi continuous process. For monomer system, MMA, styrene homogeneous polymerization and 8 butyl acrylate(BA)/91 MMA/1 methacrylic acid(MAA),%wt copolymerization were covered. In all these recent publications, crosslinking in emulsion polymerization was not done.

Napper *et al* [21,22] were the first to measure radical concentrations during styrene emulsion polymerization. They first confirmed the validity of 'sample removal followed by quenching' method in the application of ESR technology. Their experimental results showed that in a typical emulsion polymerization system such as styrene emulsion polymerization at 50°C with emulsifier concentration above its CMC, the kinetic relaxation time of the free radical concentration was around 1000 second. This should permit one to sample and to freeze the latex sample without significantly changing the free radical concentration.

Lau *et al* [24,25] did a semi-continuous copolymerization of 8 (BA)/91 MMA/1 MAA %wt system at four temperatures between 50 and 65 °C. A redox initiator and two very different particle diameters were chosen in their experiments. To determine the steady-state radical concentrations, latex samples were taken out from the reactor under a nitrogen atmosphere. In order to test the validity of their sampling method, the time delay required to transfer the sample from the reactor to a freezing bath was changed from about 15 seconds (their standard sample method) to 60 seconds. No significant change in ESR signal intensity was found in agreement with Napper *et al*[21].

As mentioned above, to date, there are no publications on the application of ESR method for emulsion polymerization with crosslinking. In this chapter, the direct measurement of the propagating free radicals in MMA/EGDMA emulsion polymerization coupled with the monomer conversion is reported. Based on these data, polymerization mechanism and kinetic analysis is discussed. Free radical trapping in the crosslinked glassy reactive polymer particles, and effect of oxygen on radical concentration decay in the polymer latex are also discussed.

3.2 Experimental

In the present experiments, the polymeric radical concentrations during emulsion polymerization were measured by a Bruker ER100D ESR spectrometer equipped with a TE 110 cavity. The spectrometer was connected to an IBM PC with "EPRware" software.

The polymer latex was sampled at preset different polymerization conversions through a specially designed closed-loop vacuum sampling line. These samples were instantaneously quenched by liquid N_2 in a 3 mm O.D. ESR tube when the latex flowed into it. Thus polymerization was stopped immediately and free radicals in the samples were frozen at the same time. The sample latex was then sealed ready for testing. In the experiments, the sampling process was done in less than 10 seconds.

The ESR signal was set up auto-collecting by a computer. In order to increase the signal/noise ratio, the ESR signal was accumulated for 1000 sec and then double integrated to get the improved total signal intensity. With the solution of 2,2-Diphenyl-2-Picryhydrazyl, hydrate (DPPH) in MMA for signal calibration, the absolute polymeric radical concentration was obtained. The ESR measurement conditions are listed in Table 3.1.

Table 3.1. ESR Measurement Conditions

Parameter	Quantity	Units
Temperature	150, 170	K
Microwave power	20	dB
Microwave frequency	9.46	Ghz
Modulation intensity	4.0	Gpp
Modulation frequency	100	KHz
Modulation Gain	1×10^6	
Scan center	3380	G
Scan time	1000	s
Scan size	1	K
Scan width	300	G

3.3 Results and Discussion

In this section are reported the results of measurement accuracy involved in the ESR testing, time profiles of free radical concentrations in the emulsion polymerization of MMA/EGDMA, kinetic analysis of polymerization mechanism elucidated using ESR data, free radical trapping in polymer latex particles and glassy reactive polymer particles having potential applications.

3.3.1 Measurement accuracy

The most important factor in ESR measurement is the signal intensity. The measurement should be done at the lowest possible temperature, and the signal should be accumulated for a sufficiently long time to get the appropriate signal/noise ratio.

Effect of the "modulation gain" of instrument

At first, measurement accuracy of the instrument used was investigated. To increase the instrument sensitivity it was necessary to increase the "modulation gain". Theoretically, different modulation gain would give different signal intensity (integral area). The ratio of these two signal intensities should equal the ratio of two modulation gains used in the measurement. As a consequence, the converted measurement result should be the same.

The problem is that the higher the modulation gain is, the more serious will be the inadequacy of signal/noise ratio. The integrated area might have a significantly increased uncertainty error. The "modulation gain" used in the present experiment is in between (0.8 - 1.0)x10^6.

Figure 3.1 shows the results for a latex sample measured at two modulation gains. This latex was sampled during an emulsion polymerization, 50 min after the initiator solution was injected into the reactor. The recipe contained 10%wt EGDMA in monomer feed, 10x10^{-3} mol/liter-H_2O SDS and 8.76x10^{-3} mol/liter-H_2O KPS. One can see that:

$$\text{Ratio of Gain} = \frac{1x10^6}{8x10^5} = 1.25$$

And the ratio of integrated area is

$$\frac{Area_{Gain=1x10^6}}{Area_{Gain=8x10^5}} = \frac{1.632}{1.357} = 1.203$$

the relative error based on the ratio of gain is 3.76%.

To convert integrated signal intensity area to radical concentration, solution of 2,2-Diphenyl-2-Picryhydrazyl, hydrate (DPPH) in MMA was used for signal calibration. **Figure 3.2** shows the spectra measured at a temperature of 150 K with the same microwave and scan parameters but at different gains. DPPH gives a strong signal, so that based on instrument adjustments mentioned above, low field modulation gain was set. The ratio of instrument gains is 1.6 and the integrated signal intensities is given by:

$$\frac{Area_{Gain=1.6x10^5}}{Area_{Gain=1.0x10^5}} = \frac{1.406*10^7}{0.8782*10^7} = 1.60$$

Effect of cavity temperature of ESR instrument

The influence of ESR cavity temperature during the measurement is another factor one should consider. **Figure 3.3** shows the results for the same sample mentioned above (sampled at 50 min reaction time) that was measured at 150 K and 170 K respectively. It can be seen that the spectra have the same line structure but the signal intensities are different. The lower the measurement temperature is, the higher is the signal intensity. The integrated signal area at 150 K is 1.357x10^7 and that at 170 K is 1.026x10^7. The relative error of these two measurements based on the data at 150 K or the improvement of sensitivity is:

$$\left(\frac{AREA_{150K} - AREA_{170K}}{AREA_{150K}}\right) \times 100$$

that is :

$$\left(\frac{(1.357 - 1.026) * 10^7}{1.357 * 10^7}\right) \times 100 = 24.4\%$$

Theoretically the lowest possible temperature is preferred. Recording of spectra the lowest temperature has three distinct advantages in sensitivity terms of measurement. First, the aqueous emulsion system is in the solid phase therefore the adsorption of microwaves by water is greatly reduced, allowing large samples to be investigated; secondly, there is a increase in sensitivity due to the temperature dependence of the Boltzmann factor; and finally the radical concentration is stable, therefore the ESR signal can be accumulated or be multi-scanned to increase the sensitivity.

In the present experiments, the technically lowest possible temperature that could be used was 150 K. Below this temperature, the cavity temperature could not be maintained stable during the measurement. As a consequence all real measurements were carried out at 150 K.

3.3.2 Free radical concentrations in MMA/EGDMA emulsion polymerization

Characteristics of ESR spectra

Figure 3.4 shows the ESR spectra of polymer latex sampled from the reactor at different polymerization times. Polymerization conditions were: EGDMA in monomer feed (10%wt), SDS ($10x10^{-3}$ mol/liter-H_2O) and KPS ($8.76x10^{-3}$ mol/liter-H_2O). **Figure 3.5** shows the ESR spectra change with polymerization time in a 3-D plot. It can be seen that the spectra gradually develop the characteristics of PMMA 5+4-line hyperfine structure.

In bulk polymerization of MMA/EGDMA, Zhu *et al* [19] observed an interesting ESR spectra transition from 13-line to 9-line in a 15%wt EGDMA bulk polymerization near the final conversion. It was explained that a 13-line signal structure indicated that the MMA radical radicals in the reaction mass were in a liquid environment, while a 9-line signal structure was contributed from the EGDMA radicals and/or the MMA radicals in a solid matrix.

In the above example measurement, because the sample quenching technology is always used before ESR testing, the 13-line spectrum can not be expected. But the final 9-line structure is very clear. This revealed the accumulation of trapped radicals in polymer particles and change to a more heterogeneous radical structure as the glassy state transition is approached.

The 9-line ESR spectrum of PMMA radicals in a solid-state matrix was, probably first reported by O'Donnell *et al*[27]. Napper *et al*[21] also reported that the 9-line spectrum was also found in the latex sample taken from the reactor at the final conversion range of polymerization. In the above mentioned semi-continuous emulsion polymerization of monomer feed containing 98%wt MMA, this 9-line spectrum was detected as well.

Radical concentration and total monomer conversion

Figure 3.6 shows the change of total radical concentration and total monomer conversion versus polymerization time. The numbers in brackets are the total polymer particle numbers. The measurement shows two regions. Total radical concentration is almost constant in the early stage of polymerization and then increases dramatically. No radical concentration level-off can be observed.

In the above mentioned seeded MMA emulsion polymerization experiment [21], the concentrations of PMMA propagating radicals in latex samples were measured by ESR. The radical concentration versus polymerization time curve showed a sigmoidal shape. It displayed three regions for radical concentration corresponding to the polymerization rate curve: (1) a low radical concentration value (ca. 10^{-7} mol/liter) during the stage II of polymerization (i.e., in the absence of particle nucleation wherein the growth of the seed latex particles proceeding in the presence of monomer droplets); (2) a rapid radical concentration increase during the period of accelerating region in stage III of polymerization (i.e., polymerization of monomer within the latex particles after exhaustion of monomer droplets) and a final level-off limiting radical concentration value ca. 10^{-5} mol/liter near complete conversion.

Kinetic analysis of mechanism

The two regions for radical concentration versus polymerization time is related to the two stages in total monomer conversion change and total particle number change periods that could be kinetically analyzed to deduce the polymerization mechanism.

During the rapid monomer consumption period, total particle number increases but total radical concentration is constant. It is clear that monomers are mainly consumed in this period, so that radicals produced in the water phase are primarily consumed in particle nucleation.

It can be understood that in this stage the spectra should have an EGDMA type character due to predominance of EGDMA-based radical centers. EGDMA monomer has lower water solubility than MMA. EGDMA molecules will transfer directly from monomer droplet to polymer particles. Because EGDMA monomer has a higher propagation rate constant ($k_{p22,p} \approx 2k_{p11,p}$), at this early stage the copolymer chains will be richer in EGDMA monomer units. The EGDMA-based radicals have a higher concentration than MMA-based radicals in the polymer latex.

In the second stage, total monomer conversion and particle number do not seem to change with time. However in this period, the total radical concentration continues to increase and the ESR spectra gradually evolve to that of PMMA chains. In this stage, oligomeric radicals entering particle would experience instantaneous termination due to the small size of recently nucleated polymer particles and/or they might most likely be immediately trapped by the high crosslinked network before further propagation with monomers or with PDB in particles. Based on the "critical chain length" controlled radical entry explanation, the oligomeric radicals which form in water phase basically consist of a KPS end group and a few MMA monomer units.

It is of interest to note in bulk MMA/EGDMA polymerization, Zhu *et al*[19] found that the time profile of radical concentration has four stages related to coupled conversion rate data. In stage one, radical concentration remains relatively constant for low monomer conversion in which the polymerization rate can be described by chemically controlled reaction kinetics. In the second stage, both the radical concentration and the conversion rate showed a synchronous increase. This verified the hypothesis that the rapid auto-acceleration in polymerization rate is due to a dramatic increase in radical concentration. In stage 3, the radical concentration fell slightly after reaching a peak value. This peak corresponded closely to the maximum conversion rate. Thereafter, the conversion started to fall. Finally, in stage 4, the radical concentration increased again, then leveled off while the conversion rate also leveled off.

In the present MMA/EGDMA emulsion polymerization, that 'slight drop in radical concentration' has not been observed. The reason is that the decrease in total radical concentration in bulk polymerization is attributed to the a dramatic reduction in initiator efficiency because of the cage effect. However, in emulsion polymerization, since radicals are generated from initiator decomposition in the water phase, the initiator efficiency does not change over the entire conversion range.

3.3.3 Free radical trapping and glassy reactive polymer particles

To verify the assumption that the ESR signal is for the trapped radicals in the polymer particles rather than oligomeric radicals frozen in the water phase, the decay in radical concentration in the network was measured.

At the end of the polymerization (polymerization was stopped at time=70 min.), the reactor temperature was reduced below the polymerization temperature (to about ambient temperature). The reactor was then opened to the atmosphere. Five days later, latex was sampled and measured again under the same conditions as before. The ratio of signal intensities of these two spectra is:

$$\frac{Area_{Time=70\,\mathrm{min}}}{Area_{Five\ days}} = \frac{1.96*10^{7}}{2.0*10^{7}} = 0.98 \approx 1$$

The intensity of these two spectra is almost unchanged within the tolerance measurement error range. This means that the radicals trapped in the polymer were not consumed. If the radicals measured at the end of emulsion polymerization (time=70 min) do include those in the water phase, after five days in the presence of oxygen, it is certain that water-phase radicals would have reacted with oxygen.

At ambient temperature, the polymer particles are in the glassy state. According to the result of ESR study on permeation of oxygen in crosslinked polymers[28] at 110°C the permeability of oxygen (DH) is around 10^{-16} (cm^3*cm/cm^2*s*Pa) in a MMA/EGDMA polymer network. The activation energy of permeation for oxygen in temperatures below Tg is 7.3 kJ/mol. The following estimation could be made:

$$Ln\left(\frac{DH_{110^0C}}{DH_{25^0C}}\right) \approx \frac{7300}{8.314}\left[\frac{373-298}{373*298}\right] = 0.59$$

The permeability of oxygen at room temperature (DH_{25^0C}) is around $5x10^{-17}$ (cm^3*cm/cm^2*s*Pa). Assuming a polymer particle with 0.1 μm in diameter, under $1x10^5$ Pa pure oxygen atmosphere condition [28], a characteristic diffusion time (t_{oxy}) could be estimated with the following calculation:

$$t_{oxy} \approx \frac{\left(0.1x10^{-4}\right)^2}{5x10^{-17}} = 2x10^6(\sec) \approx 556(hour) \approx 23.2(day)$$

It could be understood that at room temperature and 1×10^5 Pa pure oxygen atmosphere condition, over a 5 days period, the diffusion of oxygen into polymer particles with a crosslinked network could be around $(5/23.2) \approx 21.5\%$. However, considering the oxygen content in the normal atmosphere (c.a. 21%) this effect would be neglected.

Also the diffusion of trapped (not chemically bonded) radicals from the polymer particles into water phase can also be neglected. It is clear that radicals in polymer particles will not be consumed during this 5 days delay. The signal measured after five days does represent that of trapped radicals at the end of polymerization.

The major structure of the spectrum was found unchanged over 5 days. However, the center line structure has changed somewhat. The reason might be that due to the long relaxation time of the network after polymerization, the micro environment of trapped radicals has changed.

Napper *et al* [21] also confirmed that in seeded MMA emulsion polymerization, radicals measured by ESR are trapped in the latex particles and not in the aqueous phase. At the end of stage III of polymerization, a sample was removed from the reactor, placed in to a 1.0mm internal diameter ESR tube without freezing. Then ESR testing was carried out at 323 K. The spectrum obtained was unchanged from that recorded at 100 K. After storing at 25 ^{0}C for 16 hours, ESR testing was done again, and no change in shape and signal area was found. Therefore, the radicals are in a solid and not a mobile phase. This conclusion was further verified by recording the spectrum at 323 K and then at 100 K and at 323 again. No significant ESR change was observed on freezing and re-melting it.

Lau *et al* [24] performed a more deliberately designed experiment. They found that when comparing polymer particles with 50 and 500nm diameters, the steady-state radical concentration is larger for the larger particles. When the polymerization temperature was increased from 50 ^{0}C to 65 ^{0}C, for 500nm particles, the steady-state radical concentration decreased from $5.5\text{x}10^{-5}$ to $0.6\ \text{x}10^{-5}$ (mol/liter), while for 50nm particles, it decreased from $1.8\text{x}10^{-5}$ to $0.61\ \text{x}10^{-5}$ (mol/liter). This also verified that the observed radicals were within the polymer particles.

In section 2.3.4.3, results of DSC measurement of PDB for EGDMA 10%wt system was reported. DSC spectra show only one reaction peak. The total area of those peaks are a monotonous decreasing function of total monomer conversion. As has been mentioned, all these samples were washed and vacuum dried at 30^{0}C to remove the residual monomer. Besides DSC testing, all these samples were tested by ESR for trapped residual radicals.

Figure 3.7 shows a typical spectrum. **Figure 3.8** shows a 3-D plot of ESR spectra versus total monomer conversion. It could be clearly seen that after careful sample cleaning, these samples still have a very high radical concentration (ca. 0.4-6.0 x 10^{-5} mol/liter).

Two things could be deduced from these data. First, the reaction peak tested by DSC at elevated temperature really involves pendant double bonds and free radicals. Both of them were trapped in highly crosslinked polymer particles during the emulsion polymerization process. Based on these experiment results, it should be clear that one kind of chemically reactive, highly crosslinked nano polymer latex particle has been prepared that may have a potential application in synthetic rubber, engineering plastics, polymer modification and controlled chemical release substrate area.

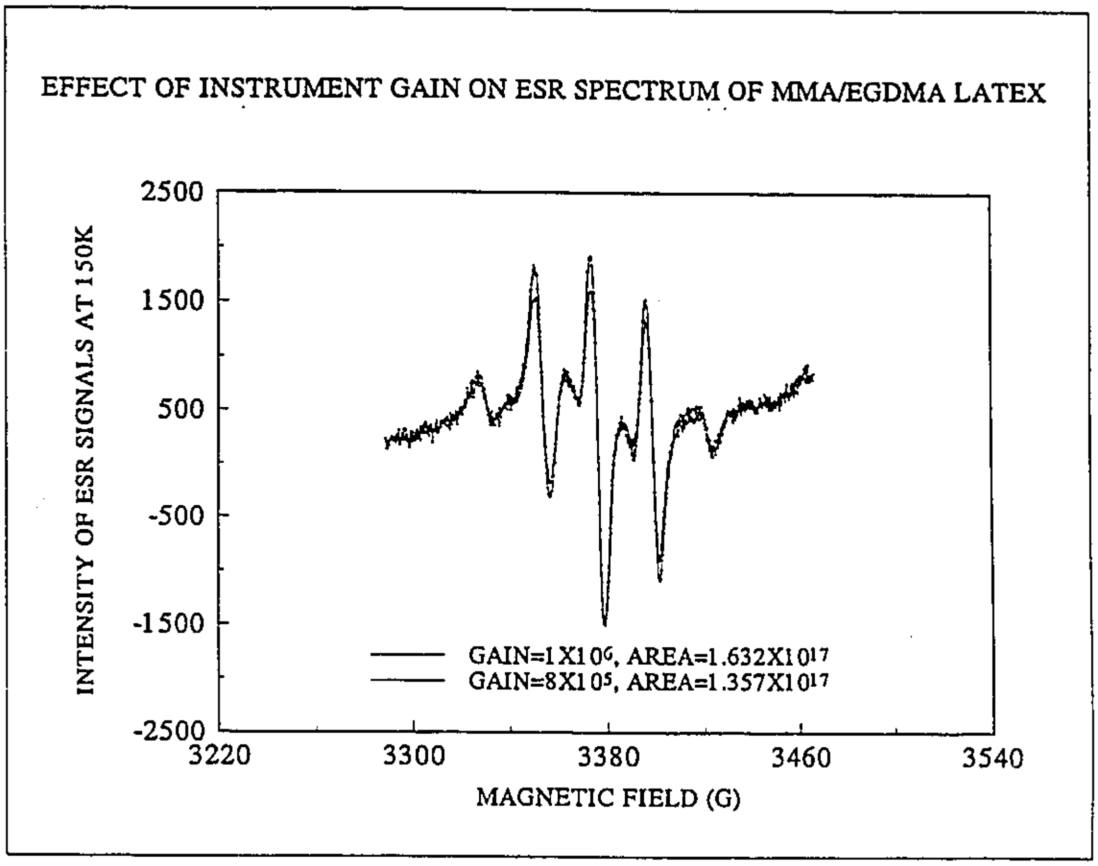

Figure 3.1 Effect of instrument gain on ESR spectrum of MMA/EGDMA copolymer latex sampled at time 50 min. Polymerization conditions: T=50°C, EGDMA: 10%wt, KPS: 8.76×10^{-3} mol/liter-H_2O, SDS: 10×10^{-3} mol/liter-H_2O. Cavity temperature: 150 K. For other ESR instrumental conditions see page 87.

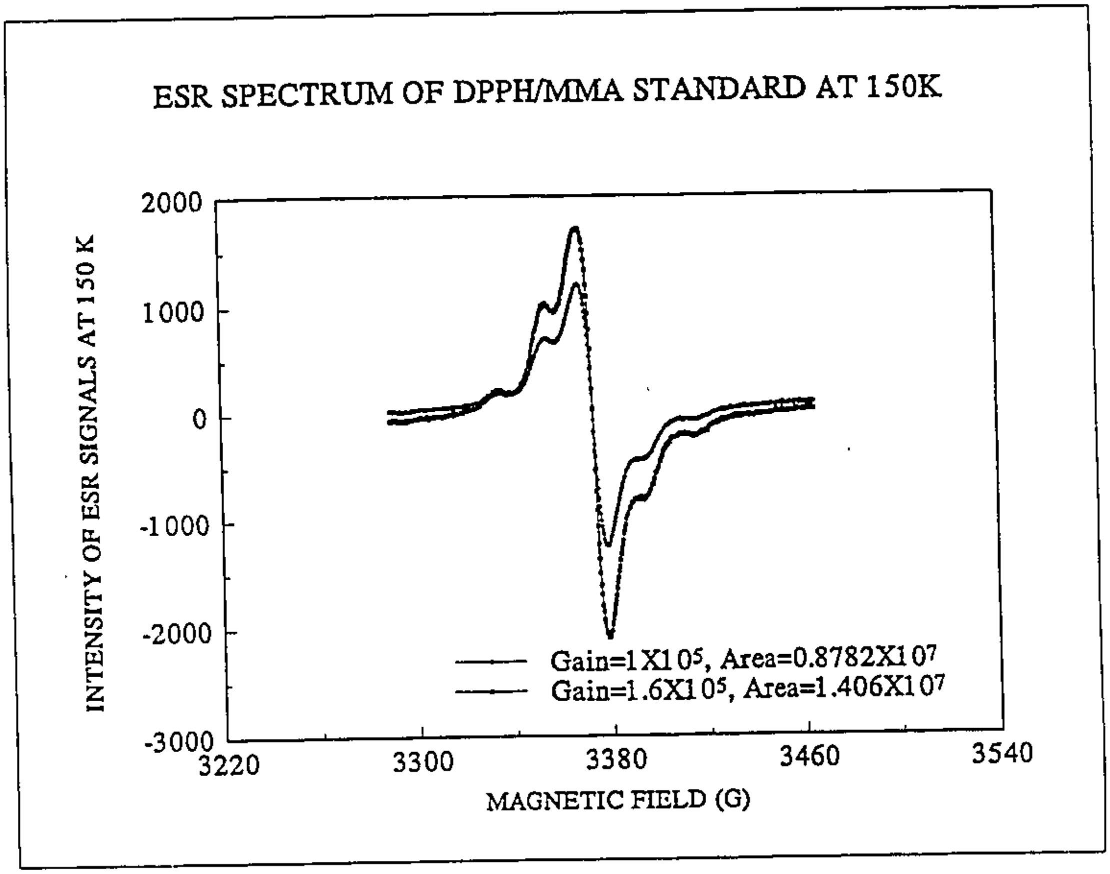

Figure 3.2 ESR spectra of DPPH/MMA solution standard (1.325×10^{-4} mol/liter). For other ESR instrumental conditions see page 87.

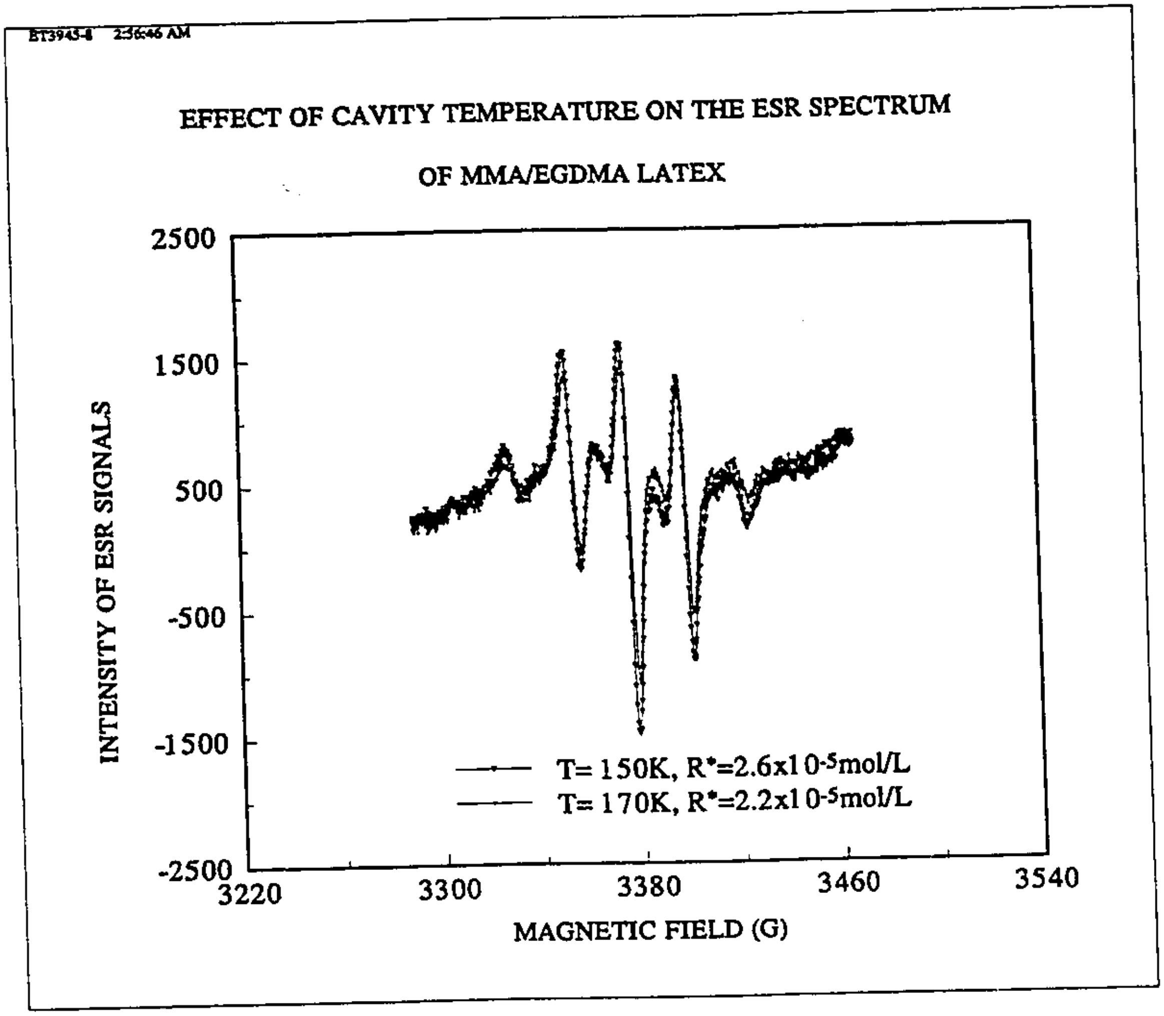

Figure 3.3 Effect of cavity temperature on ESR spectra of MMA/EGDMA latex sampled at time 50 min. Polymerization conditions: EGDMA: 10%wt, KPS: 8.76×10^{-3} mol/liter-H_2O, SDS: 10×10^{-3} mol/liter-H_2O, T=50^0C. Instrument gain: 8×10^5. For other ESR instrumental conditions see page 87.

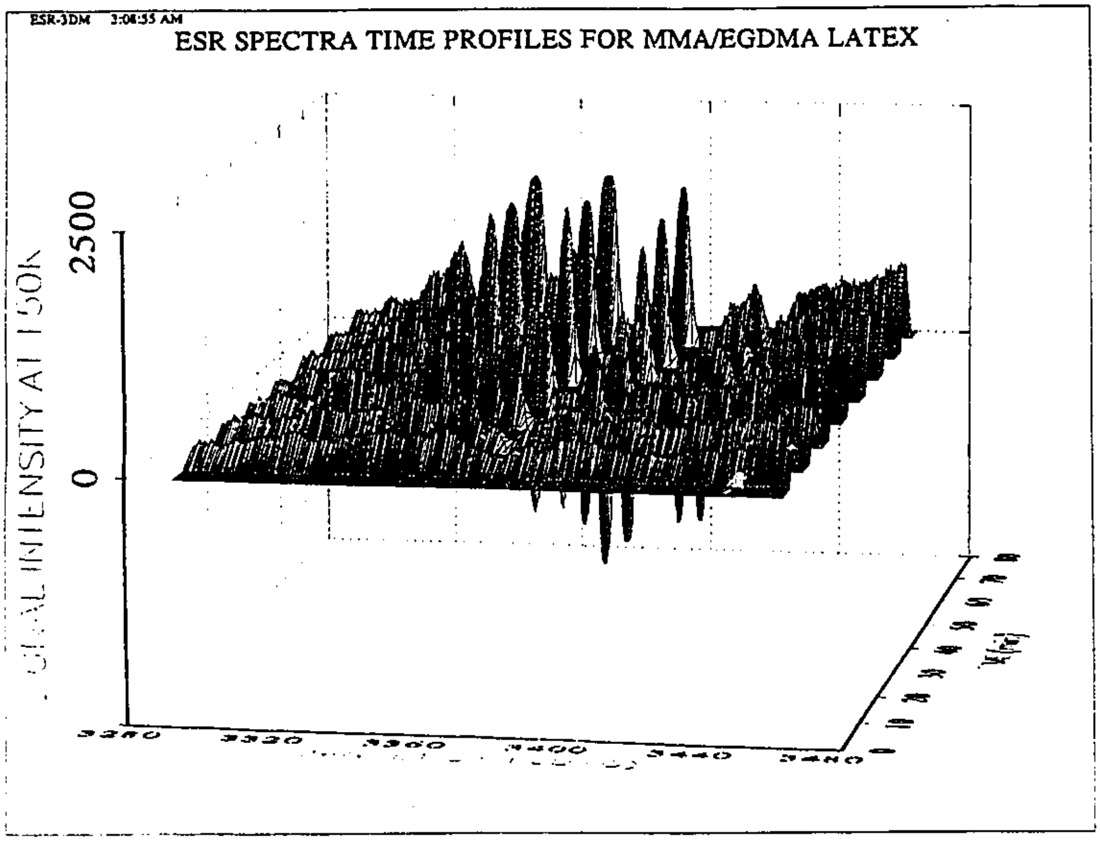

Figure 3.4 ESR spectra of MMA/EGDMA latex sampled at different polymerization times. Polymerization conditions: EGDMA: 10%wt, KPS: 8.76×10^{-3} mol/liter-H_2O, SDS: 10×10^{-3} mol/liter-H_2O, T=50°C. For other ESR instrumental conditions see page 87.

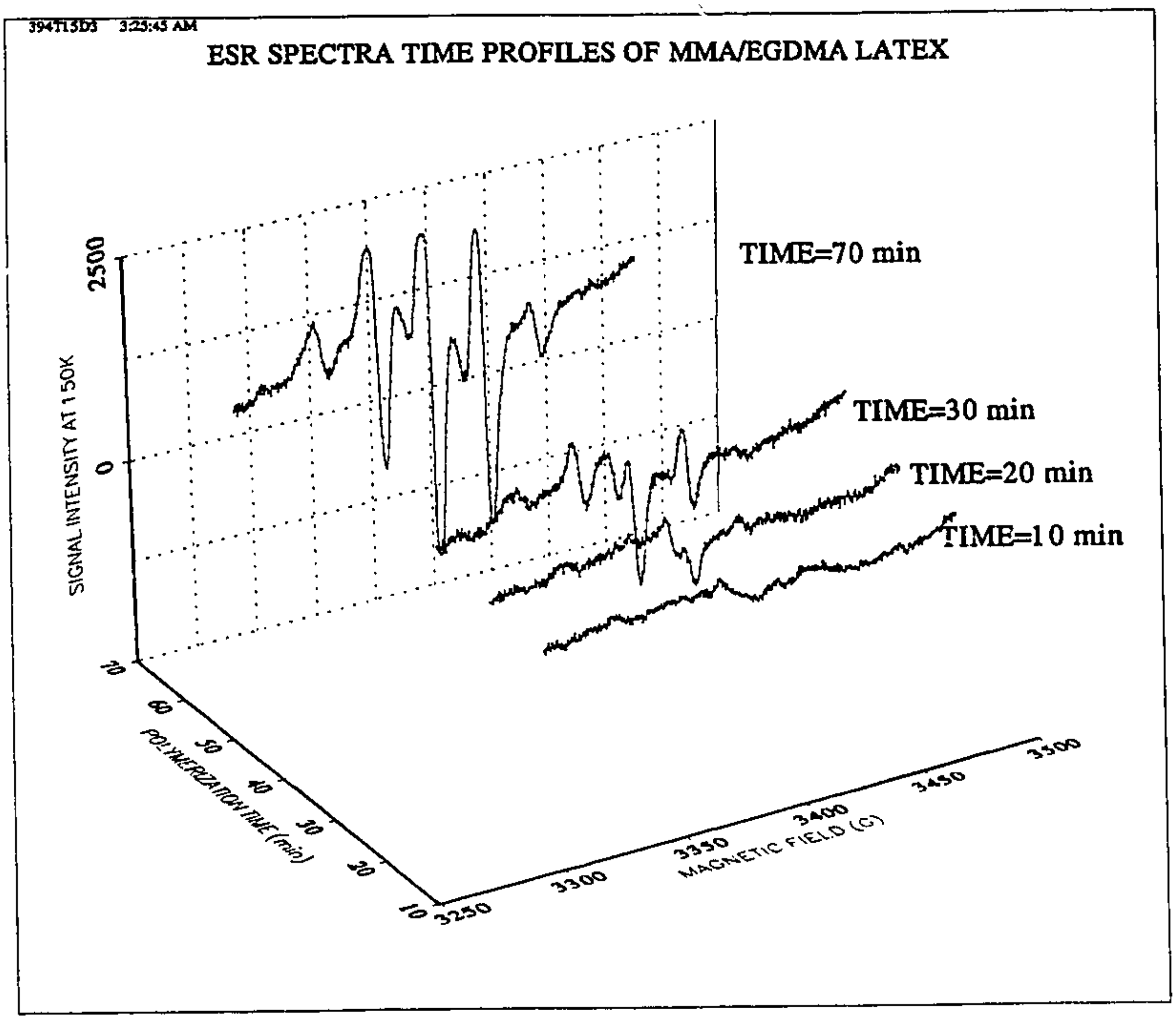

Figure 3.5 3-D ESR spectra time profiles showing structure developing with polymerization time in MMA/EGDMA polymer latex. Polymerization conditions: EGDMA: 10%wt, KPS: 8.76x10^{-3} mol/liter-H_2O, SDS: 10x10^{-3} mol/liter-H_2O, T=50^{0}C. For other ESR instrumental conditions see page 87.

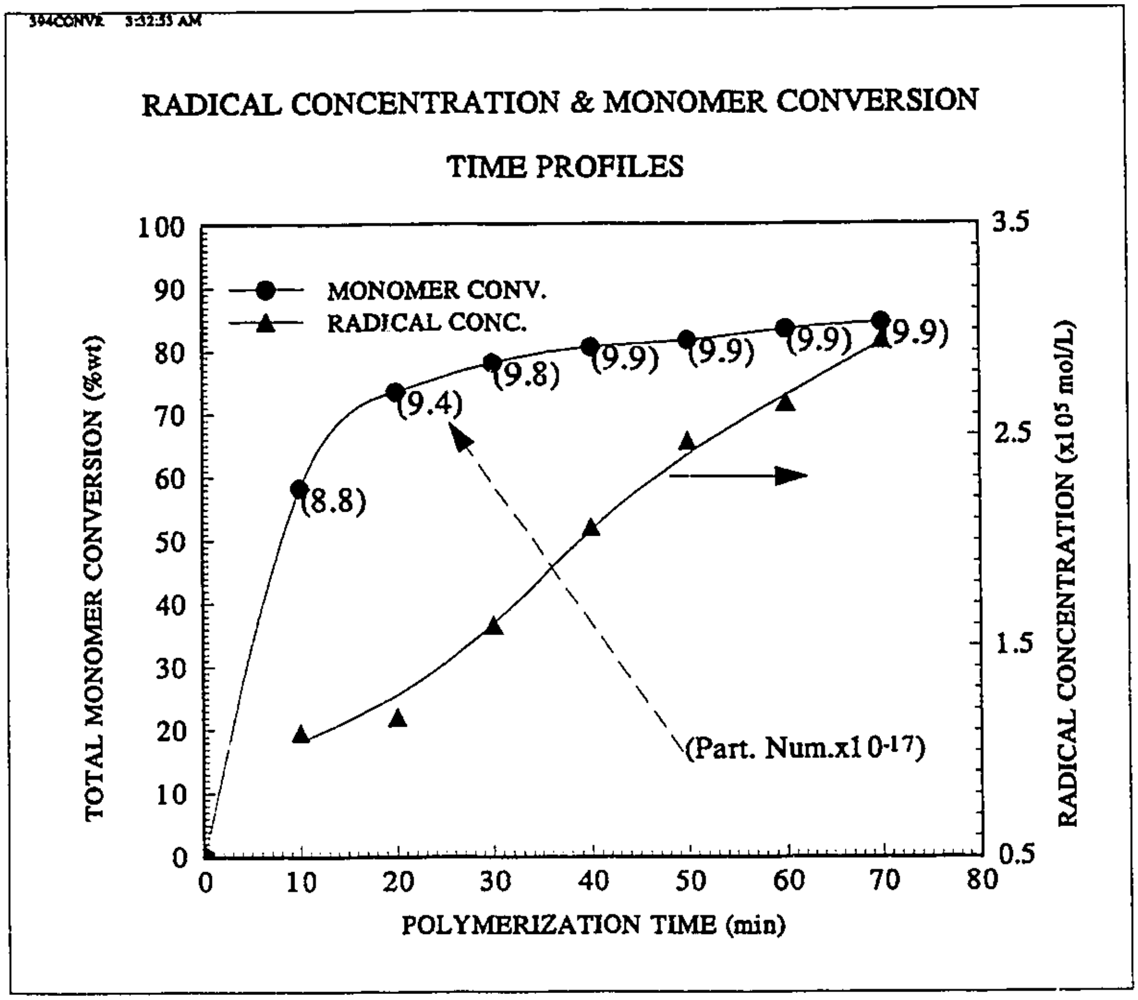

Figure 3.6 Radical concentration and monomer conversion time profiles in MMA/EGDMA polymer latex. Polymerization conditions: EGDMA: 10%wt, KPS: 8.76x10^{-3} mol/liter-H_2O, SDS: 10x10^{-3} mol/liter-H_2O, T=50^0C. For other ESR instrumental conditions see page 87.

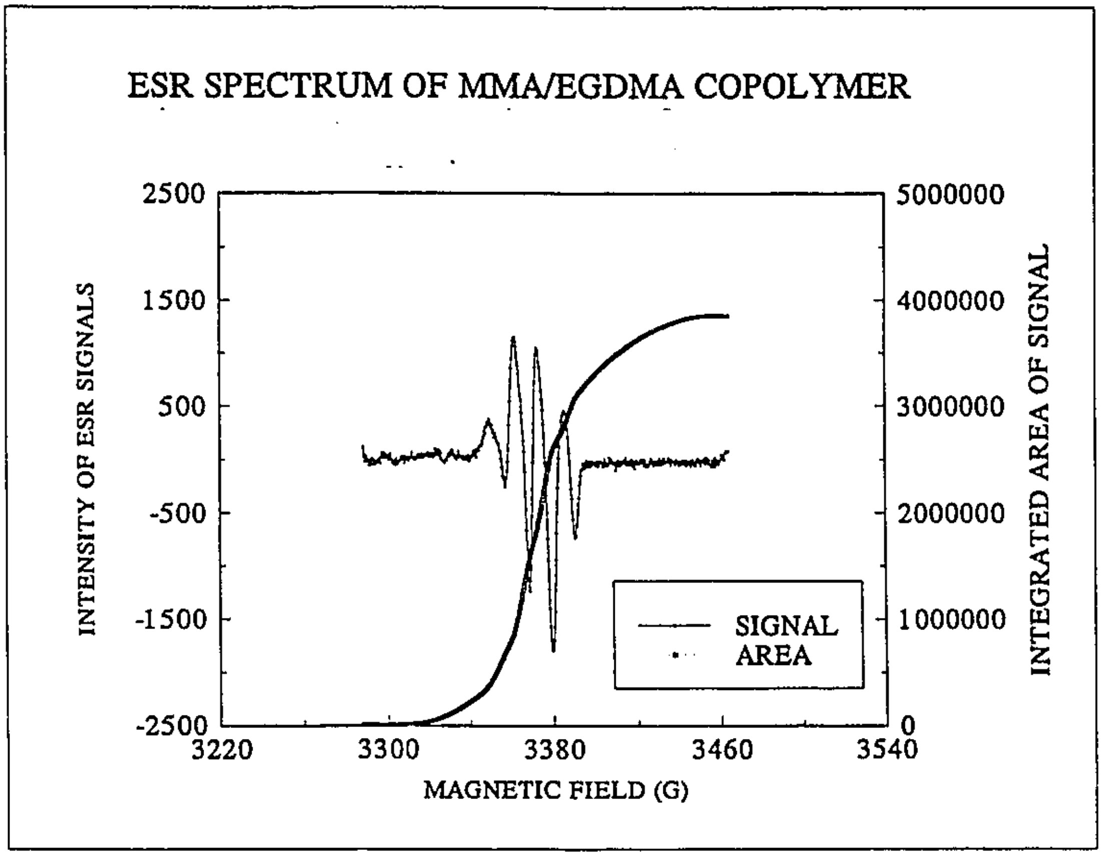

Figure 3.7 ESR spectrum of MMA/EGDMA copolymer sampled at monomer conversion 83.3%wt and after being dried in a vacuum oven. Polymerization conditions: T=50^{0}C, EGDMA: 10%wt, KPS: 2.2x10^{-3} mol/liter-H_2O, SDS: 3.47x10^{-3} mol/liter-H_2O. For other ESR instrumental conditions see page 87.

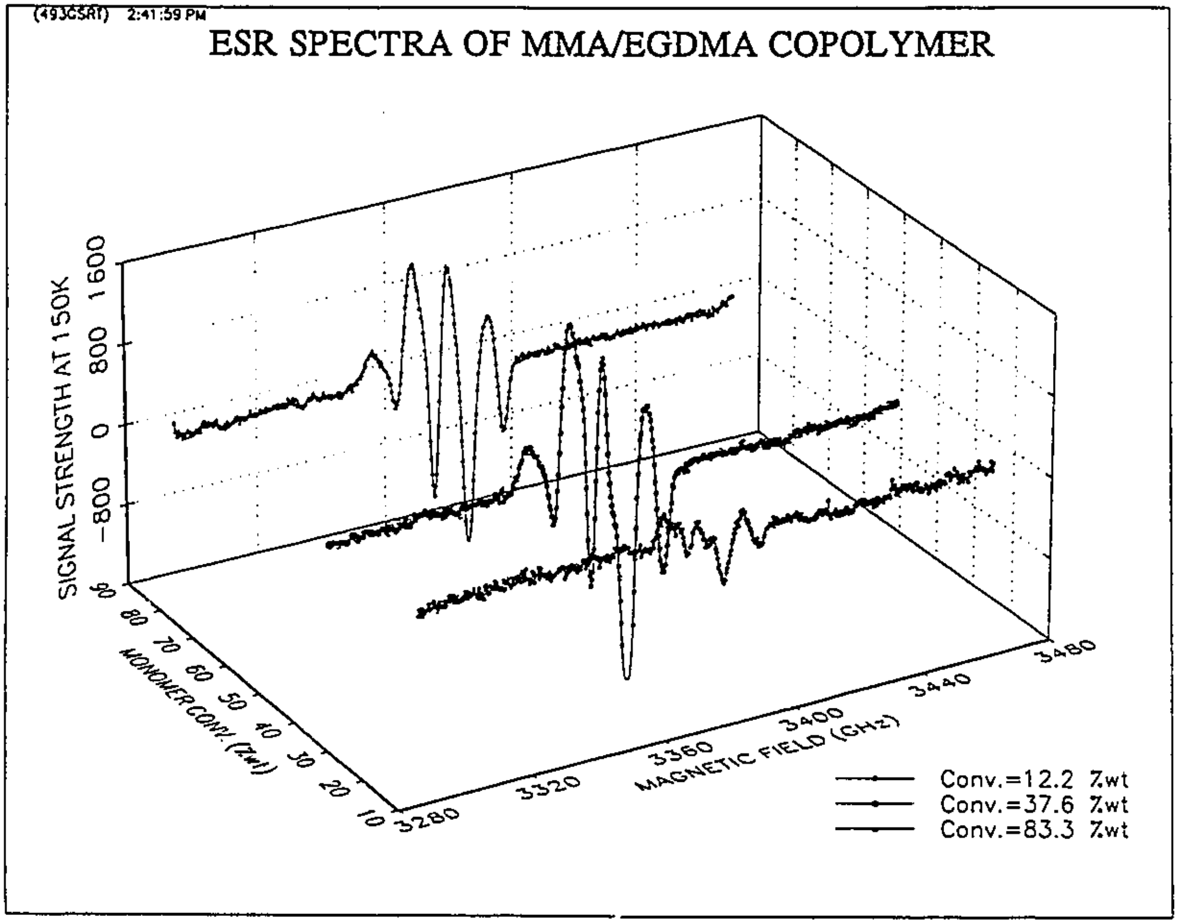

Figure 3.8 3-D spectra conversion profiles showing structure developing in MMA/EGDMA polymer sampled at different monomer conversion and after being dried in a vacuum oven. Polymerization conditions: T=50^{0}C, EGDMA: 10%wt, KPS: 2.2x10^{-3} mol/liter-H_2O, SDS: 3.47x10^{-3}mol/liter-H_2O. For other ESR instrumental conditions see page 87.

3.4 Summary

ESR has been applied to measure the concentration of propagating radicals in emulsion polymerization with crosslinking. A special closed-loop vacuum sampling method has been set up to ensure that the sampling is without atmosphere contamination and can be completed within 10 s.

Time profiles of propagating radical concentration have two regions. A relative constant radical concentration region couples with a rapid monomer conversion rate and polymer particle concentration increase. A dramatic radical concentration change appears when monomer conversion rate and polymer particle concentration level off. These indicates a trapping of radicals within crosslinked polymer network during emulsion polymerization.

Radical trapping is further confirmed by ESR testing of solid polymer samples coupled with DSC testing of residual PDB in the same samples. These results indicate the achievement of a reactive, high crosslinking nano polymer particles which might have many potential applications in the manufacture of specialty polymer-based products.

For future research, with the availability of ESR instruments having high microwave power and high sensitivity, it might be possible to directly monitor the entire kinetics of crosslinking emulsion polymerization in the cavity.

3.5 References

1 Murray, M. J., and Snowden, M. J. *Advances in Colloid and Interface Science*, 1995, **54**, 73

2 Funke, W. *J. Coating Tech.*, 1988, **60**, 767, 69

3 Obrecht, W., Seitz, U, and Funke, W, in "Emulsion Polymerization, ACS Symp. Series 24", Piirma, I. and Gardon, J. L. eds, New York Academic Press, page 92, 1976

4 Funke, W. *British Polymer J.*, 1989, **21**, 107

5 Pelton, R. H., Chibante, P. *Colloid and Surface*, 1986, **20**, 247

6 Pelton, R. H. *J. Polym. Sci., A: Polym. Chem.*, 1988, **26**, 918

7 Pelton, R. H., Pelton, H. M., Morfesis, A. and Rowel, R. L. *Langmuir*, 1989, 5, 816

8 Wu, X. Y., Ph.D. Thesis, McMaster University, Hamilton, Canada, 1992

9 Heskins, M. and Guillet, J. *J. Macromol. Sci.*, 1968, **A2**, (8), 1441

10 Pelton, R., Wu, X., McPhee, W. and Tam, K. Chiu, in "Colloidal Polymer Particles", Goodwin, J. W. and Buscall, R. eds, Academic Press Limited, page 81, 1995

11 Priest, W. J., *J. Phys. Chem.* 1952, **56**, 1077

12 Maxwell, Ian A., Morrison, Bradley R., Napper, D. H. and Gilbert, Robert G. *Macromolecules* 1991, **24**, 1629

13 Casey, Brendan S., Morrison, Bradley R. and Gilbert, Robert G. *Prog. Polym. Sci.* 1993, **18**, 1041

14 Maxwell, Ian A., Morrison, Bradley R., Napper, D. H. and Gilbert, Robert G. *Makromol. Chem.* 1992, **193**, 303

15 Bresler, S. E., Kozbekov, E. N., Fomichev, V. N. and Shadrin, V. N. *Makromol. Chem.* 1974, **175**, 2875

16 Kamachi, M., Kuwae, Y., Kohno, M. and Nozakura, S. *Polym. J.* 1985, **17**, 541

17 Kamachi, M., Kuwae, Y., Kohno, M., Nozakura, S. and Hatada, K. *Polym. J.* 1981, **13**, 919

18 Shen, J., Tian, Y. and Qiu, Z. *Makromol. Chem., Rapid Commun.* 1987, **8**, 615

19 Zhu, S., "Advances in Free Radical Polymerization Kinetics", Ph.D. Thesis, McMaster University, Canada, (1990)

20 Stricker, J., Fischer, F. and Hoffman, W. *Plaste Kautsch* 1970, **17**, 253

21 Ballard, M. J., Gilbert, Robert G., and Napper, Donald H. *Macromolecules* 1984, **17**, 504

22 Ballard, M. J., Gilbert, Robert G. and Napper, Donald H., Pomery, Peter J., O'Sullivan, Paul W. and O'Donnell, James H. *Macromolecules* 1986, **19**, 1303

23 Leslie, Gregory L., Maxwell, Ian A., Ballard, M. J., Gilbert, Robert G. and Napper, Donald H. *Aust. J. Chem.* 1988, **41,** 279

24 Lau, W., Westmoreland, D. G. and Novak, R. W. *Macromolecules* 1987, **20**, 459

25 Westmoreland, D. G. and Lau, W. *Macromolecules* 1989, **22**, 496

26 Cutting, G. R. and Tabner, B., J. *Macromolecules* 1993, **26**, 951

27 Bowden, M. J. and O'Donnell, J. H. *J. Phys. Chem.* 1986, **2,** 1577

28 Li, D., Zhu, S. and Hamielec, A. E. *Polymer* 1993, **34**, 1383

CHAPTER 4

KINETIC MODELING OF VINYL/DIVINYL MONOMER EMULSION COPOLYMERIZATION

The history of emulsion polymerization can be tracked back to 1930's, when the initial realisation that natural rubber could be replaced by dispersing some monomers or together with polymers in an aqueous medium (based on the intuitive similarity to the natural rubber latex) led to the development of emulsion polymerization. The first viable method for emulsion polymerisation was presented by Luther and Heuck in 1932[1].

The classic oil-in-water emulsion polymerization system contains the following typical components: about 65% water, 30% monomers which normally are partially soluble in water, water soluble free radical initiators, water soluble ionic and/or non-ionic emulsifiers and some other additives such as a chain transfer agent. Emulsification of those immiscible monomers in a continuous water phase followed by free radical polymerization mechanisms include the major characteristics. The main steps are radical generation in the water phase, latex particle formation, polymerization within the monomer swollen polymer particles. The resulting product is a colloidal latex containing up to 30%wt polymer particles [2].

The objective of the present kinetic modelling is to develop a mathematical model for the kinetics of emulsion polymerization of vinyl and divinyl monomers. An attempt is now made to elaborate on the mechanisms and kinetics involved in batch emulsion polymerization with crosslinking for the MMA/EGDMA system.

4.1 Literature Review

For this very complicated heterogeneous process the first set of hypotheses on its mechanisms and a reasonable qualitative kinetic model was given by Harkins in the early 1940s[3]. During the more than half a century of development, several important summaries of emulsion polymerization have been given by Bovey for 1950's [4], Blackley and Pirmma for the 1970's[5], Bassett and Hamielec [6], Napper and Gilbert for the 1980's [2] and Barton and Capek for the 1990's[7].

These reviews focused on major developments in the typical emulsion polymerization kinetics for synthesis of linear polymer chains. For the present research, it is desired to investigate the interrelation between the free radical crosslinking and emulsion polymerization. Therefore, the major study done on theoretical modelling of free radical crosslinking needs to be carefully considered as well as that for emulsion polymerization.

Studies on the emulsion polymerization of vinyl monomers have been progressing step by step since the foundation of the theoretical basis for emulsion polymerization by Smith-Ewart [8]. There are many comprehensive books about the development of emulsion polymerization fundamentals for successive periods. Theoretical studies considering the effect of crosslinking have only been published since the late 1980's.

Hamielec and co-workers [9,10] developed a dynamic mathematical model for the multi-component free radical emulsion polymerization for the production of styrene-butadiene rubber (SBR). This model was derived by including elementary reaction steps in both water phase and polymer particle phase combined with mass and heat balances, and diffusion control for termination and propagation using the free volume concept. It can be used to calculate monomer conversion, copolymer composition, average molecular weight, long/short branches and crosslinking frequencies as well as average particle number and size.

Recently a kinetic model considering the crosslinking density distribution for vinyl/divinyl monomers emulsion polymerization was published [11-13] and applied to

MMA/EGDMA emulsion polymerization. With this model the monomer concentration of stage II was calculated by using the concept of free energy of mixing, elasticity influenced by crosslinking density that are positive to monomer swelling, and interfacial tension that causes particle shrinking, negative to monomer swelling [14, 15].

It might be noticed that in the development for monomer concentration in particles, the structure of the particle was assumed to involve a homogeneous network as assumed by Guillot [15]. This seems to conflict with the concept of crosslinking density distribution leading to a very heterogeneous polymer particle, and to the result that the crosslinking density is much higher in emulsion polymerization especially in the initial stages of polymerization.

4.1.1 Crosslinking kinetics in free radical polymerization

Carothers [16] was the first to define "gel" as a three dimensional molecule with an infinitely large molecular weight. After that there were two kinds of theories to explain the mechanism of network formation. Flory [17] created the basis for the so-called "classical gelation model". It is based on an "ideal network assumption": all functional groups (vinyl groups in the free radical polymerization) have the same reactivity; no cyclization which will consume pendant double bonds with or without contribution to the formation of a "four branched node"; all functional groups are independent of each other which means there are no effects of substituted groups.

These models require that all crosslinking points be formed randomly on the accumulated polymer chains at all levels of monomer conversion which means gelation is a thermodynamic or equilibrium process. Equivalently, all primary chains formed at different times (different birth times) have the same crosslinking density.

However, synthesis of a network by free radical polymerization is kinetically controlled and hence it is necessary to use a kinetic approach to account for the reaction path dependence of polymer network properties.

Gordon [18], Pearson [19], Dotson [20], Peppas [21] developed various statistical models to describe several crosslinking radical polymerization systems. They took into account the effects of cyclization, used various models of diffusion controlled termination, and calculated the structural averages such as gel point, molecular weight, sol/gel fraction and number of elastically effective network points.

Macosko and coworkers [22-26] have reported various studies for modeling the crosslinking kinetics from both statistical and kinetic points of view. Besides the ideal network assumption, they [26] have used the stationary-state hypothesis for radical concentration development. Their statistical model defines three ways of crosslink formation which might affect the polymer MWD [24, 25], and can predict gel-point, weight fraction of sol, PDB weight fraction and concentrations of effective junctions and strands.

Hamielec and coworkers, based on their comprehensive experimental data, proposed a new model [27-28] revealing the inherent heterogeneity of polymer networks formed during the free radical synthesis process. They proved that primary polymer chains born at different conversions in a batch reactor will not have the same density of crosslinking which means there is a crosslinking density distribution. A strategy for controlling this distribution was proposed [28].

Recently, Zhu *et al* [29] combined this model with the statistical approach to investigate the influences of crosslink density distribution on such aspects of polymer network formation as sol molecular weight, gel point and sol/gel fraction. Also, the effect of crosslinking on molecular weight distribution for the pre-gel region has been proposed [30].

Most recently, Teymour *et al* [31,32] proposed a new "Numerical Fractionation" technology for the analysis of the dynamics of gelation in free radical polymerization. This method relies on the idea of numerical segregation of polymer into populations and into a series of unimodal sub-distributions of similar structure and size defined as "generation" that could be either linear chains or branched chains with same degree of branching or clustering. In present published calculation, the transition from low generation levels to a adjacent higher level generation will occur only if two lower level members connect together forming a single polymer molecule. So that the present direct application is for the situation of "chain transfer to polymer following combination termination".

From chemical engineering point of view, this method could be considered to be similar to the "plug flow model" for a tubular reactor. The beauty of this method is that it uses the kinetic approach but is not limited to calculating moments for the overall population. Continuous kinetic problems have been simplified to a series discrete fraction. This is a very promising method in the study of crosslinking kinetics. It could provide new insight into the sol/gel transition because it is continuous through the gel point and a host of polymer properties.

The only point need to be mentioned is the effect of "back mixing" on the transition between generations. It was assumed that [32] "If reaction is between molecules of dissimilar generations, the resulting polymer always belongs to the higher generation" instead of the level summation of these two generations that might cause problem near "Pseudo-Gel" transition range in which a small change in polymer structure might cause a critical property change. It would be of great interest to apply this novel approach to emulsion polymerization. This was not attempted in the present study because this research program was near its end when it became available in the literature.

4.1.2 Reactivity of pendant double bonds

The reactivity of pendant carbon-carbon double bonds is one of the key points that needs to be elucidated in crosslinking kinetics with high levels of crosslinking. With the Flory and Stockmayer classical theories the activity of all vinyl groups is assumed equal. But there are many reports showing experimental data on the gelation point which disagree with this model. Loshack [33], Minnema [34] explained the deviation as due to a shielding effect of highly crosslinked molecular structure which causes a reduced reactivity of pendant carbon-carbon double bonds.

Kward [35] provided evidence that in the copolymerization of styrene with small quantities of *m*- and/or *p*- divinylbenzene, the reactivity of PDB of the divinyl monomer is different from that of the double bond on the unreacted monomer molecule. Peppas [36,37] developed a kinetic model using the concept of ternary copolymerization. Their model considered all possible reaction mechanisms. For styrene/m-divinylbenzene (m-DVB)system only by adjusting the reactivity ratio of

PDB to about half of the one in divinyl monomer they could explained the experimental conversion plot for this styrene/m-DVB system.

Macosko *et al* [38] derived a model which considered the PDB as the third monomer type. They found that when the reactivity of PDB is adjusted to 1/2 that of EGDMA , their model could best fit the experimental data for the gelation point plot of conversion of PDB versus total conversion for the MMA/EGDMA monomer system. Keeping the EGDMA concentration constant, changing chain length of primary polymer chains by changing the chain transfer agent (CTA) concentration did not change the reactivity of PDB. However PDB reactivity decreased with EGDMA concentration increase.

4.1.3 Influence of cyclization

The first work to ascribe the delay of the gelation point due to cyclization was done by Simpson *et al* [39]. They measured the PDB content of poly (dially phthalate) at the gel point and deduced the existence of intramolecular cyclization. They found that the ratio of intramolecular cyclization to propagation is largely influenced by the distances between the polymerizable groups.

Similarly, Loshaek [40] found that the efficiency for MMA/EGDMA system was limited by geometrical restrictions on the motion of PDB. But no distinction was found between divinyl monomers forming intramolecular cycles or forming intermolecular linking. This means that the reactivity for both reaction types is the same.

Based on these results and that of Gordon [41], Aso [42] developed a model for EGDMA bulk polymerization. The cyclization was assumed uni-molecular with respect to radical concentration. Following the conclusions drawn from a statistical model proposed by Haward [43], Aso claimed that small rings which are produced by the reaction of a polymeric radical with the "most adjacent PDB or PDB only a few units away on the same chain" are the main form of cyclization. The radicals formed by this now called "primary cyclization" are less active. This model agreed well with experimental data and explained why the content of PDB in the polymeric network was less than expected by the classical statistical models.

Macosko et al also [38] investigated the cyclization of MMA/EGDMA in solution polymerization. They distinguished between primary and secondary cyclization for their experimental data. They changed the dilution extent and CTA concentration and found that if the molecular weight of primary polymer was changed by CTA the primary cyclization will be the same, but that secondary cyclization and crosslinking will increase for systems with less CTA. They also found that if the solvent content increased there would be more primary cyclization as well as less secondary cyclization and crosslinking because the primary chain were less entangled.

4.2 Kinetic Model Development

Three phases can be present in the emulsion polymerization system. A continuous water phase contains initiator, emulsifier (as either dissolved molecule or as an aggregated micelle), and a small amount of dissolved monomer. The second phase is the monomer droplets which are protected by adsorbed emulsifier molecules. The third phase is the latex particles containing polymer and partial or all of the unpolymerized monomers.

Now it is widely accepted that there are three stages in the emulsion polymerization process. The first stage (or stage I) is called particle nucleation stage. There are two different mechanisms: homogenous and heterogeneous nucleation. The criteria for each mechanism being the dominant one is that the concentration of emulsifier in the water phase is below or above the critical micelle concentration (CMC) of the emulsifier used.

In so called homogenous nucleation, in which the concentration of emulsifier in the water phase is zero or less than the CMC for the emulsifier, monomers in the water phase will propagate with charged free radicals formed via the decomposition of initiator in the water phase. When the formed oligomeric radicals exceed their solubility in water, they will precipitate to produce unstable primary polymer particles. They coagulate and the ratio of surface to volume will decrease and the surface charge density will increase to a value which is sufficient to stabilize the particle.

Particles can also be formed by micellar nucleation. With this mechanism oligomeric radicals enter monomer swollen micelles and initiate polymerization therein changing a micelle into a monomer swollen polymer particle. Increasing the emulsifier concentration will increase the number of polymer particle formed. High radical generation rate and high temperature will decrease the nucleation time and narrow the particle size distribution (PSD).

For the monomers used in the present investigation, since MMA has a fairly high water solubility (1.5 g /100g water @ 50 °C [4]) both homogenous and micellar nucleation might occur simultaneously when the emulsifier concentration is higher than its CMC. At the same time, introducing the monomer EGDMA will produce oligomeric radicals having some short branches. Because of the low water solubility of EGDMA, the resulting oligomeric radicals, and the tendency for homogenous nucleation will be changed.

The second stage is the polymer particle growth stage. It begins when all the free monomer swollen micelles have disappeared and/or homogenous nucleation has ceased. Normally, a constant polymerization rate is a characteristic of stage II. In this stage, the particles tend to maintain an equilibrium concentration of monomer in the polymer particles with an almost constant monomer volume fraction in the polymer particles. This is based on a thermodynamic balance of free energy of mixing, surface energy and elastic energy. In stage II, surface tension increases (as particle surface area is now less than 100% covered) and particle size increases. These opposing effects maintain an almost constant monomer concentration in the polymer phase. Monomer transfers from monomer droplets through the water phase and into the polymer particles. Stage II involves a semi-batch process with respect to monomer transfer.

The kinetics in stage III of emulsion polymerisation is similar to that of bulk polymerization. All monomer droplets have disappeared. Polymer particles are the segregated polymerization loci. Therefore monomer concentration in polymer particles falls continuously. This normally leads to enhanced diffusion-controlled termination in the polymer particles, increase in radical concentration and a rate acceleration.

4.2.1 Chemical reaction mechanisms in emulsion polymerization

The reaction mechanisms include those in the water phase with: initiation of free radicals, propagation to form oligomeric radicals, entry into micelles or polymer particles with formation of polymer particles via micellar nucleation and or homogeneous nucleation. As for the reaction steps within the polymer particles these include: propagation with monomers and with pendant double bonds (PDB), chain transfer to monomer, to chain transfer agent (CTA) and to polymer, producing crosslinkages, and primary and/or secondary cyclizations.

In the following description of chemical events, M_1 stands for vinyl monomer (in this study; MMA), M_2 is divinyl monomer (EGDMA in this study) and M_3 for PDB. The subscript *w* and *p* represent the water and the polymer phases.

1. Chemical reactions in water phase:

Initiation:

$$I_w \xrightarrow{kd} 2R^{*}_{in,w} \tag{4.2.1.1}$$

Propagation with monomers in the water phase in context of terminal copolymerization model:

$$R^*_{in,w} + M_{j,w} \xrightarrow{kp_{ij,w}} M^*_{j,w}$$

$$(j = 1, 2), \qquad (4.2.1.2)$$

$$\sim M^*_{i,w} + M_{j,w} \xrightarrow{kp_{i,j,w}} \sim M^*_{j,w}$$

$$(i = 1, 2;\ j = 1, 2), \qquad (4.2.1.3)$$

At present, the PDB is not considered to react with any radical in the water phase. Also the termination reaction in the water phase is neglected. This is a good assumption when there is substantial interfacial area (micelles and/or polymer particles). When the chain length of oligomeric radicals reaches a critical chain length (CCL) it will have entered a particle, or participated to form an unstable primary particle.

2. Chemical reaction in the polymer particles:

Propagation with monomers in the polymer particle in context of terminal copolymerization model:

$$\sim M_{i,p}^{*} + M_{j,p} \xrightarrow{kp_{ij,p}} \sim\sim M_{j,p}^{*}$$

$$(i = 1,\ 2;\ j = 1,\ 2), \qquad (4.2.1.4)$$

$$\sim M_{2\,\sim\sim\sim\sim\sim}^{-\,M_{3,p}^{*}} + M_{j,p} \xrightarrow{kp_{3j,p}} \sim M_{2\,\sim\sim\sim\sim\sim}^{--\,M_{j,p}^{*}}$$

$$(j = 1,\ 2), \qquad (4.2.1.5)$$

Propagation with PDB:

$$\sim\sim M_{i,p}^{*} + \sim\sim M_{2\,\sim\sim\sim\sim\sim}^{-\,M_{3,p}} \xrightarrow{kp_{i3,p}} \sim\sim M_{2\,\sim\sim\sim\sim\sim}^{-\,M_{3,p}^{*}\,M_{i,p}\,\sim\sim}$$

$$(i = 1,\ 2), \qquad (4.2.1.6)$$

$$\sim\sim M_{2\,\sim\sim\sim\sim}^{-\,M_{3,p}^{*}} + \sim\sim M_{2\,\sim\sim\sim\sim}^{-\,M_{3,p}} \xrightarrow{kp_{33,p}} \sim\sim M_{2\,\sim\sim\sim\sim\sim}^{--\,M_{3,p}^{*}\,-\,M_{2}\overset{\sim\sim}{\sim\sim}}$$

$$(4.2.1.7)$$

Chain transfer to monomer:

$$\sim\sim M_{i,p}^{*} + M_{j,p} \xrightarrow{k_{fmij,p}} \sim\sim M_{i,p} + M_{j,p}^{*}$$

$$(i = 1,\ 2;\ j = 1,\ 2), \qquad (4.2.1.8)$$

$$\sim M_2 \overset{M_{3,p}^{*}}{\underset{\sim\sim\sim\sim}{-}} + M_{j,p} \xrightarrow{k_{fm3j,p}} \sim M_2 \overset{M_{j,p}}{\underset{\sim\sim\sim}{-}} + M_{j,p}^{*}$$

$(j = 1, 2)$, (4.2.1.9)

Chain transfer to chain transfer agent (CTA):

$$\sim\sim M_{i,p}^{*} + CTA_p \xrightarrow{k_{fiT,p}} \sim\sim M_{i,p} + CTA_p^{*}$$

$(i = 1, 2)$, (4.2.1.10)

Transfer to polymer:

$$\sim\sim M_{i,p}^{*} + \sim M_{j,p} \sim \xrightarrow{k_{fpij,p}} \sim\sim M_{i,p} + \sim M_{j,p}^{*} \sim$$

$(i = 1,2;\ j = 1,2)$, (4.2.1.11)

$$\sim\sim M_{i,p}^{*} + \sim\sim M_2 \overset{M_{3,p}\,\sim}{\underset{\sim\sim\sim}{-}} \xrightarrow{k_{fpi3,p}} \sim\sim M_{i,p} + \sim\sim M_2 \overset{M_{3,p}^{*}\,\sim}{\underset{\sim\sim\sim}{-}}$$

$(i = 1, 2)$, (4.2.1.12)

$$\sim M_{2,p\sim}^{-M_{3,p}^{*}} + \sim\sim M_{i,p}\sim \xrightarrow{k_{fp3i,p}} \sim\sim M_{i,p}^{*}\sim + \sim M_{2,p\sim}^{-M_{3,p}}$$

$(i = 1, 2)$, (4.2.1.13)

$$\sim M_{2,p\sim}^{-M_{3,p}^{*}} + \sim M_{2\sim}^{-M_{3,p}} \xrightarrow{k_{fp33,p}} \sim M_{2,p\sim}^{-M_{3,p}} + \sim M_{2\sim}^{-M_{3,p}^{*}}$$

(4.2.1.14)

Termination by combination:

$$\sim\sim M_{i,p}^{*} + \sim M_{j,p}^{*} \xrightarrow{k_{tcij,p}} \sim\sim M_{i,p}M_{j,p}\sim$$

$(i = 1, 2;\ j = 1, 2)$, (4.2.1.15)

$$\sim\sim M_{i,p}^{*} + \sim M_{2,p\sim}^{-M_{3,p}^{*}} \xrightarrow{k_{tci3,p} \Leftrightarrow k_{tc3i,p}} \sim M_{2,p\sim}^{-M_{3,p}M_{i,p}\sim\sim}$$

$(i = 1, 2)$, (4.2.1.16)

$$\sim M_{2,p\sim}^{-M_{3,p}^{*}} + \sim M_{2,p\sim}^{-M_{3,p}^{*}} \xrightarrow{k_{tc33,p}} \sim M_{2,p\sim}^{-M_{3,p}M_{3,p}^{-\widetilde{M_{2,p}}\sim}}$$

(4.2.1.17)

Termination by disproportionation:

$$\sim\!\sim\!\sim M^{*}_{i,p} + \sim\!\sim M^{*}_{j,p} \xrightarrow{k_{tdij,p}} \sim\!\sim\!\sim M_{i,p} + \sim\!\sim M_{j,p}$$

$$(i = 1,\ 2;\ j = 1,\ 2). \qquad (4.2.1.18)$$

$$\sim\!\sim M^{*}_{i,p} + \sim\!\sim M^{-M^{*}_{3,p}}_{2,p\sim\sim} \xrightarrow{k_{tdi3,p} \Leftrightarrow k_{td3i,p}} \sim\!\sim M_{i,p} + \sim\!\sim M^{-M_{3,p}}_{2,p\sim\sim}$$

$$(i = 1,\ 2), \qquad (4.2.1.19)$$

$$\sim\!\sim M^{-M^{*}_{3,p}}_{2,p\sim\sim} + \sim\!\sim M^{-M^{*}_{3,p}}_{2\sim\sim} \xrightarrow{k_{td33,p}} \sim\!\sim M^{-M_{3,p}}_{2,p\sim\sim} + \sim\!\sim M^{-M^{*}_{3,p}}_{2\sim\sim}$$

$$(4.2.1.20)$$

Radical desorption from particles:

At present it is considered that only two radicals may desorb from polymer particles :

(1) oligomeric radical just entered into the particle (OLI^{*})

$$\sim\!\sim OLI^{*}_{p} \xrightarrow{k_{dep}} \sim\!\sim OLI^{*}_{w}$$

$$(4.2.1.21)$$

(2) chain transfer agent radical(CTA*)

$$\sim CTA_p^* \xrightarrow{k_{de,CTA}} \sim CTA_w^*$$

(4.2.1.22)

4.2.2 Kinetics of network formation in polymer particles

As for crosslinking in emulsion polymerization of vinyl and divinyl monomers, there are two different mechanisms. When chain transfer from a propagating radical to a dead polymer molecule occurs, this polymer will form a backbone radical centre which will grow to form a branched chain radical. When two of these branched chain radicals terminate via combination, a tetrafunctional branch point or crosslinkage will result.

With the existence of a divinyl monomer in the polymerization system, another mechanism for crosslinking becomes important (see **Figure 4.1**). When a growing polymer radical propagates with a divinyl monomer, a pendant carbon-carbon double bond (PDB) is created. Thereafter, this PDB might propagate with a radical on its own chain to form a node of cyclization, or with a radical on another polymer chain to form a tetrafunctional branch point. The successive formation of tetra-branched nodes will ultimately lead to a three dimensional polymeric network.

In the emulsion polymerization of vinyl and divinyl monomers, crosslinking in the polymer particles can produce micro heterogeneity. This will change the monomer partitioning in different domains within the particle and the overall between polymer particles and water. The apparent behaviour due to this physical change is that the overall polymerization rate and crosslinking density will deviate from that of a bulk or solution process as it has been shown in Chapter 2.

It is clear that branching and/or crosslinking certainly confounds diffusion-controlled bimolecular termination. First the diffusing polymer species have a more complex structure and at the same time the diffusion matrix (the polymeric network) is also more complex. These more complex micro-environments will likely shield the PDB, and reduce their effective reactivity. Accepting the assumption that PDB born at the same time will have the same reactivity for the entire polymerization time, the reactivity of PDB born at different times will be different. This assumption is not consistent with different micro-environments being present, since PDB born at same time may later experience a different micro-environment. That means that even if the composition of all polymer chains is constant in a semi-batch process, the effective PDB concentration will change with time which in turn will alter the process of crosslinking.

4.2.3 Modification of the Crosslinking Density Distribution Model

The present model is to be a generalization of an existing dynamic model for SBR (styrene butadiene rubber) production by emulsion polymerization [9,10]. The contribution of the present work is to account for the crosslinking density distribution and the shielding effect on pendant double bond reactivity.

4.2.3.1 Effect of termination mechanism

The principal mechanism for the formation of crosslinks in a vinyl/divinyl monomer system involves the propagation of a polymeric radical with a pendant double bond. In the original derivation of the crosslinking density distribution [27,28], it was concluded that chain transfer to polymer followed by disproportionation termination will not cause gelation. Using their "generations transition" criteria Teymour et al [32] proposed a systematic approach for *a priori* determination of the possibility of generation for any reaction mechanism and confirmed this point.

Herein, another detailed mathematical proof is presented. The fundamental normalized second moment equation at this condition (no combination termination) is given by:

$$\frac{dq_2}{dx} = \frac{2(1+C_{p2})}{\tau + C_{p1}} = \frac{2(1+\varepsilon\frac{q_2}{1-x})}{(\tau + \varepsilon\frac{x}{1-x})} = \frac{2[(1-x)+\varepsilon q_2]}{(1-x)\tau + \varepsilon x}$$

(4.2.3.1)

$$C_{p2} = \frac{k_{fp,p}q_2}{k_{p,p}(1-x)} \;; \quad \text{and} \quad C_{p1} = \frac{k_{fp,p}x}{k_{p,p}(1-x)}$$

(4.2.3.2)

$$\tau = \frac{k_{td,p}[R]}{k_{p,p}[M]} + \omega, \quad \omega = \frac{k_{fm,p}}{k_{p,p}} + \frac{k_{fT,p}[CTA]}{k_{p,p}[M]}$$

(4.2.3.3)

$$\varepsilon = \frac{k_{fp,p}}{k_{p,p}}$$

(4.2.3.4)

wherein:

q_2 is the normalized second moment of the dead polymer molecular weight distribution (MWD)

$k_{p,p}$ is the pseudo propagation rate constant in the polymer phase (in the polymer particle), and for the terminal copolymerization model is given by

$$k_{p,p} = \sum_{i=1}\sum_{j=1} k_{pij,p}\phi_i^{*} f_j$$

(4.2.3.5)

$k_{fm,p}$ is the pseudo chain transfer to monomer rate constant in the polymer phase

$$k_{fm,p} = \sum_{i=1}\sum_{j=1} k_{fmij,p}\phi_i^* f_j$$

(4.2.3.6)

$k_{fp,p}$ is the pseudo chain transfer to polymer rate constant in the polymer phase

$$k_{fp,p} = \sum_{i=1}\sum_{j=1} k_{fpij,p}\phi_i^* \overline{F}_j$$

(4.2.3.7)

$k_{td,p}$ is the pseudo disproportionation termination rate constant in the polymer phase

$$k_{td,p} = \sum_{i=1}\sum_{j=1} k_{tdij,p}\phi_i^* \phi_j^*$$

(4.2.3.8)

$k_{fT,p}$ is the pseudo chain transfer to CTA rate constant in the polymer phase

$$k_{fT,p} = \sum_{i=1}\sum_{j=1} k_{fTi,p}\phi_i^*$$

(4.2.3.9)

ϕ_i^* , ϕ_j are number fractions of polymeric radicals of type *i* and *j* in the polymer phase

f_j is the mole fraction of monomer of type j in the polymer phase

$\overline{F_j}$ is the mole fraction of monomer j bond in the accumulated copolymer chains

x is the monomer conversion (mole fraction)

There is a limitation in the original mathematical derivation [27,28]. A preliminary assumption of a constraint condition $\tau > (k_{fm,p}/k_{p,p})$ has been made. Also that proof has a limiting condition that $\tau = \tau_{min.}$ This restricts the application of their result to "extreme diffusion controlled situation" only. To prove that in the absence of termination by combination (only disproportionation termination occurs) one must (under general constraint condition) prove that:

$$\lim_{x \to 1}\left(\frac{dq_2}{dx}\right) = \lim_{x \to 1}\frac{2(1-x)+\varepsilon q_2}{\tau(1-x)+\varepsilon x} \neq \infty \tag{4.2.3.10}$$

<u>**Case 1:**</u>

If the majority of dead polymer chains produced in the polymerization process will not be re-activated again by chain transfer to the polymer mechanism, ($\varepsilon = 0$), so that one gets:

$$\lim_{x \to 1}\left(\frac{dq_2}{dx}\right) = \lim_{x \to 1}\frac{2(1-x)}{\tau(1-x)} = \left.\frac{2}{\tau}\right|_{\tau \Rightarrow finite} \neq \infty \tag{4.2.3.11}$$

For the limiting situation where $k_{td,p} \approx 0^+$ (with perhaps strong diffusion controlled termination), one obtains:

$$\lim_{\substack{x \to 1 \\ \tau \to \omega}} \left(\frac{dq_2}{dx}\right) = \lim_{\substack{x \to 1 \\ \tau \to \omega}} \frac{2(1-x)}{\tau(1-x)} = \frac{2}{\omega}\bigg|_{\omega = finite} \neq \infty$$

(4.2.3.12)

In the present proof, there is no preliminary requirement for $\tau > (\ \omega = k_{fm,p}/k_{p,p}\ )$.

<u>**Case 2:**</u>

For the ($\varepsilon \neq 0$) monomer system, chain transfer to polymer will re-activate the dead polymer chain. After analytically solving differential equation (4.2.3.1) and substituting into the limiting condition one gets:

$$\lim_{x \to 1} \left(\frac{dq_2}{dx}\right) = \lim_{x \to 1} \left(q_2\right) = \frac{1}{\varepsilon + \tau}\left[1 + \left(\frac{\varepsilon}{\tau}\right)^{\frac{2\varepsilon}{\varepsilon - \tau}}\right] \neq \infty$$

(4.2.3.13)

It is clear that for extreme diffusion controlled termination that is (x → 1, $k_{td,p} \to 0^+$), one may get:

$$\mathop{Lim}_{\substack{x\to 1\\ k_{td,p}\to 0}} \left(\frac{dq_2}{dx}\right) = \mathop{Lim}_{\substack{x\to 1\\ \tau\to\omega}} (q_2) = \left\{ \frac{1}{\varepsilon+\omega}\left[1+\left(\frac{\varepsilon}{\omega}\right)^{\frac{2\varepsilon}{\varepsilon-\omega}}\right]\right\}_{\omega = finite} = finite$$

(4.2.3.14)

It can be seen from equation (4.2.3.3) that the parameter τ represents the mechanism by which the dead polymer chain is produced. Among those three terms (chain termination , chain transfer to monomer, and chain transfer to CTA)

$$\frac{k_{td,p}[R]}{k_{p,p}[M]},\quad \frac{k_{fm,p}}{k_{p,p}},\quad \frac{k_{fT,p}[CTA]}{k_{p,p}[M]}$$

one of these three terms should not be zero in order to produce dead polymer chains. In above extremely limiting cases ($k_{td,p} \to 0^{-}$) there must exist either chain transfer to monomer or chain transfer to CTA. In this way τ will approach τ_{min} ($\tau_{min} \approx \omega$) to make reasonable above basic equation (4.2.3.1). Otherwise one will get a misleading result:

$$\mathop{Lim}_{\substack{x\to 1\\ \tau\to 0}} \left(\frac{dq_2}{dx}\right) = \mathop{Lim}_{\substack{x\to 1\\ \tau\to 0}} \frac{2(1-x)}{\tau(1-x)} \Rightarrow \infty$$

(4.2.3.15)

$$\lim_{\substack{x\to 1\\ \omega\to 0}}\left\{\frac{1}{\varepsilon+\omega}\left[1+\left(\frac{\varepsilon}{\omega}\right)^{\frac{2\varepsilon}{\varepsilon-\omega}}\right]\right\}=\infty$$

(4.2.3.16)

4.2.3.2 Shielding effect on pendant double bond reactivity

The main contribution of the derivation of the crosslinking density distribution is showing that the crosslink density of a primary polymer chain depends on its birth time as well as on the present time and is composed of instantaneous crosslinking and additional crosslinking.

At any specific present time *y*, consider the primary chains (the primary chains are the linear macromolecules which would exist if all crosslinks connecting them were severed) born at time *x* ($y > x$). Since the total double bond conversion is a monotonous increasing function of polymerization time, one can derive the following mass balance for PDB **(see Figure 4.2):**

$$k_{p,p}^{*0} * \{[F_2(x) - D_a(x,y) - D_{pc}(x) - D_{mlp}(x) - D_{sc,a}(x,y)] * N_x\} * [R_T^*] * \Delta t$$
$$= N_x * [D_a(x, y + \Delta y) - D_a(x,y)]$$

(4.2.3.17)

Where:

$k^{*o}_{p,p}$	is the pseudo propagation constant for PDB in the polymer phase.
N_x	is the total number of primary polymer chains born at time *x*.
$F_2(x)$	is the mole fraction of divinyl monomer in polymer chains born at time *x*.
$[R_T^{\bullet}]$	is the total concentration of polymeric radicals
$D_a(x,y)$	is the additional crosslinking density at time y for primary chains born at time *x* (crosslinking units formed by consuming PDB in primary polymer chains born at time *x* by chains born in the time interval, *x* to *y*).
$D_{pc}(x)$	is the primary cyclization (formed at time *x* through a chain growth while consuming PDB on the same primary polymer chain).
$D_{mlp}(x)$	is the divinyl monomer loop (cycle formed at time *x* through propagation successively with the double bond on the same divinyl monomer).
$D_{sc.a}(x,y)$	is the additional secondary cyclization (crosslinked units formed through consuming PDB on chains born at time *x* by chain born in the time interval, *x* to *y*).

Using the equation:

$$\frac{dy}{dt} = k_{p,p} * (1 - y) * [R]$$

(4.2.3.18)

One gets the following fundamental equation for the calculation of additional crosslinking density:

$$\frac{\partial D_a(x,y)}{\partial y} = \left(\frac{k_{p,p}^{*o}}{k_{p,p}}\right) * \frac{F_2(x) - D_a(x,y) - D_{pc}(x) - D_{mlp}(x) - D_{sc.a}(x,y)}{1-y}$$

(4.2.3.19)

In **Figure 4.2** one can see that each crosslinkage connects two crosslinked monomer units $D_a(x,y)$ and $D_i(y)$. Strictly speaking, the total crosslinking density for chains born at time x at present time y is given by:

$$D(x,y) = D_i(y) + D_a(x,y)$$

(4.2.3.20)

and $D_i(y)$ is given by

$$D_i(y) = \int_0^y \frac{\partial D_a(\theta,y)}{\partial \theta} d\theta$$

(4.2.3.21)

There are some assumptions in the derivation of the above equation:

(1) All PDB on primary polymer chains born at time x are statistically distributed, and have the same probability to be attacked by a growing radical

(2) All PDB born at same and/or different time x have the same reactivity

Therefore $F_2(x)$ was assumed to be only controlled by reaction with divinyl monomer. Also it shows that at present time y, all primary polymer chains born at time x will have the same crosslinking density.

But owing to crosslinking, the micro-local-environment of PDB born time x might change with time (shielding effect). And for the same reasons, the PDB born at different times may have different reactivity , as well. From the above discussion, it can be seen that the shielding effect of the pendant double bond comes from the accessibility of the pendant double bond. There are two ways to correct for this shielding effect.

First, (assuming $F_2(x)$ will be unchanged):one could modify the pseudo reaction constant rate $k^{*o}_{p,p}$

$$k^{*o}_{p,p} = \sum_{i=1}^{3}\left(k^{*}_{pi3,p} * \phi^{*}_{i}\right) = \sum_{i=1}^{3}\left(A_{i3} * \exp\left(\frac{-E_{i3}}{RT}\right)\right) * \phi^{*}_{i} \tag{4.2.3.22}$$

where:

A_{i3} is the collision frequency of polymeric radicals with PDB

E_{i3} is the activation energy for PDB adding to a polymeric radical

ϕ_i^* is the number fraction of polymeric radical of type i

Applying the "long chain hypothesis", it might be assumed that E_{i3} is the same for all PDB formed at different times. With a crosslinking increase, more polymeric radicals will be trapped in the polymer network, so that ϕ_i^* will increase. At the same time, the pendant double bonds formed will also be trapped at the polymer network. Therefore, A_{i3} will decrease causing a strong "shielding effect". After some critical point, the decrease in A_{i3} will balance the increase in radical concentration so that $k_{p,p}^{*o}$ will begin to decrease.

What has been done in the present study is to assume a constant $k_{p,p}^{*o}$ and to try to introduce $F_{2,ef}(x)$ which is defined as the "effective concentration" of PDB born at time x:

$$F_{2,ef}(x) = K_F(x) * F_2(x)$$

(4.2.3.23)

where $K_F(x) \in (0,\ 1]$ is a correction factor for the shielding effect. At present study, it is assumed to be only a function of birth time of PDB. The up limit value of $K_F(x)$ is "one" which means no shielding effect. The smaller this correction factor is, the more serious is the shielding effect, therefore the lower is the "effective concentration" of PDB born at this time.

Accepting the assumption that all PDB on primary polymer chains born at time x are statistically distributed, $K_F(x)$ should be a function of divinyl monomer type, concentration of divinyl monomer in the feed, and the polymerization conversion at which a PDB is born. One empirical form of this factor might be assumed to have following most probable distribution function:

$$K_F(x) = (\frac{1}{B}) * \exp(\frac{-x}{B}) \tag{4.2.3.24}$$

In this equation, $K_F(x)$ is the fraction of PDB that maintain their reactivity in the time interval, x to y. B is defined as the "average residence time" of PDB.

It might be proper to assume that when the chemical structure of divinyl monomer, divinyl monomer concentration level in the polymerization system and polymerization temperature are fixed, B could be considered as a constant. The longer the average lifetime time, the larger is the "shielding effect" for this monomer system. Because for this condition there will more PDB left unreacted at the end of the polymerization.

It is clear that B reflects the "average-micro-local-environment" of the polymerization system. For a given limit B, $K_F(x)$ represents the "instantaneous-micro-local-environment" of PDB born at different times x. It is a monotonous decreasing function of birth time of the PDB. The later the birth time of PDB, the more crosslinked will the surrounding be. These PDB would therefore have a longer "life time" which is equivalent to a larger "shielding effect".

The formation of divinyl monomer loops is a function of divinyl radical concentration. At present simplification, it might be defined as a first order function of effective PDB concentration with a dimensionless constant K_{mlp}:

$$D_{mlp}(x) = f\left\{\phi_2^*(x)\right\} \equiv K_{mlp} F_{2,ef}(x)$$

(4.2.3.25)

The PDB consumed by forming divinyl monomer loop do not partake in primary cyclization. According to the "random flight model", it might be formulated as a first order reaction of PDB available with a dimensionless constant K_{pc}:

$$\begin{aligned} D_{pc}(x) &= K_{pc}\left[F_{2,ef}(x) - D_{mlp}(x)\right] \\ &= F_{2,ef}(x) K_{pc}\left[1 - K_{mlp}\right] \end{aligned}$$

(4.2.3.26)

The additional secondary cyclization by definition is associated with the additional crosslinking with a dimensionless constant $K_{sc,a}$:

$$D_{sc,a}(x,y) = K_{sc,a} D_a(x,y) \tag{4.2.3.27}$$

4.3 Model Application

In this section, parameter estimation and one calculation example is presented to show the shielding effect on the crosslinking density distribution. The kinetic equations describing above mechanisms of emulsion polymerization with crosslinking will be simulated by a Monte-Carlo method in next chapter. The simulation is based on the distribution of time interval between adjacent radical entry, the time interval distribution between two adjacent reaction steps between each radical entry and the probability for a specific reaction to happen in this step.

4.3.1 Parameter estimation

It can been seen from above derivation that constant K represents the ratio of the pseudo propagation constant for PDB and the pseudo propagation constant for all double bonds in the polymer phase.

$$K = \frac{k^{*\circ}_{p,p}}{k_{p,p}} = \frac{\sum\limits_{i=1}\left(k^*_{pi3,p}\phi^*_i\right)}{\sum\limits_{i=1}\sum\limits_{j=1}\left(k_{pij,p}\phi^*_i f_j\right)}$$

(4.3.1)

It might be suitable to make following assumptions at present $k^*_{p23,p} \approx k^*_{p33,p}$, and $k_{p31,p} \approx k_{p21,p}$, and $k_{p32,p} \approx k_{p22,p}$. Then what follows is:

$$k^{*\circ}_{p,p} = \sum_{i=1} k^*_{pi3,p}\phi^*_i \approx k^*_{p13,p}\phi^*_1 + k^*_{p23,p}(1-\phi^*_1)$$

(4.3.2)

$$\begin{aligned} k_{p,p} &= \sum_{i=1} k_{pij,p}\phi^*_i f_j \\ &\approx (k_{p11,p}f_1 + k_{p12,p}f_2)\phi^*_1 + (k_{p21,p}f + k_{p22,p}f_2)(1-\phi^*_1) \end{aligned}$$

(4.3.3)

It has been mentioned above that normally the pendant double bonds are less reactive, so that it might be reasonable to assume that :

$$k^*_{p13,p} = \frac{1}{2}k_{p12,p}, \text{ and } (k^*_{p23,p} = k^*_{p33,p}) \approx (\frac{1}{2}\ k_{p22,p} = \frac{1}{2}k_{p32,p})$$

(4.3.4)

so that :

$$K = \frac{k_{p,p}^{*\circ}}{k_{p,p}}$$

$$\approx \frac{0.5\left[k_{p12,p}\phi_1^* + k_{p22,p}(1-\phi_1^*)\right]}{\left[k_{p12,p} + f_1(k_{p11,p} - k_{p12,p})\right]\phi_1^* + \left[k_{p22,p} + f_1(k_{p21,p} - k_{p22,p})\right](1-\phi_1^*)}$$

(4.3.5)

It is shown that K is usually smaller than one. Also it could be considered as a constant if only the monomer compositions and polymerization temperature are kept constant.

4.3.2 Calculation example

In this section, one simplified calculation result is presented with the aim of showing the effect of shielding on the crosslinking density distribution.

Substituting equations of (4.2.3.25) to (4.2.3.27) into equation of (4.2.3.19), one can get the following equation:

$$\int_0^{D_a(x,y)} \frac{dD_a(x,\xi)}{F_{2,ef}(x)\left[(1-K_{pc})(1-K_{mlp})\right] - (1+K_{sc,a})D_a(x,\xi)} = \int_x^y K \frac{d\xi}{1-\xi}$$

(4.3.6)

Following the assumption that K is a constant and that $F_{2,ef}(x)\left[(1-K_{pc})(1-K_{mlp})\right]$ is a constant if $F_{2,ef}(x)$ could be considered as only the function of PDB birth conversion, one can get that:

$$D_a(x,y) = F_{2,ef}(x)\frac{(1-K_{pc})(1-K_{mlp})}{1+K_{sc,a}}\left\{1-\left[\frac{1-y}{1-x}\right]^{K(1+K_{sc,a})}\right\}$$

(4.3.7)

Based on the equation of (4.2.3.21), it can be shown that:

$$D_i(y) = \int_0^y \frac{K}{1-y}\left\{\left[F_{2,ef}(\theta)(1-K_{mlp})(1-K_{pc})\right]\left[\frac{1-y}{1-\theta}\right]^{K(1+K_{sc,a})}\right\}d\theta$$

(4.3.8)

For $K(1+K_{sc,a}) \neq 1$:

$$D_i(y) = KF_{2,ef}(y)\frac{(1-K_{pc})(1-K_{mlp})}{1-K(1+K_{sc,a})}\left\{[1-x]^{K(1+K_{sc,a})-1}-1\right\}$$

(4.3.9)

For *$K(1+K_{sc,a})=1$:*

$$D_i(y) = -KF_{2,ef}(y)(1-K_{mlp})(1-K_{pc})Ln(1-x)$$

(4.3.10)

Figure 4.3 shows the result of a sample calculation comparing the original model with the present modified model. The parameters used in this calculation are: B=1, F_2 =0.05, K_{pc}=0.1, K_{mlp}=0, $K_{sc,a}$=0.1 and K=0.75. In **Figure 4.3**, subscript m means modified model.

From equation (4.3.7) one can understand that: (1) for any present conversion y, the PDB birth conversion can vary in the region $x \in [0, y)$; (2) $D_a(x,x)=0$ which means that additional crosslinking occurs among primary chains with different birth time; (3) for any present time y, $D_a(0,y)$ is the maximum value which means that the primary chain born at $x=0^+$ has the maximum reactivity to crosslink because the PDB born at this low conversion is readily available with minimal shielding effect from the network structure and (4) if $K_{pc,}$ $K_{sc,a}$ K_{mlp} increase the additional crosslinking will decrease because cyclization reactions will consume more PDB.

From equations (4.3.9) and (4.3.10) one can understand that $D_t(x=0^+)=0$ and it is a monotonous increasing function of time for both conditions. Note that the total crosslinking density $D_t(x,y)$ seems to decrease.

In the present calculation F_2 is assumed constant. From an understanding of the principles of semi-batch operation, adding parts of the two monomers at the start to get the required copolymer composition and feeding both of them incrementally, one might be able to keep the polymer composition constant during the polymerization.

But as the present model predicts that due to the shielding effect of PDB, the "crosslinking effective composition" of polymer chains might not be the same as the stoichiometric composition. So that it could be understood that even though the composition $F_2(x)$ is kept constant by way of some semi-batch operation, the effective PDB concentration $F_{2,ef}(x)$ will change with conversion. At high monomer conversions, one can expect that more PDB are trapped in the polymer network. It should be noted that with semi-batch feeding of monomers, copolymer composition may be kept constant, however, it should also be noted that copolymer concentration increases with time and this will affect branching, crosslinking and microstructure.

4.4 Summary

In this chapter, an attempt has been made to elaborate on the mechanisms involved in batch emulsion polymerization for the MMA/EGDMA system. The effect of termination mechanism on the network formation has been elucidated. The crosslinking density distribution model has been modified to account for the shielding effect on the PDB reactivity. A Monte-Carlo simulation of the kinetic equations for the emulsion polymerization with crosslinking described in section 4.2.1 will be presented in the next chapter.

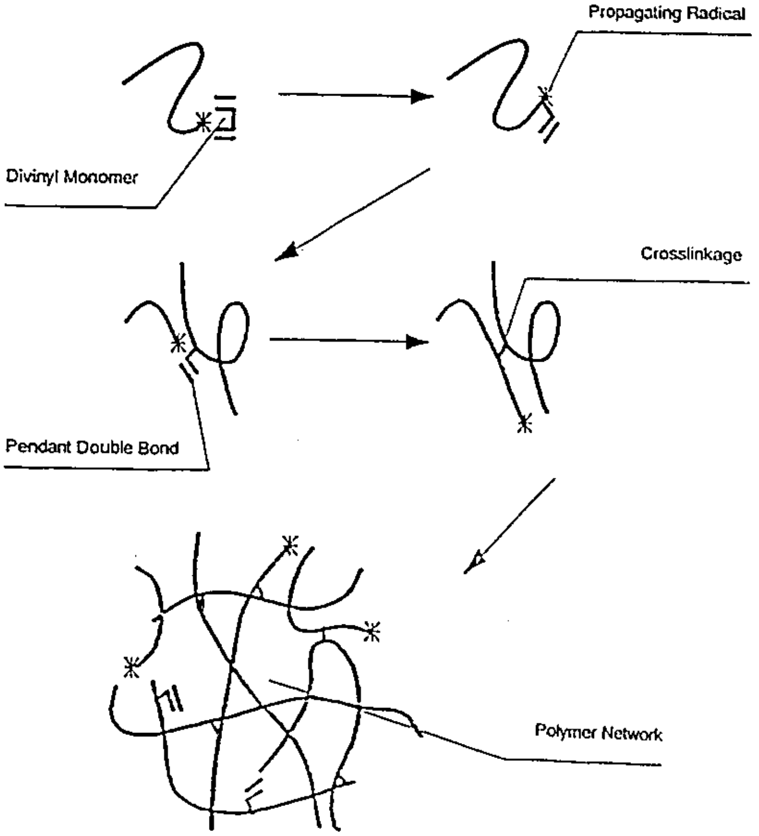

Figure 4.1 Schematic drawing of crosslinking process -- (propagation with PDB) in free radical polymerization of vinyl/divinyl monomers.

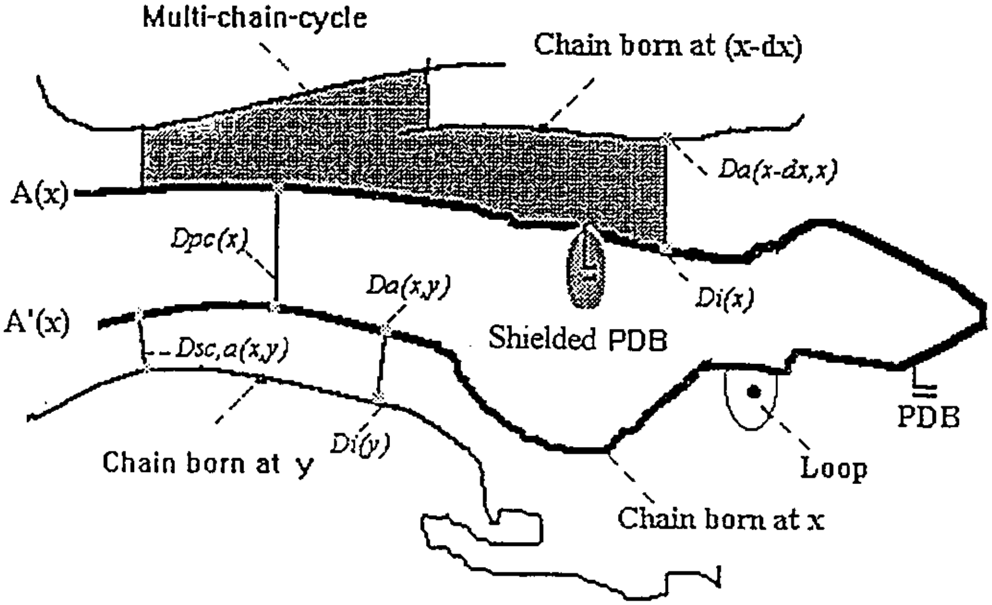

Figure 4.2 Schematic drawing of polymer network formation in free radical polymerization. Chain propagation direction is from A(x) to A'(x). Shielded PDB is the pendant double bond having reduced reactivity because of the shielding effect by chains which are part of the crosslinked polymer network.

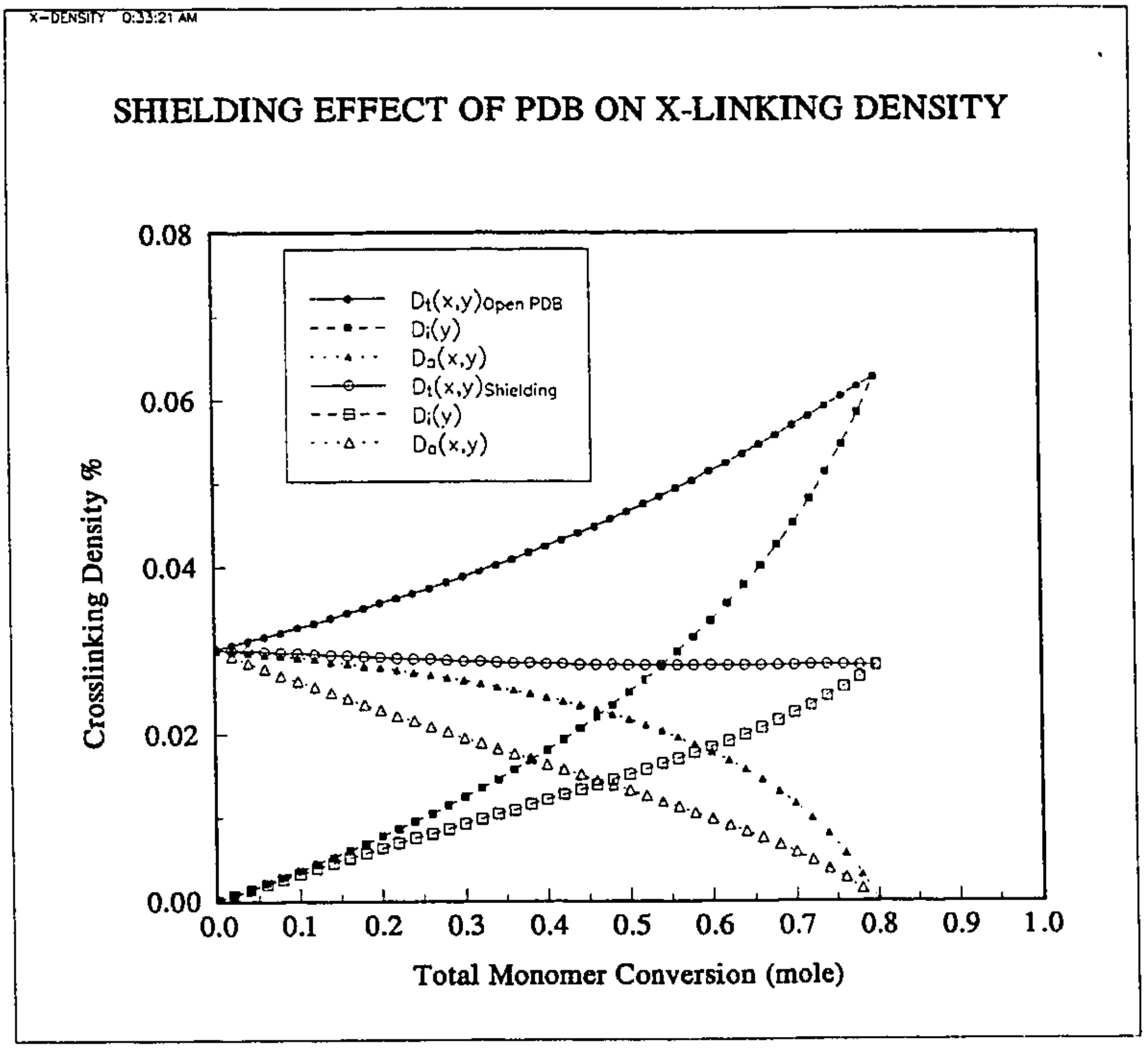

Figure 4.3 Calculated crosslinking density distribution using original model and modified model. $F_2=0.05$; B=1; K=0.75; $K_{pc}=0.1$ and $K_{sc,a}=0.1$, $K_{mlp}=0$.

4.5 References

1 Luther, M., and Heuck, C. (I. G. Farbenindustries A. G.), *US Pat.* 1932, 1864078, (Chem. Abstr., 1932, **26**, 4505)

2 Napper, D. H. and Gilbert, R. G. in "Comprehensive Polymer Science", vol. **4**, page 171, Pergamon Press, 1989

3 Harkins, W. D. *J. Am. Chem. Soc.* 1947, **49**, 1428, *J. Polym. Sci.* 1947, **5**, 217

4 Bovey, F. A. "Emulsion Polymerization,-- High Polymer Series vol. IX", 1955

5 Piirma, I. and Gardon, J. L. eds, "Emulsion Polymerization, ACS Symp. Series 24", New York Academic Press, 1976

6 Bassett, D. R. and Hamielec, A. E. eds, "Emulsion Polymer and Emulsion Polymerization, ACS Symp. Series, **165**", America Chemical Society, 1981

7 Barton, J. and Capek, I. eds "Radical Polymerization in Dispersion system", Ellis Horwood, 1994

8 Smith, W. V., and Ewart, R. H. *J. Chem. Phys.* 1948, **16**, 592

9 Broadhead, T. O., Hamielec, A. E. and MacGregor, J. F. *Makromol. Chem. Suppl.* 1985, **10/11**, 105

10 Hamielec, A. E., MacGregor, J. F. and Penlidis, A *Makromol. Chem. Macromol Symp.* 1987, **10/11**, 521

11 Tobita, H. and Hamielec, A. E. *Makromol. Chem., Macromol. Symp.* 1988, **20/21**, 501.

12 Tobita, H. and Hamielec, A. E. *Makromol. Chem., Macromol. Symp.* 1990, **35/36**, 193

13 Tobita, H. *Macromolecules*, 1992, **5**, 2671

14 Gardon, J. L. *J. Polym. Sci., Polym. Chem.* 1968, **6**, 2859

15 Charmot, D. and Guillot, J *J. Makromol. Chem. Suppl.* 1985,**10/11**, 235

16 Carothers, W. H. *Trans. Faraday Soc.* 1936, **32**, 39

17 Flory, P. J. *J. Am. Chem. Soc.* 1936, **63**, 3083, 3091, 3096

18 Gordon, M. *Proc. Roy. Soc. (London)* 1962, **A 268**, 240

19 Pearson, D. S. and Graessley, W. W. *Macromolecules* 1978, **11**, 528

20 Dotson, N. A. *Macromolecules* 1992, **25**, 308

21 Scranton, A. B. and Peppas, N. A. *J. Polym. Sci., Part A: Polym. Chem.* 1990, **28**, 39

22 Miller, D. R. and Macosko, C. W. *Macromolecules* 1978, **11**, 656

23 Miller, D. R. and Macosko, C. W. *Macromolecules* 1980, **13**, 1063

24 Miller, D. R. and Macosko, C. W. *J. Polym. Sci., Part B:, Polym. Phys.* 1987, **25**, 2441

25 Miller, D. R. and Macosko, C. W. *J. Polym. Sci., Part B:, Polym. Phys.* 1988, **26**, 1

26 Dotson, N. A. and Macosko, C. W. *Macromolecules* 1988, **21**, 2560

27 Tobita, H. "Crosslinking Kinetics in Free Radical Copolymerization". Ph.D. Thesis, McMaster University, Canada,(1990)

28 Tobita, H. and Hamielec, A. E. *Polymer* 1992, **33**, 3647

29 Zhu, S., and Hamielec, A. E. *Macromolecules* 1992, **25**, 5457

30 Zhu, S., and Hamielec, A. E. *Makromol. Chem., Theory & Simulation* 1993, **2**, 587

31 Teymour, F. and Campbell, J. D. DECHEMA-Mongr. 1992, **127**, 149

32 Teymour, F. and Campbell, J. D. *Macromolecules* 1994, **27**, 2460

33 Loshaek, S. and Fox, T. G. *J. Am. Chem. Soc.* 1953, **75**, 3544

34 Minnema, L. and Staverman, A. J. *J. Polym. Sci.* 1958, **29**, 281

35 Kwant, P. W. *J. Polym. Sci., Part A: Polym. Chem.* 1979, **17**, 1331

36 Mikos, A. G. and Peppas, N. A. *Macromolecules* 1986, **19**, 2174

37 Mikos, A. G., Takoudis, C. G. and Peppas, N. A. *Polymer* 1987, **28**, 998

38 Landin, D. T. and Macosko, C. W. *Macromolecules* 1988, **21**, 846

39 Simpson, W. and Holt, T. *J. Polym. Sci.* 1953, **10**, 489; 1955, **18**, 335

40 Loshaek, S. *J. Polym. Sci.* 1955, **15**, 391

41 Gordon, M. and Roe R. J *J. Polym. Sci.* 1956, **21**, 27, 39, 57, 75

42 Aso, C. *J. Polym. Sci.* 1959, **39**, 475

43 Haward, R. N. *J. Polym. Sci.* 1954, **14**, 535

CHAPTER 5

MONTE-CARLO SIMULATION OF EMULSION POLYMERIZATION KINETICS WITH CROSSLINKING

5.1 Introduction

The theoretical derivation of the kinetic equations for free radical polymerization is usually based on the steady-state assumptions. Although these assumptions are valid in most cases, under certain conditions the steady-state hypothesis is not valid ^{1}. In the emulsion polymerization process, in addition to all the chemical reaction steps, there are the diffusion processes for monomer molecules, free radical initiator and chain transfer agent fragments as well as the polymeric radicals which may have one or more radical centers. The description of these phenomena involves a very complicated set of coupled ordinary differential equations (ODE). This set of coupled non-linear ordinary differential equations is difficult to solve. In these situations, Monte-Carlo simulation method shows its power. In this chapter, a new general stochastic Monte-Carlo simulation algorithm has been developed for emulsion polymerization with crosslinking.

In general, Monte-Carlo methods involve making a large number of random choices among potential outcomes to approximate an average property or property distribution. In the chemical engineering or chemistry area, Monte-Carlo simulation methods have been applied to coupled chemical reactions [2], reaction-diffusion systems[3,4], and for calculating molecular weight distribution in condensation polymerization such as reported by Speckhard *et al* [5,6] in the late 1980s' for the synthesis of polyurethane block copolymers.

Recently, Monte-Carlo methods have been extended to describe the kinetics of free radical polymerization. Several reports have been published for the simulation of molecular weight distribution and copolymer composition heterogeneity [7,9,10], of molecular weight distribution development in pulsed laser polymerization [13,14], crosslinking and microgel formation in free radical polymerization containing multi-vinyl monomers [17-26], as well as of molecular weight distribution in emulsion polymerization [27]. However, the general stochastic Monte-Carlo simulation algorithm for crosslinking emulsion polymerization with the potential to cover all mass transfer and reaction steps involved from stage I to stage III and to describe a host of process kinetic behaviors and polymer properties has not been found in the literature.

5.1.1 Molecular weight distribution and composition heterogeneity of copolymers

Mirabella [7] examined the variation in the cumulative copolymer composition with chain length. Choosing only initiation and propagation reaction steps, he calculated the instantaneous and cumulative copolymer composition for any desired chain length as a function of initial feed composition by Monte-Carlo method. Calculation was compared with experimental results of three (styrene/vinyl sterate) copolymers containing initial styrene mole fraction of 0.5, 0.8 and 0.9 separately. Results showed that for short polymer chains the initiation reaction could have a significant influence on the commutative copolymer composition. No comparison was made with Stockmayer's bivariate distribution [8].

O'Driscoll [9] has used the Monte-Carlo method to examine the compositional heterogeneity of binary and ternary copolymers. He recognized that both the initiation and termination reactions could influence the compositional heterogeneity. In his calculation he assumed that there was no particular selectivity between these two steps to simplify the calculations.

Galbraith *et al*[10] claimed that there was significant selectivity in the initiation and termination, that this effect should be examined and that ignoring this effect could lead to a significant error in the simulated copolymer composition. They used Monte-Carlo methods to calculate influences of the initiation and termination reactions on the molecular weight distribution and compositional heterogeneity.

In Galbraith's[10] calculation, the basic polymerization mechanism was assumed to be the terminal model. The initiation via initiator-derived radical and the termination via mutual reaction of polymeric radicals were neglected. Reaction of chain transfer agent radical with monomer molecules (initiation), propagation with monomers, and chain transfer of polymeric radicals to chain transfer agent molecules (chain termination) were considered in their simulation.

Their method was applicable for systems containing two to four monomer types and could calculate the copolymer composition and sequence distribution. There were three setting options in this program: (a) constant monomer composition; (b) varying monomer composition with conversion; (c) semi-batch process with a chosen number of monomer addition steps. Particularly, their model was suitable for the simulation of copolymerization carried out in the presence of a chain transfer agent. The calculation results showed that the effects of initiation and termination were most noticeable for low molecular weight copolymers. Again, in that work, Galbraith *et al* [10] did not compare their calculation results with the Stockmayer bivariate distribution [8] model or experimental results.

5.1.2 Pulsed laser polymerization (PLP)

Pulsed laser initiation of free radical polymerization and the resulting molecular weight distribution was first investigated by Aleksandrov *et al* [11]. The idea of using a pulsed laser to evaluate rate constant separately was first suggested by Olaj and coworkers [12] who showed that with this method they could distinguish k_d and k_t individually from the combined group (k_d / k_t).

As a kinetic method, PLP consists of repetitively irradiating a monomer mixture containing a photo initiator for very short time period (ca. 10 ns) at a specific (constant or other configuration) time interval (in second order of time) for relatively long time (ca. 1000 s). During the laser pulse, radicals are generated. During the dark period, these radicals can grow by propagation, chain transfer or can terminate bi-molecularly. Those radicals that survive the dark period will join fresh radicals produced in the next laser pulse. In this manner, monomer conversion and polymer chain length distribution can develop gradually.

O'Driscoll *et al* [13] reported the application of a Monte-Carlo method for PLP. Their results showed that the molecular weight distribution consists of two superimposed distributions. One had a relatively broad distribution representing the termination reaction during the dark time. The other was a rather sharply peaked distribution representing the termination reactions occurring as a result of a large number of small radicals coexisting for a very short period the laser pulse time. The postulate that the inflection point on that sharp peak could be used to calculate the propagation rate constant was tested and found to be accurate to within 3%.

At almost the same time, Yang *et al* [14] independently reported similar results. For the first step in their simulation, this method was tested by the radical polymerization with a continuous initiation mechanism. They assumed combination termination and compared their simulation of radical concentration with the analytical solution describing the time dependent radical concentration during the unsteady-state time period [15]:

$$[R^{\bullet}] = \sqrt{\frac{k_d[I]_O}{k_t}}\ \mathrm{th}\left(2\sqrt{k_d k_t [I]_O}\ \bullet \mathrm{t}\right) \tag{5.1.1}$$

Their simulation results at fixed starting initiator concentration $[I]_o$, termination rate constants k_t and different initiator decomposition rate constant k_d were in very good agreement with the analytic solution. These results clearly showed the approach to steady-state of the radical concentration in the system. To further confirm their method, the steady-state assumption was applied to simulate the time-dependent monomer conversion, chain length distribution and these were compared with the following analytical solutions [16]:

$$Ln\frac{[M]}{[M]_O} = k_p\sqrt{\frac{k_d[I]_O}{k_t}}\ t \tag{5.1.2}$$

$$v = \frac{k_p[M]}{2\sqrt{k_d k_t [I]}} \tag{5.1.3}$$

Again, their simulation results agreed with the analytical solutions very well. In the above tests of the model, the starting monomer and initiator molecule numbers were set. What they did was to count the numbers of monomer, initiator, free radical (of different chain length) and dead polymer (of different chain length) for a specific time scale. That was calculated via different probabilities for each reaction event. For the application of Monte-Carlo simulation to the PLP, their method is similar to that of O'Driscoll *et al* [13] and consisted of the following steps:

(1) At time zero, the system contained a certain number of monomer molecules.

(2) During the laser pulse a certain number (limited) of radicals were generated.

(3) During the dark period, the fate of these radicals was checked via different probabilities for the reaction types involved.

(4) The time evolution of monomer, polymeric radical and dead polymer concentration were calculated.

The convenient part of this simulation was that the number of radicals generated via each laser pulse could be set to a finite value. The common weakness of this simulation method is that the total volume of polymerization system should be chosen to transfer the concentration to number. This total volume was assumed as a constant used in the entire calculation.

5.1.3 Free radical polymerization with crosslinking

The emulsion polymerization of multi-vinyl monomers can lead to a heterogeneous mixture of monomer, sol polymer, microgel polymer and polymer gel. This heterogeneous internal structure for the polymer particle can affect the reactivity of monomer and pendant double bonds. Generally, for this system, model solution approaches that have been tried can been divided into three categories: (1) kinetic models, (2) statistical gelation models and (3) Monte-Carlo simulation methods [22].

The kinetic theory describes the crosslinking and branching process as a set of kinetic differential equations. These equations can usually be transferred into a single partial differential equation of the generating function describing the distribution of all molecules. Solutions can only be obtained for chain polymerization with equal and independent reactivity. The kinetic equations can sometime only be conveniently solved using the method of moments. The kinetic models are conceptually and mathematically simple and yet can provide very important infonnation about reactivity and reaction path.

With statistical models, the molecules and structures are generated for monomer units occurring in the different reaction states. The reaction state is characterized by the number and the type of reacted functional groups and the type of their neighbors. The statistical methods are relatively easy extended to multi-functional monomers and enable one to treat complex system. They provide structural information such as elastically effective crosslinking density and primary cyclization. But the methods use state functions instead of time function. Therefore they can not provide the time-dependent reaction information. Also, due to the assumption of reversible reactions, they show good agreement with experimental data for polycondensation reactions but are not satisfactory for free radical polymerizations that are chemically or diffusion controlled.

For the application of Monte-Carlo simulation, there are two different sub-directions: lattice or off-lattice. For the lattice model, the simulation in space takes into account the spatial correlation. It is based on random connections of points of a rigid lattice. Therefore it is able to describe the high extent of cyclization for bulk chain polymerization. Very recently, Chiu and Lee [22] reviewed the key work done to date.

Manneville and De Seze [23] first introduced the simulation method for free radical polymerization of multi-functional monomers. They used a cubic lattice. Each site on the lattice represented either a vinyl or divinyl monomer molecule. Mobility of either monomer or polymer was not considered. All radicals were activated in a short time prior to the polymerization that this was refereed to as "fast initiation". This model could give reasonable trends of polymerization of multi-functional monomers, however the predicted kinetic chain lengths were too smaller and thus in disagreement with experiment.

Boots and Pandey [24] modified the "fast initiation" model. They developed a model allowing a randomly selected monomer molecule to be initiated to a radical at a constant rate. Therefore this model did not consider the different initiator types nor the exponentially decaying rate of initiation. Later, Boots *et al* [25, 26] modified this model by accounting for the polymer diffusion thus termination took place through trapped radicals.

Chiu and Lee [22] realized that in all those earlier models each site on the lattice was considered being occupied by one monomer molecule with all its functional groups represented by this lattice site. Because if this limitation, these models were not sensitive to structural change of monomer or polymer chains. Therefore, they developed a 2-D lattice model of homo-polymerization of divinyl monomer.

In their simulation [22], a lattice of 90 x 90 was introduced. Initiator molecules were first distributed on this lattice randomly. Each was assumed to occupy two adjacent lattice sites that were connected by a bond. Then monomers were randomly placed on the lattice with a pre-specified molar ratio. Each monomer molecule was assumed to be a rigid rod and occupying four lattice sites either horizontally or vertically. After initiation, each radical occupied one site and had four nearest neighbors. The fate of radicals was determined by the status of those four nearest neighbors as well as the setting of probabilities for possible reaction types, monomer translational diffusion and segmental diffusion of polymers.

It can be understood that the obvious limitation of this lattice method is that this model is performed on a lattice, while the actual polymerization proceeds in a continuous phase. However, this model can give a fairly good description of some typical properties for free radical polymerization with crosslinking. These included the general trends of primary polymer size distribution, the pendant double bond conversion, the cyclization fraction, and the heterogeneity of the polymer matrix.

Tobita [17-20] applied the Monte-Carlo method to simulate the molecular weight distribution in free radical crosslinking copolymerization. This method effectively used the crosslinking density distribution of the primary polymer molecules. At any present time (conversion) ψ, considering a randomly selected primary polymer chain born at time θ, $(0<\theta<\psi)$, this randomly selected primary polymer chain will form instantaneous crosslinking point with primary polymer molecules formed at z $(0<z<\theta)$. Also this randomly selected primary polymer chain will form additional crosslinking points with primary polymer chains formed at u $(\theta<u<\psi)$.

Tobita introduced two probabilities to represent these two crosslinking mechanisms [17-20]: one is the probability that the primary polymer molecule formed at $(x=\theta)$ will be connected via instantaneous crosslinking point to the primary polymer molecules formed in the conversion interval $\{z<x<z+\Delta z\}$

$$P_i(z|\theta)\Delta z = \frac{\frac{\partial \rho_a(z,n)}{\partial n}\Big|_{n=\theta}\Delta z}{\int_0^{\theta}\frac{\partial \rho_a(z,n)}{\partial n}\Big|_{n=\theta}dz} \tag{5.1.4}$$

The other is the probability density that the primary polymer molecule formed at $(x=\theta)$ will be connected via the additional crosslinking points to the primary polymer molecules formed in the conversion interval $\{u<x<u+\Delta u\}$.

$$P_a(u|\theta)\Delta u = \frac{\frac{\partial \rho_a(n,u)}{\partial n}\Big|_{n=\theta}\Delta u}{\int_\theta^\psi \frac{\partial \rho_a(n,u)}{\partial n}\Big|_{n=\theta}du}$$

(5.1.5)

It is worth noticing that following the definition of these two probabilities, one can see that the physical meaning of the probability densities of them are the ratio of the local additional crosslinking density to the accumulated instantaneous crosslinking density and the ratio of local additional crosslinking density to the accumulated additional crosslinking density separately.

The first step in his simulation was to randomly select a primary polymer chain in the time range *$(0<\theta<\psi)$*. Because this was a continuous time interval, this sample method was equivalent "to sampling polymer molecules from an infinite number of polymer molecules in the reaction mixture on a weight basis" [17, 18]. Then the chain length of this primary polymer chain (r) was randomly sampled from either the "instantaneous chain length distribution W(r,θ)"[19] or from the "Schulz-Zimm distribution" [19, 20]. The third step was to calculate the number of crosslinking points on this randomly selected primary chain at time θ and with chain length r. This was done using the crosslinking density distribution. The last step was to determine how each crosslinking point connects other primary polymer chains with different birth time.

The power of this method was that crosslinking density distribution was a very important feature of polymer networks synthesized in a kinetically controlled system; it provides information on how each chain is connected to others, therefore the full molecular weight distribution can be simulated by the Monte-Carlo method. The drawback of this model is that there existed an assumed molecular weight distribution type for all primary polymer chains to be sampled, and that for any primary polymer chain, when it was selected will not be put back to the "source" for future sampling. This means that each primary polymer chain sampled from the "source" was always a new one. This does not really happen and is a major weakness of the method.

As for the application of the Monte-Carlo method to the crosslinking emulsion polymerization of vinyl and divinyl monomer systems, to date, publications involving the number of polymer chains in polymer particles, molecular weight distribution, copolymer composition, crosslinking density distribution, and pendant double conversion are virtually nonexistent [27]. The difficulty in the use of Monte-Carlo methods stems from the fact that crosslinking emulsion polymerization is a heterogeneous process with transfer processes occurring between phases and heterogeneity in the polymer particles.

A simplifying factor, however, is that the number of monomer molecules as well as the number of polymer chains in the polymer particle are relatively small. With transfer to polymer and termination by dispropartionation, the polymer chain number will be the same as that for linear chains. With crosslinking (transfer to polymer plus termination by combination and propagation with PDB), the polymer chain number is reduced. This opens the prospect of using Monte-Carlo methods to efficiently simulate the kinetic features of the emulsion polymerization process.

In the following part of this chapter, a new stochastic simulation algorithm has been presented. In the present study, this method is developed to describe the kinetics in stage II where all polymer particles have been generated and their number remains constant.

5.2 Stochastic simulation algorithm

The Monte-Carlo simulation of a chemical reaction system is based on the master equation which describes the stochastic time evolution of this system. [2,28] Few publications have been found in which the application of the Monte-Carlo method to free radical polymerization has been shown probably because of the large number of species. For emulsion polymerization processes, there will be only a relatively small number of polymer chains in the tiny monomer swollen polymer particles.

5.2.1 General algorithm design

For the present simulations, the probability functions for several kinetic events (reaction channels) described in the mechanism described earlier (Chapter 4) must be formulated. It can be understood that one needs knowledge of the following probabilities. **Figure 5.1** shows the flow-sheet for this general algorithm. It shows that the entire simulation consists of four major steps:

(1) the time interval probability density for one radical entering a particle,

(2) the probability for one oligomeric radical to desorb from a particle,

(3) the probabilities for specific reaction steps,

(4) the probability for the time interval between two successive reaction steps.

5.2.2 Time interval distribution for radical entry into a particle

Similar to the PLP simulation, the starting point for the application of the Monte- Carlo method in emulsion polymerization is to generate a reactive center. That is to let a polymer particle receive a radical from the water phase. In the PLP situation, the monomer receives a laser pulse and all the radicals formed are assumed to be introduced into the system in the same short time interval.

However, in emulsion polymerization the situation is different. Free radicals are generated in the water phase continuously. They diffuse into the polymer particles in random manner. That means that not all polymer particles will have received the same number of free radicals at any time.

To calculate the probability density distribution of time interval for a radical to enter a polymer particle, it is necessary to calculate the average time interval (over all time intervals) for radicals to enter into all polymer particles. For the present simulations, the total number of polymer particles is considered as constant (stage II). However, the algorithm could be extended to include the nucleation stage with little difficulty.

As mentioned in the above mechanism, because in a normal emulsion polymerization the time interval for a radical to be deactivated by bimolecular termination in the water phase is much longer than that for it to enter a polymer particle, chain termination in the water phase is neglected, the total rate of radical entry ρ [#/s] in stage II of emulsion polymerization is given by:

$$\rho = \rho_w + \rho_{\mathrm{ren}} \tag{5.2.1}$$

where the ρ_w is the entry rate into polymer particles for radicals produced by decomposition of initiator in the water phase [#/s] and ρ_{ren} is the re-entry rate of radicals desorbed from polymer particles [#/s]. If one assumes that all desorbed oligomeric radicals will re-enter the polymer particles, ρ_{ren} could be represented as the total rate of radical desorption from polymer particles:

$$\rho_{ren} = k_{de}\bar{n}N_T = \frac{a}{d_p^2}\bar{n}\,N_T = \frac{a}{V^{\frac{2}{3}}}\bar{n}N_T$$

(5.2.2)

where:

k_{de} is the overall desorption rate constant of oligomeric radicals from polymer particles (1/s), dp is the diameter of a monomer swollen polymer particle, N_T is the total number of particles in the system, $\bar{n}$ is the average number of radical per particle and V is the volume of one swollen polymer particle, if volume change on mixing monomer and polymer is neglected (i.e. regular solution), $V=V_m+V_p$:

$$V = \frac{1}{\phi_p}V_p = \frac{i}{\phi_p}\left[n_p \frac{M_m}{\rho_p * N_A}\right]$$

(5.2.3)

where:

Vp is the volume of polymer in the polymer particle, ϕ_p is the volume fraction of polymer in the particle, ρ_p is the density of polymer, M_m is the molecular weight of the repeat unit, N_A is the Avogadro's number and n_p is the total number of monomer units in polymer chains within a particle which include the dead polymer and polymeric radicals. Using the assumption that polymer particle system is a regular solution, one gets:

$$n_p = \sum_{i=1}(i*n_{p,i}) + \sum_{j=1}(j*n_{R,j})$$

(5.2.4)

where, $n_{p,i}$ is the number of the dead polymer chains with chain length (i), $n_{R,j}$ is the number of polymeric radicals with chain length (j).

The average time interval for radical entry T_{ave} is given by:

$$T_{ave} = \frac{N_T}{\rho}$$

(5.2.5)

To calculate the time interval probability density distribution for one radical entering into a particle, an assumption has been made that the probability of radical entry is the same for all polymer particles. This assumption does not inroduce a serious error for systems with a narrow particle size distribution. The concept is that for an average time interval T_{ave} considering all particles in the system (N_T) the probability density distribution for number of particles having a radical entry (*Ne*) could be given by following most probable distribution:

$$P(Ne) = \frac{1}{N_T}\exp\left(\frac{-Ne}{N_T}\right)$$

(5.2.6)

Based on the same above assumption, if one specific particle is focused on, the above most probable distribution could be transferred to present the probability density distribution for time interval of radical entry into this particle:

$$P(t_e) = \frac{1}{T_{ave}}\exp\left(\frac{-t_e}{T_{ave}}\right)$$

(5.2.7)

In the present simulation process, one has to transform the continuous random number t_e which is distributed in the interval [0, ∞] with a density distribution function *P(Ne)* by a random number R_1 that has a *uniform distribution function in [0,1]* [29,,30,31] :

$$R_1 = \int_0^{t_e} \frac{1}{T_{ave}}\exp\left(\frac{-t_e}{T_{ave}}\right)dt_e = 1 - \exp\left(\frac{-t_e}{T_{ave}}\right)$$

(5.2.8)

The constraint conditions for this construction function are:

$$\{t = 0\;;\; \mathrm{R}_1 = 0\} \quad \{t = \infty\;;\; \mathrm{R}_1 = 1\} \tag{5.2.9}$$

5.2.3 Radical desorption from a polymer particle

The second step in the simulation is to evaluate the probability of radical desorption from a particle. It is generally accepted that in emulsion polymerization, the principle mechanism for radical transfer between water and polymer particle phases is by the migration of oligomeric radicals with small chain length. If one assumes that a specific radical which has just entered into a polymer particle can undergo desorption, propagation, chain transfer and termination, the required probability for this radical to desorbe out of the particle could be given by:

$$P(des) = \frac{\alpha\, k_{de}}{k_{p,p}[M]_p + k_{fm,p}[M]_p + k_{fT,p}[T]_p + k_{t,p}\left(\dfrac{n-1}{V N_A}\right) + \alpha\, k_{de}} \tag{5.2.10}$$

where:

n is the total number of radicals in the particle (including the newly entered one), α is the coefficient to correct for the difference between the overall desorption rate constant for all type of radicals and the desorption rate constant for that newly entered oligomer radical. N_A is Avogadro's number. In the present simulation, the probability of this desorption can be tested with the following relation by another random number R_2 having a *uniform distribution function in [0,1]:*

$$0 < P(des) \leq R_2 \tag{5.2.11}$$

5.2.4 Time interval distribution for the adjacent reaction in a particle

In a particle of volume *V*, one has a spatially regular mixture of different chemical species shown in the above mechanisms. As polymerization proceeds the system will change its state. Essentially all one should do to simulate emulsion polymerization using the Monte-Carlo method and to move the system forward in time is to answer two questions.

To answer the first question one should solve for the fate of one specific radical when the next adjacent reaction occurs. The time interval between two successive reaction steps in the particle accounted by Δt is also a discrete stochastic variable which could be sampled by another random number with a *uniform distribution function in [0,1]* (R_3):

$$\Delta t = \frac{1}{\sum\limits_{\xi=1}^{M_T} R(\xi)} \ln\left(\frac{1}{R_3}\right) = \Delta t_{ave} \ln\left(\frac{1}{R_3}\right)$$

(5.2.12)

where Δt_{ave} is defined as the average time interval between two successive reaction steps which reflects the kinetic characteristics of emulsion polymerization system under consideration. That is in the summation over all reaction types M_T:

$$\Delta t_{ave} \frac{1}{a} = \frac{1}{\sum\limits_{\xi=1}^{M_T} R(\xi)}$$

(5.2.13)

In the above equations R(ξ) is the rate of type ξ reaction in the particle. Reaction rates of propagation, chain transfer to monomer, chain transfer to polymer, chain termination by recombination or by disproportionation, and propagation with pendant double bonds can all be included in this term. The faster the over all reaction rate, the less is the average time internal for next reaction step to occur.

There are two ways to express the reaction rate of each reaction step involved in the calculation process. One is to express it by the mole concentration of each component. the other is to use the molecule numbers of each one. In the present simulation, because only stage II was considered, monomer molecules were not in the "sample pool". therefore, it would be more convenient to use mole concentrations. Polymeric radicals, dead polymer chains and pendant double bond had to be transferred to those units. For example, for propagation with monomer or chain transfer to monomer, the reaction rates are $R_{p,p} = k_{p,p}[M]_p$, $\mathrm{R}_{\mathrm{fm,p}} = k_{fm,p}[M]_p$, while for chain transfer to polymer it can be expressed as $R_{fp,p} = k_{fp,p}\left(\frac{n_{dp}}{VN_A}\right)$.

5.2.5 Criteria in the adjacent reaction type determination

The second question is: *what kind of reaction will this radical undergo for its next reaction step.* Focusing on any one of the statistically chosen radicals in a particle, if there are totally M_T reactions which can occur with the same statistical probability, the reaction type that will happen in time interval ($t \rightarrow t + \Delta t$) could be constructed as a discrete random variable μ. This discrete random variable has the probability $P(\xi)$ representing the reaction type $\xi \in [1, M_T]$. In the process of Monte-

Carlo simulation it could be sampled by a random number (R_4) with a *uniform distribution function in [0,1] also*

$$\sum_{\xi=1}^{\mu-1} P(\xi) < R_4 \leq \sum_{\xi=1}^{\mu} P(\xi)$$

(5.2.14)

where the probability

$$P(\xi) = \frac{R(\xi)}{\sum_{\xi=1}^{M_T} R(\xi)}$$

(5.2.15)

and P(ξ) satisfies the normalization condition:

$$\sum_{\xi=1}^{M_T} P(\xi) = 1$$

(5.2.16)

The advantage of this algorithm is that a different kind of reaction step in the above mechanism (chapter 4) can be formulated into the simulation frame to consider their influences on the emulsion polymerization with crosslinking.

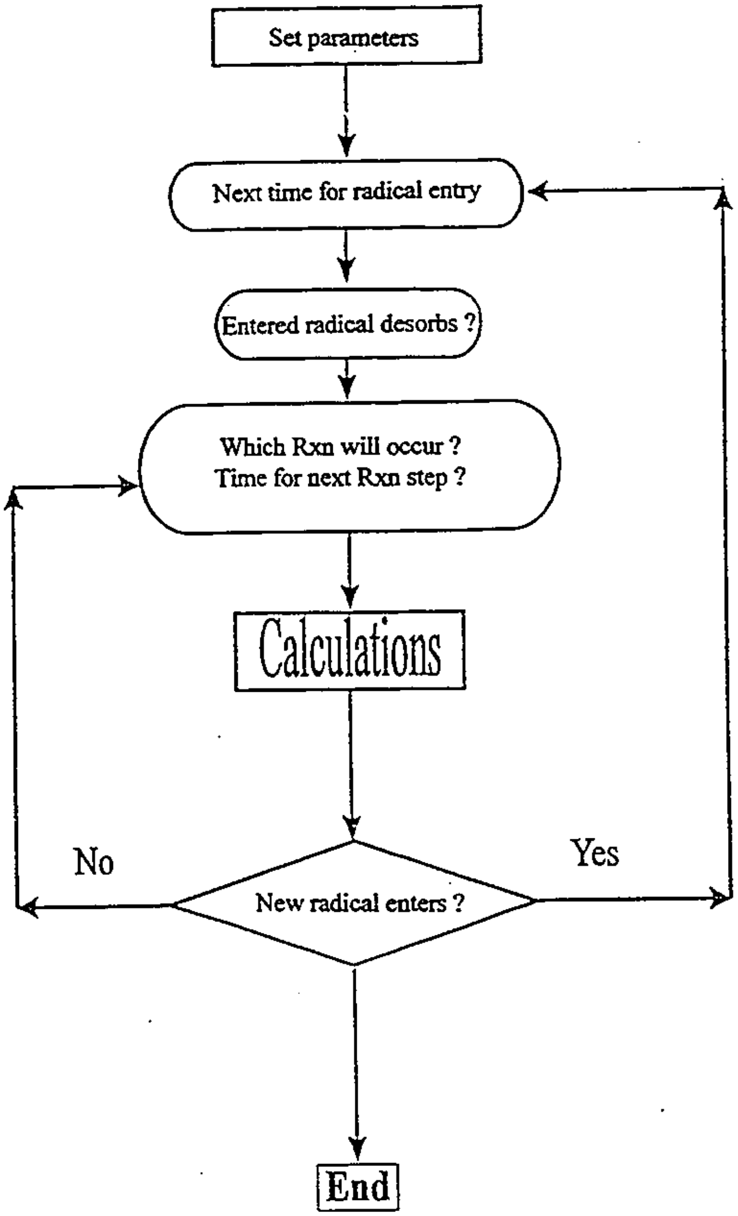

Figure 5.2.1 Schematic drawing of Monte-Carlo Simulation algorithm

5.3 Model Testing and Discussion

Model testing includes two parts. The first part is aimed at testing the basic blocks in the program which do not involve the detail requirements of the reaction kinetic information. The testing events and parameters were selected to meet the specific situation. In the second, three emulsion polymerizations with different kinetic characteristics are simulated. These covered homo-polymerization with chain transfer to polymer plus combination termination, linear copolymerization and copolymerization of vinyl/divinyl monomers causing crosslinking.

5.3.1 Basic testing

Before the real simulations of emulsion polymerization were done, tested were the random number sampling processes of the "time interval for radical to enter a particle", "probability for radical desorption", "distribution of reaction steps in a particle". The purpose is to test the present formulation of probability density and the random number quality. Table 5.1 shows the general parameters used in the following simulation. These parameters are estimated from normal kinetic constants and physical properties of MMA monomer system.

TABLE 5.1 General Parameters used in Simulation

Parameters	*Value*	*Unit*
$k_{p,p}$	210	L/mol•s
$[M]_p$	5.5	mol/L
$k_{tc,p}$	$6x10^6$	L/mol•s
ρ_m / ρ_p	.862	
ρ_p	1.089	g/cm^3
M_m	100	g/mol
V_m	0.6	
N_t	600	particles/L

Radical entry interval

Figure 5.3.1 shows the calculated time interval between radical entry into a particle versus total monomer units in polymer chains. This calculation was based on equations 5.2.1 to 5.2.5. It shows that when Nt/Rw is small, radicals enter polymer particles more often, the average time interval will be small. This value approaches "steady-state" level quickly as the particle grows which is reflected by the "total number of monomer units in polymer chains" in a polymer particle.

Figure 5.3.2 shows the results of comparing the calculation of probability density using equation 5.2.7 and the Monte-Carlo simulation using formulation 5.2.8. **Figure 5.3.3.** shows the relative error of using the Monte-Carlo simulation assuming the analytical solution is correct. The error range is within 2.5%. The simulation result is therefore considered satisfactory.

Free radical desorption probability

Figure 5.3.4 shows the simulated radical desorption probability using equation 5.2.10 and 5.2.11. Circle symbols (both solid and open) are for the situations in which at the start of calculation the polymer particle contained only one radical. It shows that desorption probability is not a function of radical entry rate. For polymer particle with one initial radical, radical termination term is zero. In this case equation 5.2.10 is a typical power law function with negative exponent $f(x) = ax^{-b};\ (b > 0)$. Desorption probability decreases rapidly as the polymer particle volume increases and then gradually approaches a constant low level.

However, if polymer particles initially contain two radicals, radical termination term in the denominator of equation 5.2.10 will reduce the radical desorption probability. In the very small particle volume range, radical termination has a predominant effect on the fate of the entered radical. In fact termination may be instantaneous. When particle volume increases, P(des) will initially increase.

Then gradually the numerator of equation 5.2.10 will become the controlling factor because it has a higher exponent and P(des) will then decrease with further increase in particle volume. The two curves approach each other as particle volume increases. This shows that the radical termination term will have less and less influence. At the limit condition two situations will become one governed by equation $f(x) = ax^{-b};\ (b > 0)$.

Distribution of reaction steps in a particle

To simulate the polymerization events proceeding with time, one has to know how many reaction steps will happen in between two successive radical entries. The probability density distribution of time interval for the radical entry has been available. Using formulation 5.2.12, the probability density distribution for two successive reaction steps in a polymer particle can be calculated. So the distribution of reaction steps in a particle can be derived.

Figure 5.3.5 shows one of the simulation results. In this case the average time between radical entry is $\Delta T_{avg} = 10s$. The average reaction step between each radical entry was set at $a = \sum_{\xi=1}^{M_T} R(\xi)$ = 100 (1/s). In this figure, X axis is the simulated reaction (polymerization) time. The distance between two date points in X axis is the time of simulated time interval between radical entry. The left Y axis is the simulated reaction steps which occur in each interval between radical entry (shown in Bar). The right Y axis is the average number of reaction steps calculated from the above two values $(Y_{left} \div X,)$ shown in solid diamond symbols that should be around the average time interval between two reaction steps (a=100 1/s).

From **Figure 5.3.5** one can see that the longer the time interval between radical entry is, the greater is the number of reaction steps in this interval, but the average reaction step number seems to approach a constant 100 (dot reference lines).

To test the present simulation algorithm, specifically the quality of the "pseudo random number generator" used in the present program that is very important in the application of Monte-Carlo simulation methods, four simulation runs were done under above conditions. **Figure 5.3.6** shows the results. This figure shows all data were around a=100 (1/s) average value. Also there was no correlation of simulated "average Rxn step" change with reaction time. Statistically, the results are satisfactory.

In order to test if the present simulation algorithm could suit different polymerization kinetic situations that is the different combination of reaction steps, four different "a" values (100-500 1/s) have selected for further calculation. It could be understood that the larger the number a is, the faster will be the overall polymerization rate. **Figure 5.3.7 to 5.3.10** show the simulation results. The average time between radical entry that means initiation rate in the water phase was fixed at 10 sec. The profiles do reflect the desired results. Statistically, the results are satisfactory.

Based on above testing results, it has been confirmed that the present simulation algorithm can work properly to meet the different requirements involved in the emulsion polymerization process including different initiation system (initiation rate, radical desorption extent) in the water phase. It has the flexibility to be extended to cover different monomer systems reflected by the "average reaction steps" combinations.

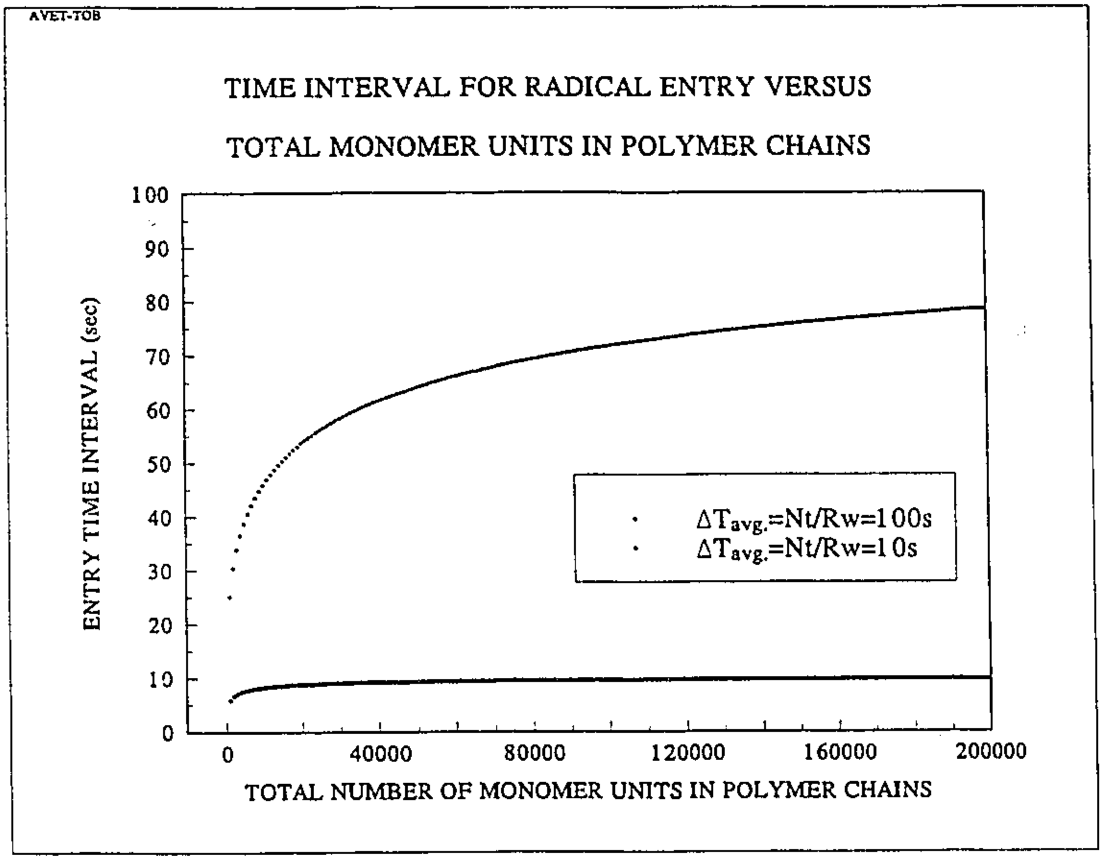

Figure 5.3.1 The calculated average time interval between radical entry into a particle vs total monomer units in polymer chains.

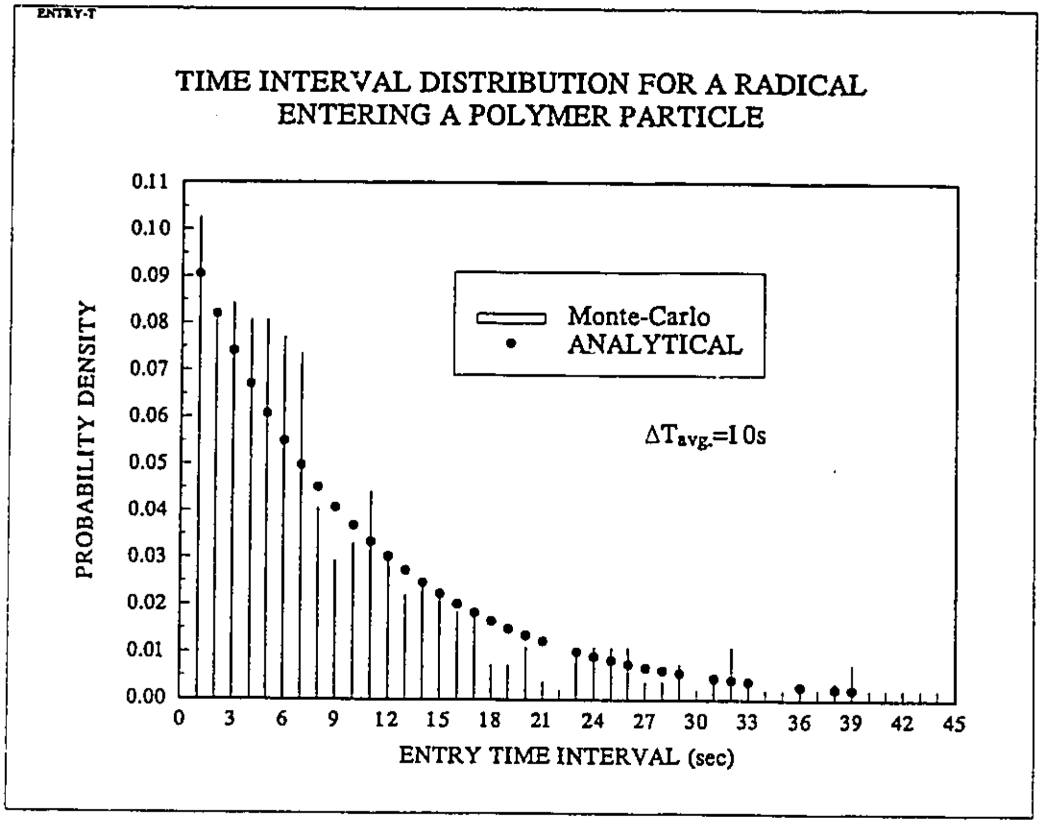

Figure 5.3.2 Probability density distribution of time interval between radical entry into a polymer particle.

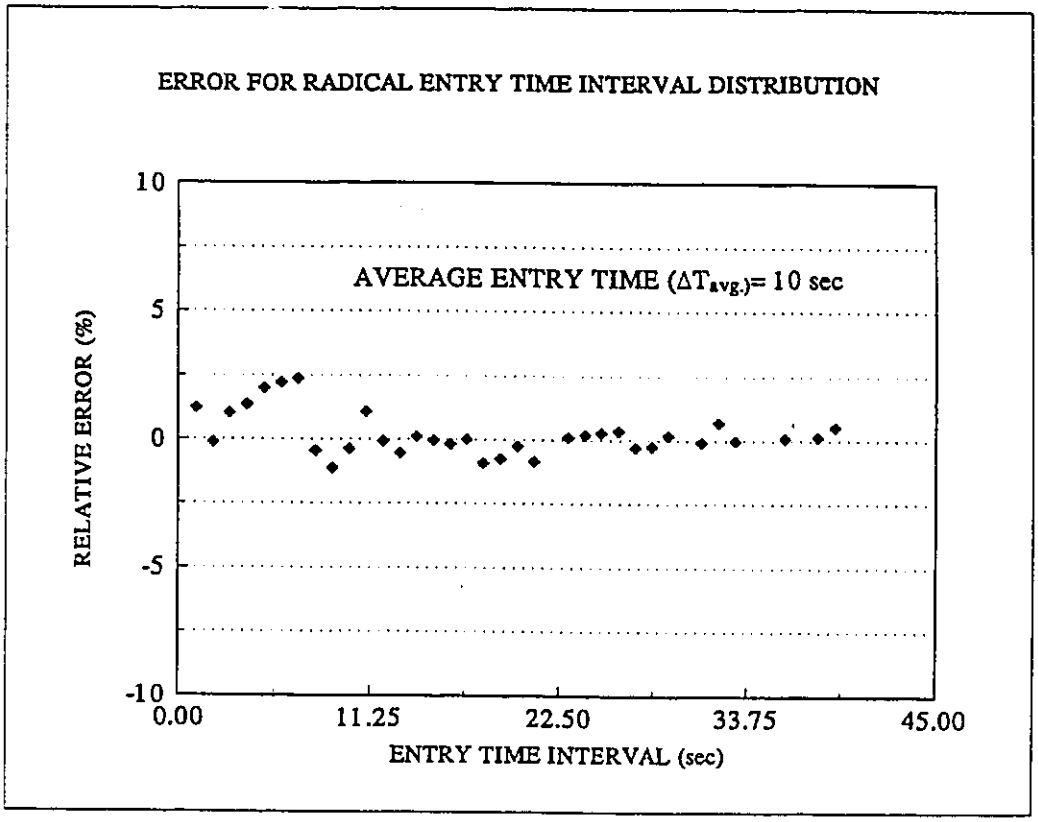

Figure 5.3.3 Error between analytic solution and Monte-Carlo simulation for probability density distribution of time interval between radical entry into a polymer particle.

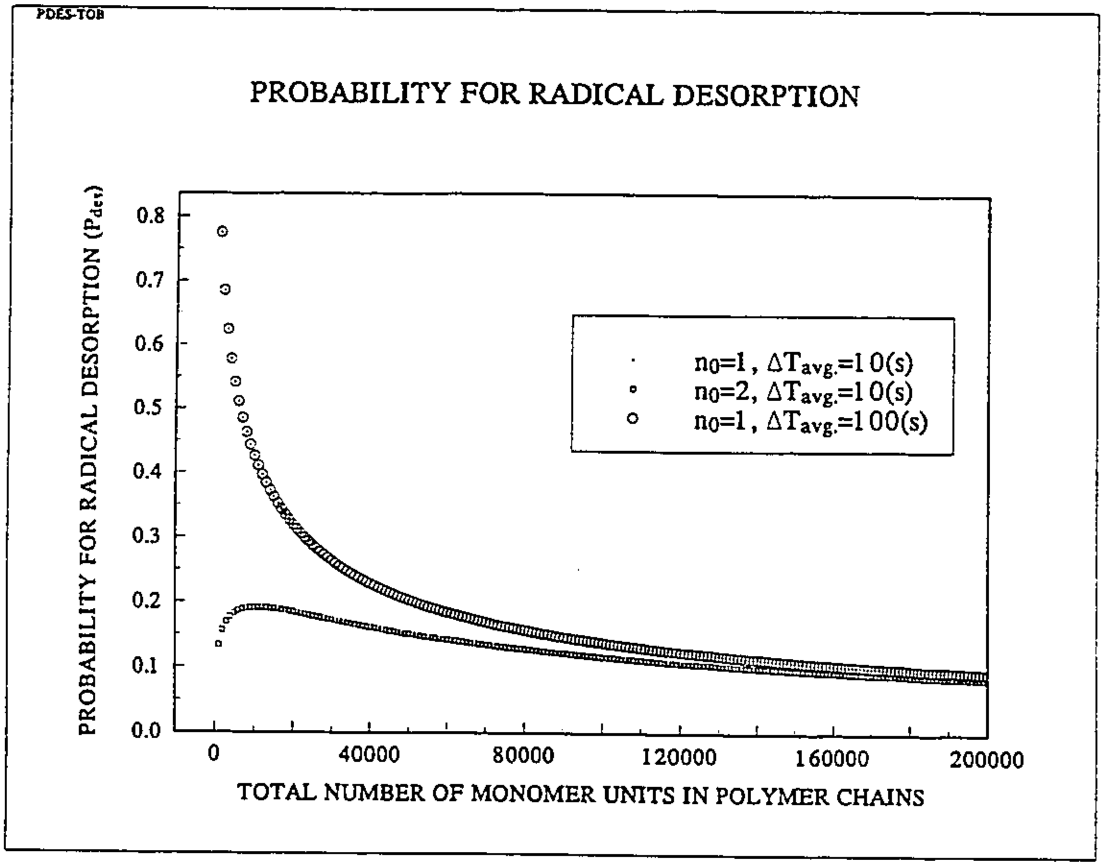

Figure 5.3.4 Probability density distribution for radicals desorbing from a polymer particle.

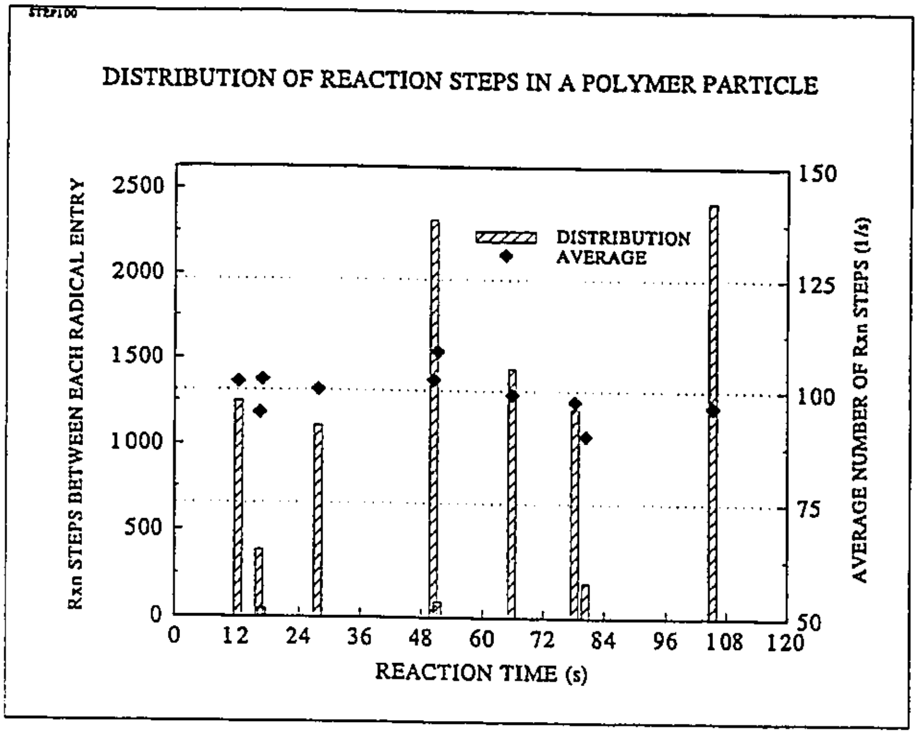

Figure 5.3.5 Probability density distribution for number of reaction steps between two successive radical entries. $\sum_{\xi=1}^{M_T} R(\xi) = {}^{1}\!/_{\Delta t_{ave}} = 100(1/s)$. Average time interval between radical entry: $\Delta T_{avg}=10s$.

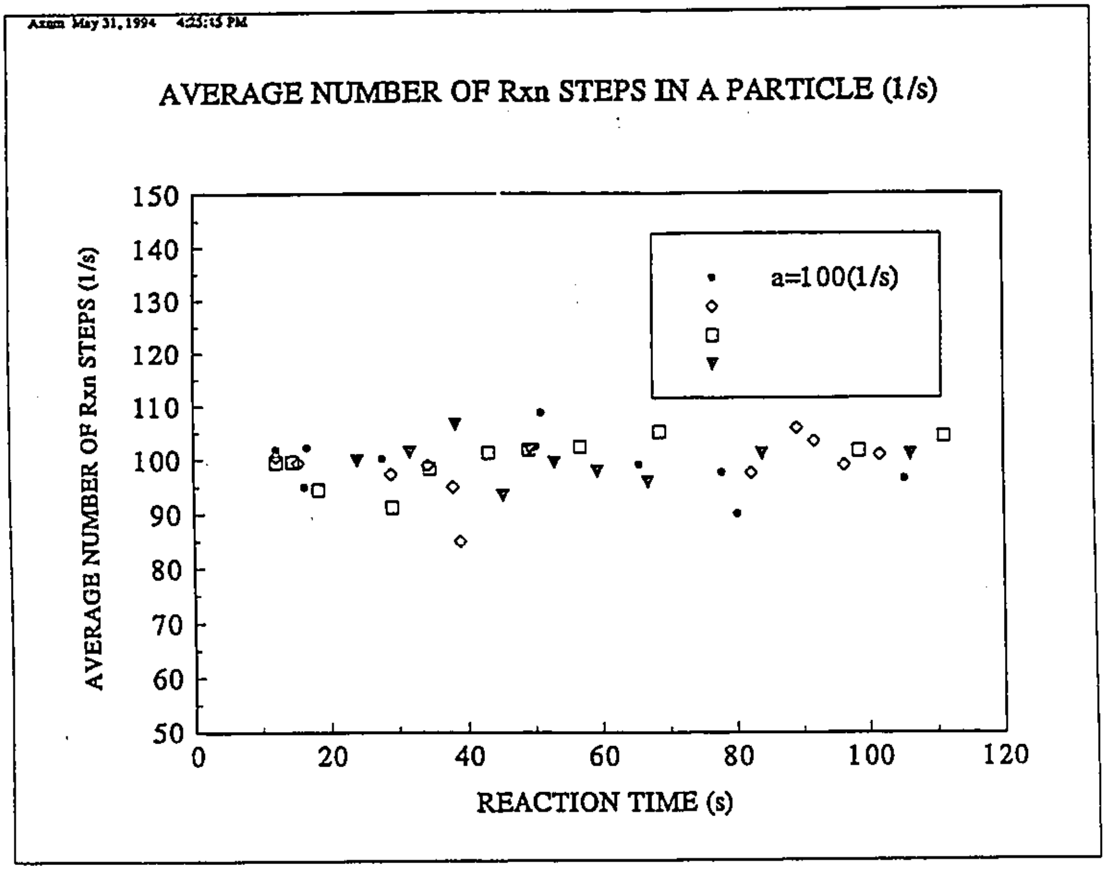

Figure 5.3.6 Reproducibility of simulation of probability density distribution for number reaction steps between two successive radical entries. Average time interval between radical entry: ΔT_{avg}=10s. $\sum_{\xi=1}^{M_T} R(\xi) = 1/\Delta t_{ave} = 100(1/s)$

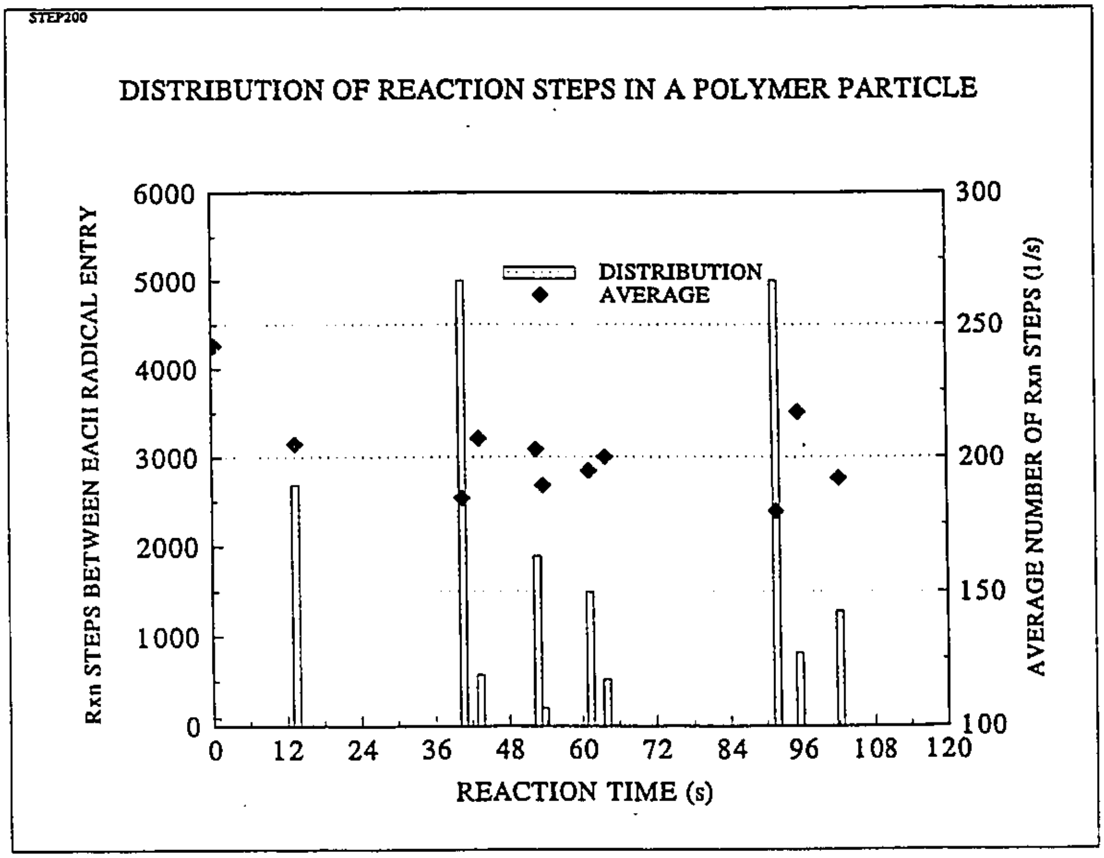

Figure 5.3.7 Probability density distribution for number of reaction steps between two successive radical entries. $\sum_{\xi=1}^{M_T} R(\xi) = {}^{1}\!/_{\Delta t_{ave}} = 200(1/s)$. Average time interval between radical entry: ΔT_{avg}=10s.

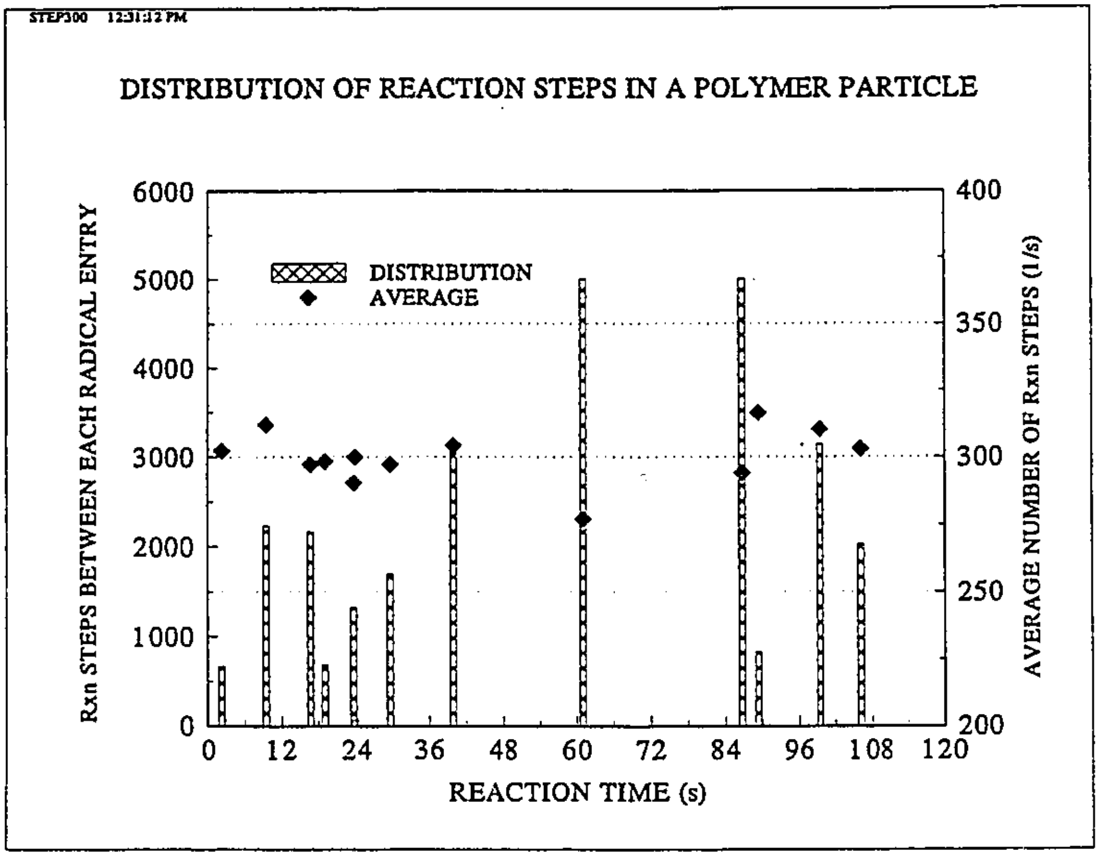

Figure 5.3.8 Probability density distribution for number of reaction steps between two successive radical entries. Average time interval between radical entry: ΔT_{avg}=10s. $\sum_{\xi=1}^{M_T} R(\xi) = 1/\Delta t_{ave} = 300(1/s)$

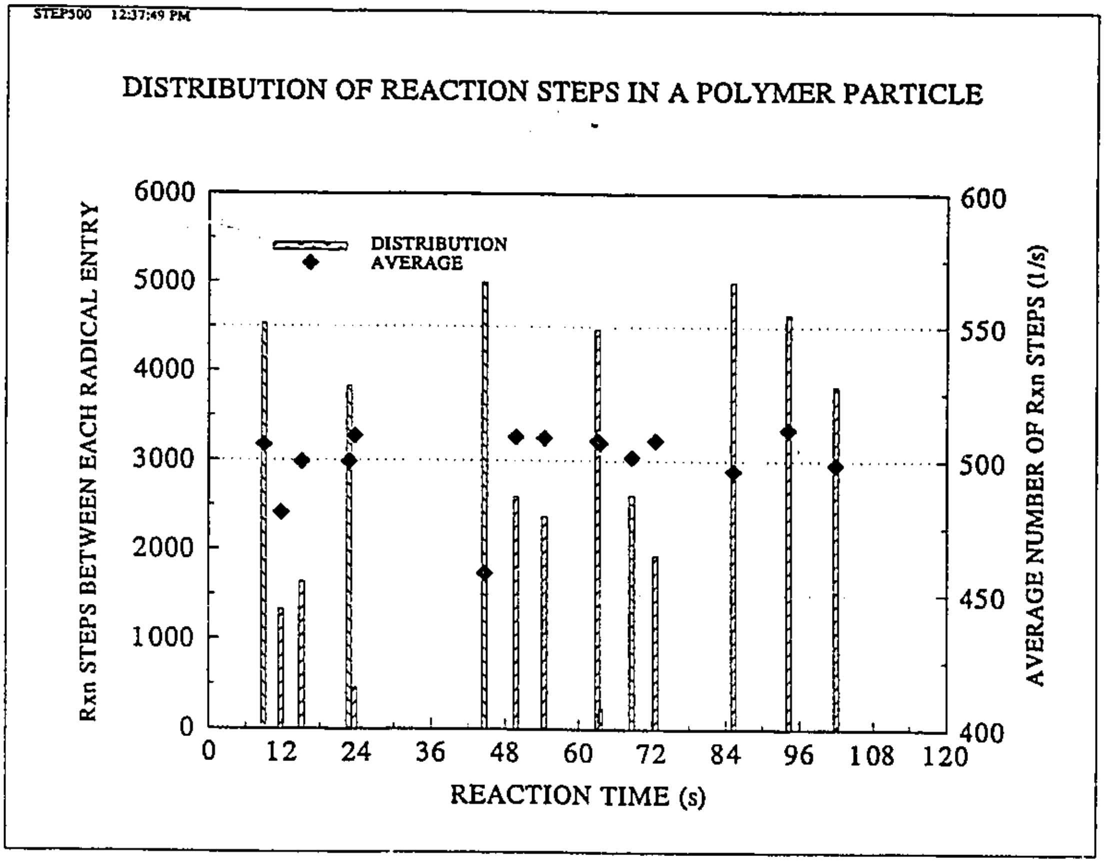

Figure 5.3.9 Probability density distribution for number of reaction steps between two successive radical entries. Average time interval between radical entry: $\Delta T_{avg}=10s$. $\sum_{\xi=1}^{M_T} R(\xi) = {}^{1}\!/_{\Delta t_{ave}} = 500(1/s)$.

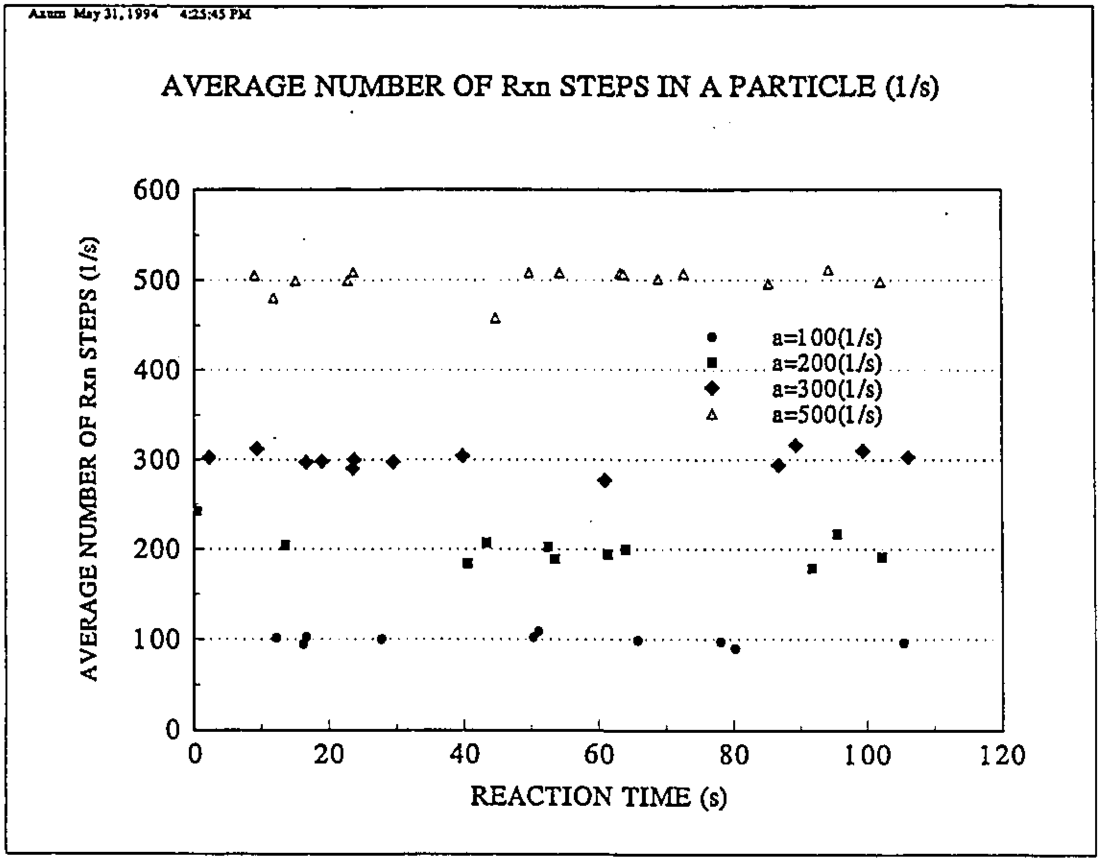

Figure 5.3.10 Probability density distribution for number of reaction steps between two radical entries for different $\sum_{\xi=1}^{M_T} R(\xi) = 1/\Delta t_{ave.}(1/s)$. Average time interval between radical entry: ΔT_{avg}=10s.

5.3.2 Emulsion polymerization with chain transfer to polymer

Long chain branches on polymer chains occur both intentionally and fortuitously. In bulk polymerization, especially in the high monomer conversion region, the possibility of long chain branching via chain transfer to polymer should be considered for most free radical polymerizations. The long chain branches can have a significant effect on the molecular weight distribution.

On the basis that the rate of chain transfer to polymer is proportional to the degree of polymerization, it can be understood that in emulsion polymerization, compared with bulk polymerization, the loci of polymerization (the polymer particle) will have a high polymer concentration for the instant of birth. The long chain branching, if any, will have an influence on the system over the whole conversion range.

Because of its importance, the Monte-Carlo simulation was next applied to "emulsion homo-polymerization with chain transfer to polymer". In the present simulation, besides the basic kinetic parameters mentioned in the Table 5.1, three chain transfer to polymer constant ratios ($C_{fp,p} = \frac{k_{fp,p}}{kp,p}$) were chosen ($C_{fp,p}$ = 0.0001; 0.0005; 0.001). The average time between radical entry was taken as ΔT_{avg}=10s.

With the method of moments, one critical assumption is that each polymer radical is allowed to possess only one radical center regardless of the structure and size of this polymeric radical. In the present simulation, as can be seen from the above development of the algorithm, there was no such assumption made. Also, in the present simulation, in the polymer particle considered, the propagation with monomer, chain transfer to polymer and termination reactions occur simultaneously. No primary polymer chain concentrations and molecular weight distributions have to be assumed.

Figure 5.3.11 is a simulated result showing the effect of chain transfer to polymer on the number average chain length (Ln) and weight average chain length of polymer chains (Lw). In this figure, the "open symbols with lines" stand for the time profiles of "number average chain length". The solid symbols represent the "weight average chain length". Triangle symbols (solid and open) are for the largest chain transfer to polymer rate constant ratio.

It can be seen that with these three chain transfer to polymer rate constant ratios the time profiles for number average chain length are similar and do not change with time. However, for the weight average chain length, the changes with reaction time can be very dramatic. With chain transfer to polymer, the total chain number in the polymer particle will not change and therefore the number average chain length should not change with respect to time (monomer conversion) or with level of the transfer to polymer constant ratio. However, chain transfer to polymer will create long chain branches on some polymer chains increasing their weight without changing these number and that causes significant increases in Lw. In the present simulation, considering the molecular weight of monomer (Mm=100 g/mol) the weight average molecular weight of the polymer changes from $3x10^6$ to $7\ x10^6$ (g/mol) in 300 sec when $\beta = (k_{tc,p}/k_{p,p}) = 2.85x10^4$ and $C_{fp,p} = 0.001$.

One calculation has been reported by Tobita [32] for bulk polymerization with $\beta = (k_{tc,p}/k_{p,p}) = 5x10^{-4}$ (a very low value) and $C_{fp,p} = 0.001$. The calculated weight average chain length changed from $8x10^3$ to $2x10^5$ up to 30% conversion level. This demonstrates that in bulk polymerization molecular weights can be much lower than that in emulsion polymerization. This is clearly due to the fact that from the time of birth of a polymer particle it has a high polymer concentration.

Figure 5.3.12 clearly shows the polymer dispersity index (PDI) increase with reaction time. In this figure, an interesting observation is that when the chain transfer to polymer constant ratio $C_{fp,p}$ equals 0.0001 and 0.0005, the effects of this transfer reaction on the PDI are fairly moderate and do not increase so rapidly with reaction time. However, when $C_{fp,p}$ is 0.001 the effect is very strong and appears almost from the very beginning (zero conversion). This result basically tells that in emulsion polymerization there might be a critical $C_{fp,p}$ value that can be reached either by changing temperature for fix monomer feed or by adding small amount of monomer with more labile hydrogen atoms. After this critical point the chain transfer to polymer will play a most important role in raising the weight-average molecular weight.

Figure 5.3.13 and **Figure 5.3.14** show the simulated time profiles for tri-functional long chain branching frequency and the time profile of the number of dead polymer chains in polymer particles. It can be seen that only for the $C_{fp,p}$=0.001 case, does the tri-functional long chain branching frequency show a clear increase with time after a certain reaction time. Also it can be seen that the dead polymer chain concentrations for all three $C_{fp,p}$ values monotonous increase with time.

The primary effect of chain transfer to polymer is to give a tri-functional branching point with a reactive radical center. The future of these branching points depends on the termination mechanism thereafter. They might cause long chain branches or crosslinkages. It should be emphasized that in the present simulations, combination termination reaction has been taken into account. So that these simulation results actually account for trifunctional long chain branching and crosslinking.

Another point should be stressed. Based on the result that the total number of dead polymer chains in above three cases are not near one and increase with time, it might be expected that at higher conversions gelation might occur. Of course, when the polymer particles are smaller (c.a. < 1000 ⮨) the capacity of a polymer particle to hold a polymer network is limited and according to Flory's criterion for gelation ($\overline{M}_w \to \infty$), these small particles may never experience gelation.

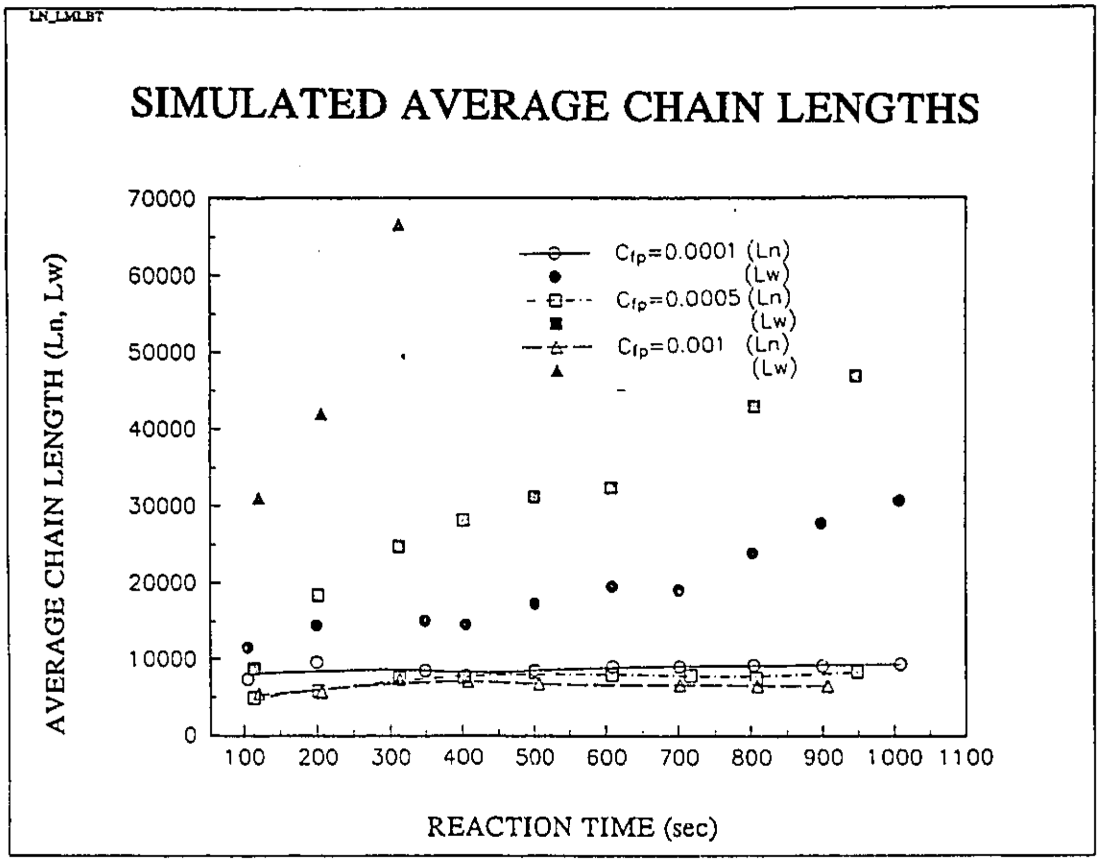

Figure 5.3.11 Monte-Carlo simulations showing the effect of chain transfer to polymer on the number average chain length (Ln) and weight average chain length of polymer chains (Lw) in emulsion polymerization of a vinyl monomer. k_p = 210 L/mol•s, k_{tc} = 6×10^6 L/mol•s.

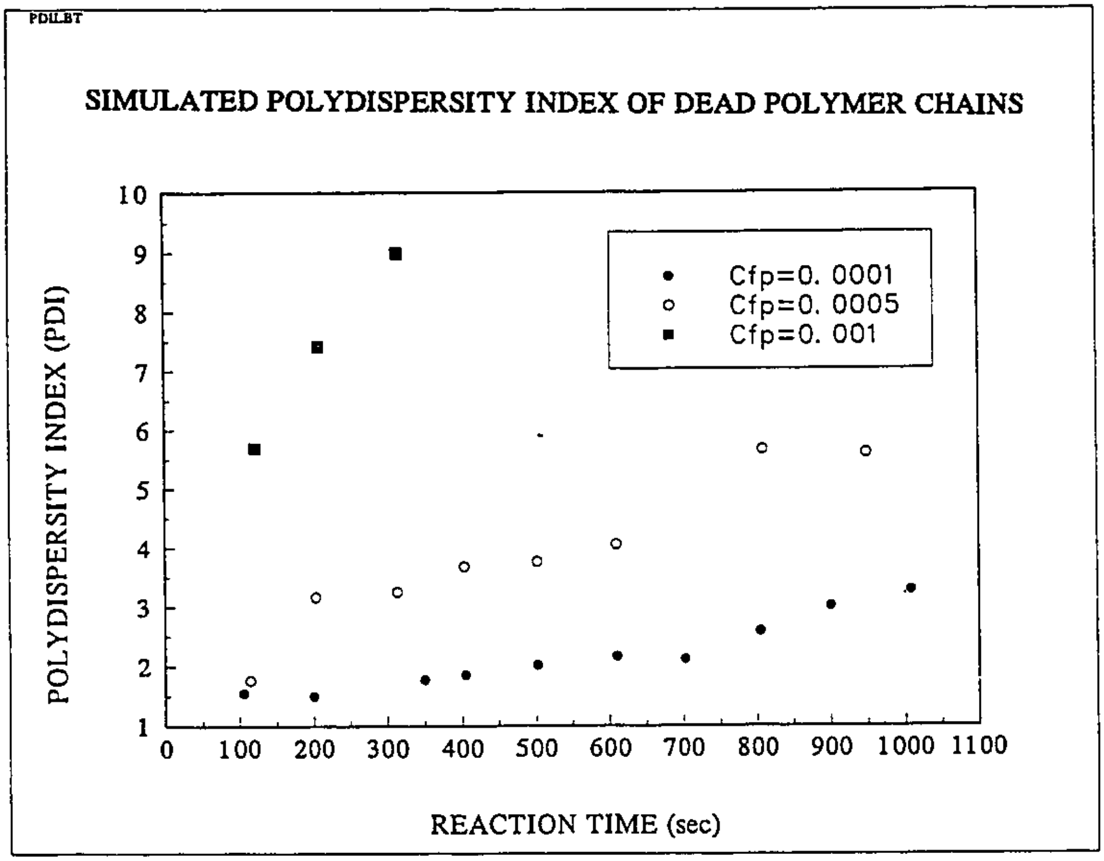

Figure 5.3.12 Simulated results by the Monte-Carlo method showing effect of chain transfer to polymer on PDI of polymer chains in emulsion polymerization of a vinyl monomer. $k_p = 210$ L/mol•s , $k_{tc} = 6x10^6$ L/mol•s.

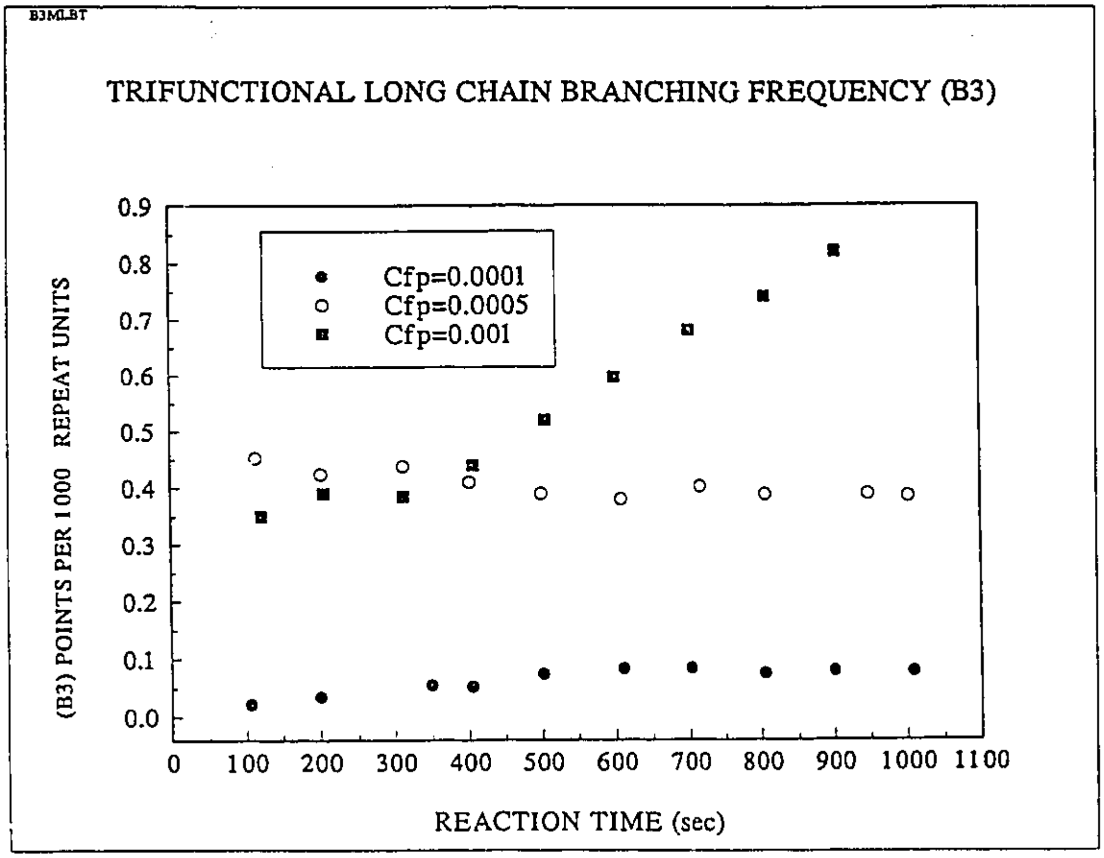

Figure 5.3.13 Simulated results by the Monte-Carlo method showing the time profile of trifunctional long chain branching frequency of polymer chains in a polymer particle during emulsion polymerization of a vinyl monomer. $k_p = 210$ L/mol•s, $k_{tc} = 6 \times 10^6$ L/mol•s.

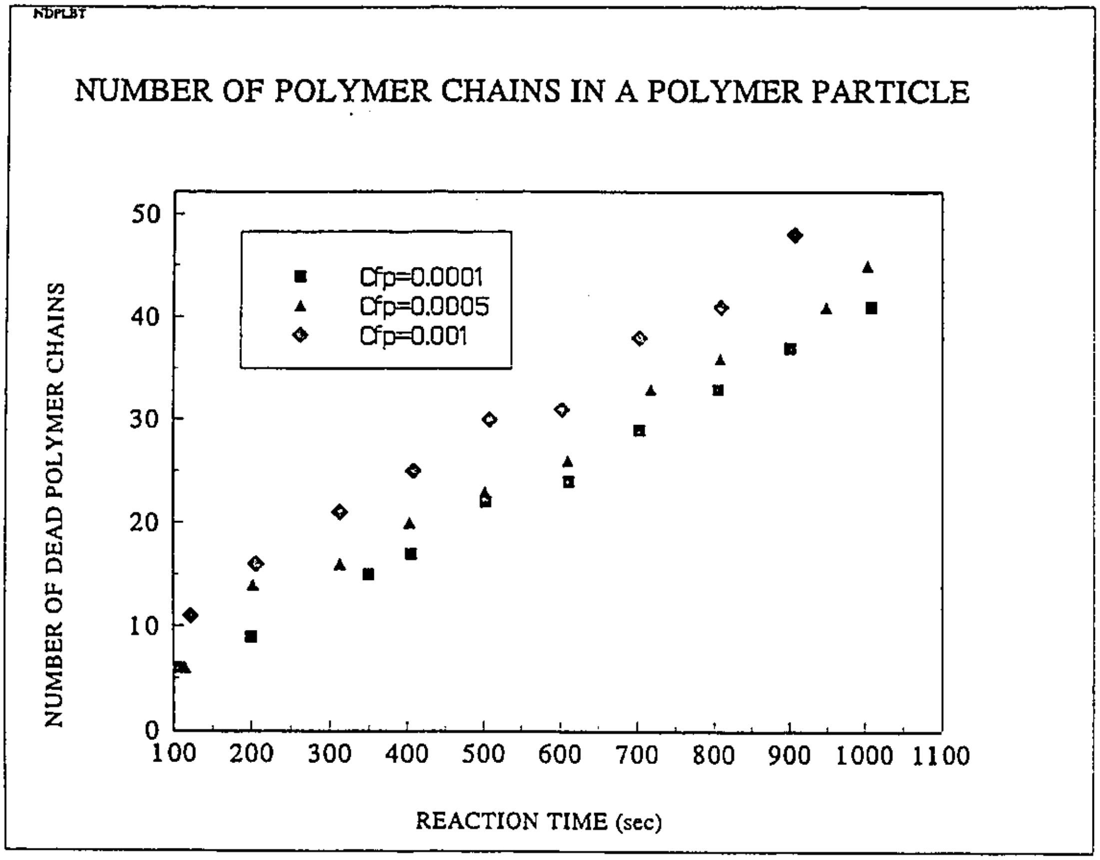

Figure 5.3.14 Simulated results by the Monte-Carlo method showing the time profile of number of dead polymer chains in a polymer particle during emulsion polymerization of a vinyl monomer. $k_p = 210$ L/mol•s, $k_{tc} = 6\times10^6$ L/mol•s.

5.3.3 Emulsion copolymerization of vinyl/divinyl monomers

In this part, the Monte-Carlo method was first tested using copolymerization in a semi-continuous process. By checking the deviation of simulated copolymer composition from calculated [33] "instantaneous copolymer composition", the validity of the extension used from one type of radical to multi-type radicals has been confirmed and this permits the set up of the Monte-Carlo simulation for vinyl/divinyl emulsion polymerization with crosslinking.

Emulsion copolymerization of vinyl monomers

Before being applied to the polymerization of vinyl and divinyl monomer system, this program was tested for linear chain copolymerization. In these calculations, to isolate variables, the monomer composition was kept constant (semi-batch policy). Chain transfer to monomer, chain transfer agent and polymer were not considered, initially. The termination by combination reaction was accounted for. In addition to the kinetic parameters mentioned in the Table 5.1, in this case, the additional kinetic parameters used are as follows [34] :

k_{p11}: 490 (L/mol•s) $k_{p22} = 2\,k_{p11}$

r_1: 0.67 r_2: 1.49

ΔT_{avg}: 2.5, 5, 10 (s) f_{10}: 0.85

Using these kinetic parameters, the calculated "instantaneous copolymer composition" using the Mayo-Lewis equation [33] is $F_{10} = 0.791$ and should be constant theoretically because the monomer composition in the simulation was kept constant.

Figure 5.3.15 shows one example of the calculated time profiles for total number of monomer repeat units and composition of copolymer in a polymer particle. In this figure, solid circle symbols show total monomer units (monomer one and two), and open circle symbols, monomer units of monomer type one. Right Y axis means simulated copolymer composition of monomer of type one (mole fraction). Solid-triangle symbols show the calculated copolymer composition from monomer repeat units calculations shown in the same figure. The dot line is the "instantaneous copolymer composition" versus polymerization time. It is clear that Monte-Carlo simulation results do agree with calculation results by Mayo-Lewis equation.

An additional kinetic factor in emulsion polymerization is that the initiation rate (time interval between radical entry) may change because of increase in polymerization temperature, increase in initiator concentration, using of a redox initiation system or simply because of the duration of polymerization time. All these effects can be included in the present algorithm by using proper kinetic equations, initial conditions and criteria.

In the present simulation, in order to test the sensitivity and flexibility of the Monte-Carlo simulation, three average radical entry times were used. **Figure 5.3.16** shows the results of these simulations. In this figure, open symbols represent "accumulated copolymer composition" simulated from time 0 to about 100 sec, 200 sec and 300 sec separately. The solid symbols represent the total chain number in a polymer particle. It can be seen that copolymer composition does not change with change in time interval between radical entry or with increase in reaction time as expected. However, the chain number in a polymer particle does increase with "reaction time". And the longer the time interval between radical entry is, the fewer is the chain number. This means that variation in radical generation rate in the water phase has no effect on copolymer composition, but does affect the total number of copolymer chains. The reason is that when the time interval between radical entry is long, there might be some time when no reaction will occur in a polymer particle because during this time no radical exists within this particle.

As has been done in the "Basic Testing", to test the reliability and reproducibility of this program, one of above case has been simulated three times. The basic reason for doing this is that in the "Basic Testing" part, the present simulation algorithm has been only tested regarding "how many reaction steps will, on average, happen between each radical entry". Now one further step is that "what type of reaction will happen based on a certain combination of kinetic events". **Figure 5.3.17** shows the results of these simulations. Here the open symbols show the copolymer composition, and the "short dash" line is the average value that is around the value calculated by using Mayo-Lewis equation ($F_{10} = 0.791$). The solid symbols represent the time profiles of total polymer chain number in a particle. The "dot dash" line gives the average value. It is clear that the reproducibility is satisfactory.

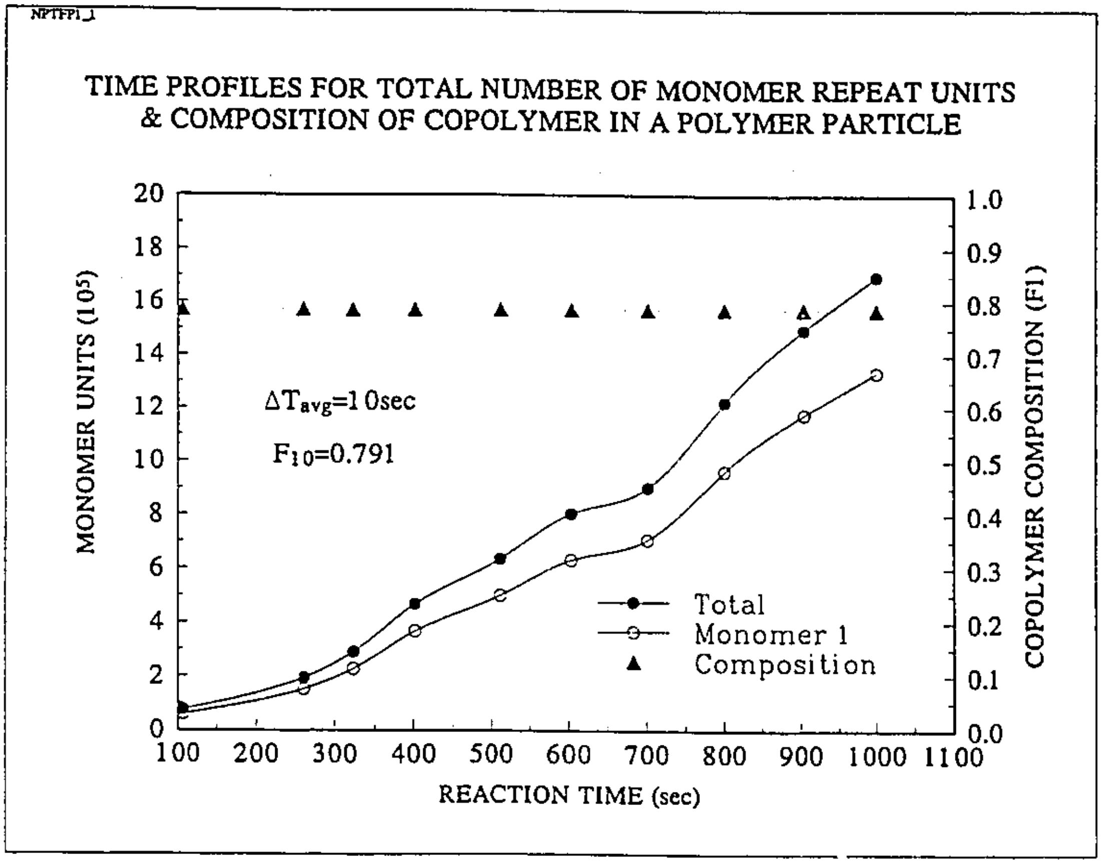

Figure 5.3.15 Calculated time profiles for number of monomer repeat units and composition of copolymer in a polymer particle during emulsion copolymerization of vinyl monomers (without crosslinking). $k_{p11} = 490$ L/mol•s, $k_{p22} = 2\ k_{p11}$, $r_1 = 0.67$, $r_2 = 1.49$.

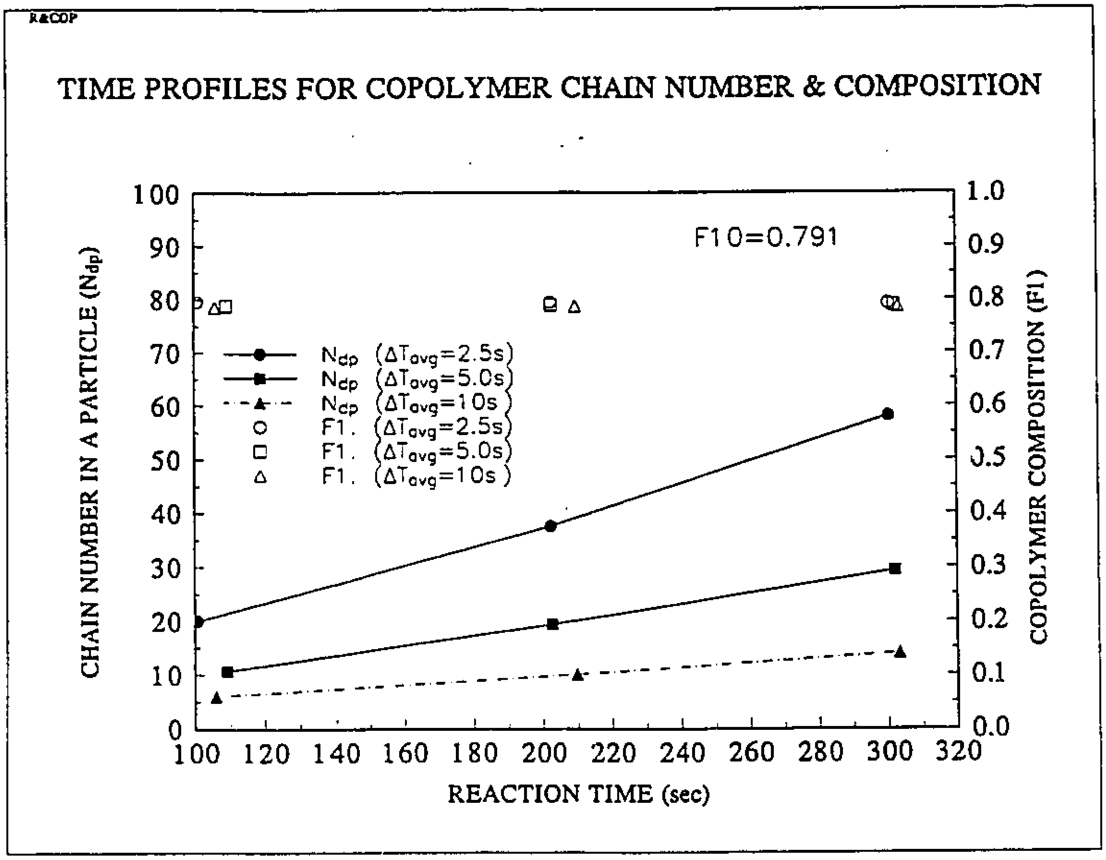

Figure 5.3.16 Effect of average time interval between radical entry (ΔT_{avg}) on calculated time profiles for polymer chain number and composition of copolymer in a polymer particle during emulsion copolymerization of vinyl monomers (without crosslinking).

$k_{p11} = 490$ L/mol•s, $k_{p22} = 2\, k_{p11}$, $r_1 = 0.67$, $r_2 = 1.49$.

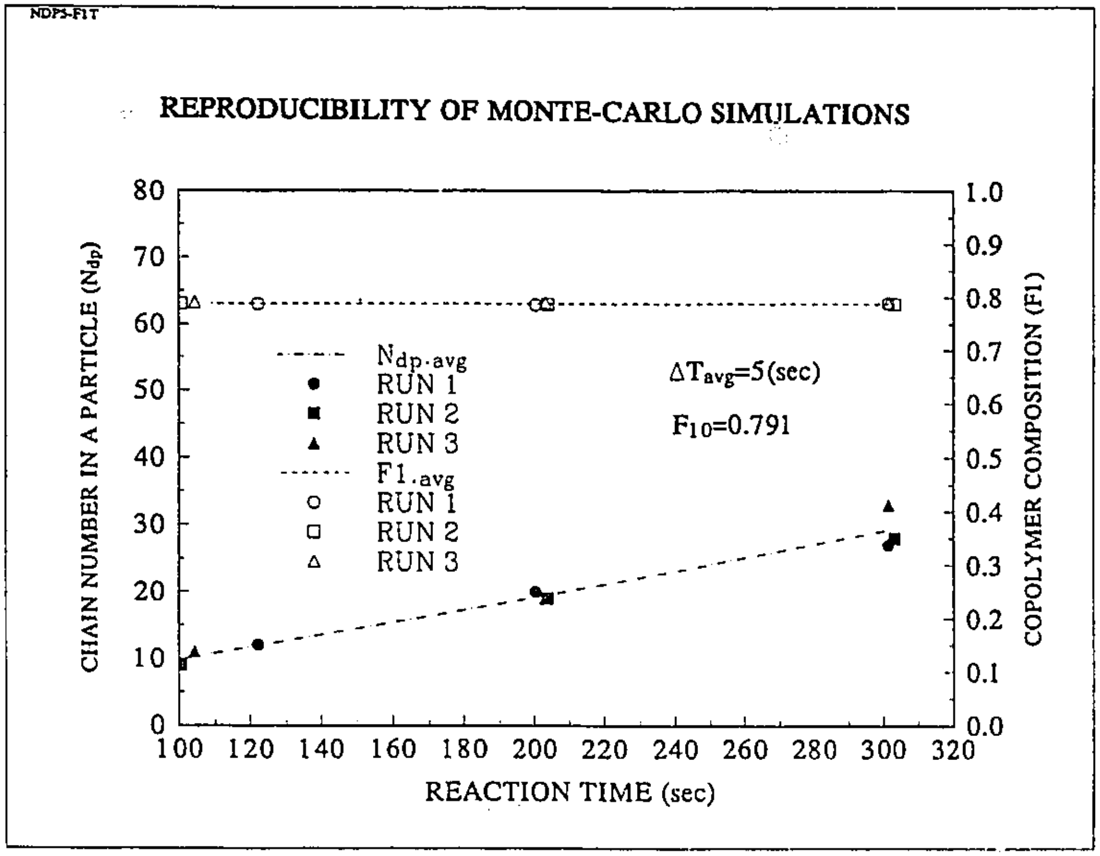

Figure 5.3.17 Reproducibility of the Monte-Carlo simulations showing the effect of average time interval between radical entry (ΔT_{avg}) on calculated time profiles for polymer chain number and composition of copolymer in a polymer particle during emulsion copolymerization of vinyl monomers (without crosslinking).

k_{p11} = 490 L/mol•s , $k_{p22} = 2\ k_{p11}$, $r_1 = 0.67$, $r_2 = 1.49$.

Emulsion copolymerization of vinyl/divinyl monomers (Crosslinking)

To simulate the polymer properties in crosslinking emulsion polymerization of vinyl/divinyl monomer system is the primary and final objective of the present development of the Monte-Carlo algorithm. At this moment, the focus is on the semi-batch process which holds for the stage II in emulsion polymerization. And chemically controlled rate phenomena have been set in order to display the major advantage of Monte-Carlo methods in the simulation of emulsion polymerization with crosslinking.

Crosslinker concentration in the monomer swollen polymer particle was from 0 to 5%wt. The average time interval for radical entry is $\Delta T_{avg} = 2$ seconds. Polymerization was done using the following typical kinetic parameters selected from literature data for MMA/EGDMA bulk polymerization reported by Li *et al*[33]:

k_{p11} : 446.2 (L/mol•s) $k_{p22} = 2\,k_{p11}$

r_1 : 0.67 r_2 : 1.49

$k_{p13} = k_{p12}/2$ $k_{p23} = k_{p33} = k_{p22}/2$

In Table 5.2 is an example of the entire copolymer chains of different length in a polymer particle simulated by the Monte-Carlo method. This is the case without crosslinking that was designed as a reference. In this table the "Number" column is the chain number of a specific length, the columns with name from X0100 to X0600 show the whole set of polymer chains accumulated up to 100 sec to 600 sec reaction times. The first left column in that table shows an ascent sequence of copolymer chain length in a particle and the total chain number at a certain time. For example, for the X0100 column, the total copolymer chain number is 29, the shortest chain has 265 units including both monomer 1 and monomer 2, and the longest chain has 15944 units. It can be seen from this Table that total polymer chain number increases with polymerization time. When a polymer chain is terminated it remains in the particle because the chain transfer to polymer reaction was not introduced in this case. The number of high molecular weight chains increases with polymerization time. **Figure 5.3.18 a** and **Figure 5.3.18 b** are the calculated number and weight chain length distributions using data in column X0350.

Figure 5.3.19 shows the effect of crosslinking on the copolymer composition and chain numbers. Herein, the second monomer level has been set at 0.1%wt. The reactivity of this comonomer (k_{p11}, k_{p22}, r_1 and r_2) were assumed constant. The only difference is that in one case this second monomer is a vinyl monomer (no crosslinking) while in the other 0.1%wt comonomer is a divinyl monomer (crosslinker). In this figure, circle symbols (solid and open) represent the crosslinking case.

It can be seen that for the copolymer composition as long as the monomer ratio in polymer particles has been kept constant, there is no effect of crosslinking on the copolymer composition. For both cases, the simulated copolymer compositions agree with the "instantaneous copolymer composition", $F_{10} = 0.9992$, calculated using the Mayo-Lewis

Table 5.2 Copolymer Chain Length Without Crosslinking

	1	2	3	4	5	6
	Number	X0100	X0200	X0350	X0500	X0600
1	1	265	265	132	132	132
2	1	501	437	172	172	172
3	1	781	501	265	265	265
4	1	874	781	432	432	432
5	1	978	798	437	437	437
6	1	1083	874	501	456	456
7	1	1332	978	519	492	492
8	1	1544	1083	781	501	501
9	1	1822	1248	783	519	519
10	1	1950	1284	798	554	554
11	1	2499	1332	874	589	589
12	1	2800	1544	978	629	598
13	1	3558	1586	1083	679	629
14	1	3976	1688	1119	781	679
15	1	4373	1822	1248	783	781
16	1	4418	1841	1271	798	783
17	1	4541	1868	1284	874	798
18	1	4962	1950	1332	938	874
19	1	5597	2180	1394	978	935
20	1	5687	2499	1544	1050	938
21	1	5785	2656	1586	1083	978
22	1	5842	2800	1688	1119	1050
23	1	5866	3061	1783	1127	1083
24	1	7089	3212	1790	1248	1119
25	1	7146	3488	1822	1271	1127
26	1	8136	3558	1841	1284	1225
27	1	8850	3976	1868	1332	1248
28	1	9205	4373	1950	1372	1271
29	1	15944	4418	2180	1394	1284
30	1		4541	2499	1544	1332

Table 5.2 Copolymer Chain Length Without Crosslinking (continued)

	1	2	3	4	5	6
	Number	X0100	X0200	X0350	X0500	X0600
31	1		4718	2656	1586	1372
32	1		4962	2699	1688	1394
33	1		5357	2800	1783	1397
34	1		5597	3061	1790	1544
35	1		5687	3167	1822	1586
36	1		5785	3212	1841	1688
37	1		5842	3240	1868	1783
38	1		5866	3271	1950	1790
39	1		5898	3488	2024	1822
40	1		5954	3558	2180	1841
41	1		6522	3787	2204	1868
42	1		7089	3883	2223	1950
43	1		7146	3976	2439	2024
44	1		7801	4133	2499	2180
45	1		8136	4183	2656	2204
46	1		8850	4373	2699	2223
47	1		9205	4418	2800	2354
48	1		10718	4471	3061	2439
49	1		11619	4541	3167	2499
50	1		13089	4718	3212	2656
51	1		13866	4719	3240	2697
52	1		14828	4787	3271	2699
53	1		15944	4962	3488	2800
54	1		16414	5357	3558	3061
55	1			5597	3787	3147
56	1			5687	3790	3167
57	1			5785	3804	3212
58	1			5842	3883	3240
59	1			5866	3976	3271
60	1			5898	4082	3466

Table 5.2 Copolymer Chain Length Without Crosslinking (continued)

	1	2	3	4	5	6
	Number	X0100	X0200	X0350	X0500	X0600
61	1			5954	4133	3488
62	1			5967	4183	3558
63	1			6374	4261	3706
64	1			6432	4373	3787
65	1			6522	4418	3790
66	1			6662	4471	3804
67	1			6956	4541	3883
68	1			7089	4718	3938
69	1			7146	4719	3976
70	1			7381	4787	4082
71	1			7708	4962	4133
72	1			7801	5113	4183
73	1			7820	5357	4261
74	1			7863	5579	4373
75	1			8136	5597	4418
76	1			8337	5687	4471
77	1			8850	5752	4541
78	1			8956	5785	4718
79	1			9205	5842	4719
80	1			10718	5866	4787
81	1			10859	5898	4853
82	1			11049	5954	4962
83	1			11619	5967	5113
84	1			12108	6166	5357
85	1			13089	6217	5579
86	1			13866	6250	5597
87	1			13904	6374	5687
88	1			14828	6432	5752
89	1			15944	6522	5785
90	1			16414	6662	5802

Table 5.2 Copolymer Chain Length Without Crosslinking (continued)

	1	2	3	4	5	6
	Number	X0100	X0200	X0350	X0500	X0600
91	1			16814	6956	5842
92	1				7089	5866
93	1				7146	5898
94	1				7310	5954
95	1				7381	5967
96	1				7708	6166
97	1				7801	6171
98	1				7810	6217
99	1				7820	6250
100	1				7863	6374
101	1				8136	6432
102	1				8337	6522
103	1				8850	6662
104	1				8956	6948
105	1				9205	6956
106	1				9312	7089
107	1				9490	7124
108	1				10718	7146
109	1				10767	7310
110	1				10859	7381
111	1				11049	7708
112	1				11619	7801
113	1				12108	7810
114	1				12278	7820
115	1				13089	7863
116	1				13678	8136
117	1				13866	8337
118	1				13904	8419
119	1				14125	8850
120	1				14828	8956

Table 5.2 Copolymer Chain Length Without Crosslinking (continued)

	1	2	3	4	5	6
	Number	X0100	X0200	X0350	X0500	X0600
121	1				15944	9205
122	1				16414	9312
123	1				16814	9490
124	1				17466	9668
125	1				17876	10718
126	1				21061	10767
127	1					10859
128	1					11049
129	1					11061
130	1					11619
131	1					12108
132	1					12129
133	1					12278
134	1					13089
135	1					13678
136	1					13866
137	1					13904
138	1					14125
139	1					14828
140	1					15272
141	1					15944
142	1					16414
143	1					16814
144	1					16905
145	1					17439
146	1					17466
147	1					17876
148	1					21061
149	1					25937
150	1					

equation [33]. The reason is that in the present simulation, the liquid volume fraction and the monomer composition in the polymer particle were assumed not to change with reaction time (stage II). However, for the polymer chain number, the effect of crosslinking is very clear. The total polymer chain number in the non-crosslinking case is a monotonous increase function of reaction time. While for the crosslinking case, the total polymer chain number is not very sensitivity to reaction time and remains a very small value (below 10). It should be pointed out that for most of the reaction time almost one polymer chain exists in the polymer particle.

The dramatic molecular weight increase is one of the major effects of crosslinking of polymer chains in polymer particles. As is shown **in Figure 5.3.20**, unlike the copolymer composition, under this condition, the molecular weight of non-crosssIinked polymer (weight average) in polymer particles (see solid-triangle symbols with a solid line) does not go through a large change, it is less than 5 million. However, for the crosslinking case the polymer molecular weight (see solid-circle symbols with a solid line) keeps increasing with time from 15 million @ 100 sec to more than 80 million @ 600 sec. One thing needs to be stressed is that in this simulation, @ 600 sec (10min) reaction time the molecular weight of polymer in the particle is not "infinite" with essentially only one polymer molecule in the polymer particle due to crosslinking. This reveals that according to Flory's criterion for gelation ($\overline{M}_w \to \infty$), the "gel point" has not been reached. But the polymer particles do contain "few polymer chains with a high molecular weight". This is characteristic of a "microgel" mentioned in Chapter 3.

In emulsion polymerization of vinyl/divinyl monomer system, changing the divinyl monomer level in the monomer mixture is an effective approach to control the crosslinking level and polymer molecular weight. In the present simulation, three crosslinker monomer levels have been selected to test the sensitivity of these properties to crosslinker level. **Figure 5.3.21** and **Figure 5.3.22** show the results of these calculations. In these figures, solid symbols (triangle, square and circle) represent the time profiles of accumulated copolymer composition (left Y-axis). Data clearly show that the copolymer composition does not change with time in stage II (semi-batch process), and that copolymer composition does shift with the divinyl monomer level around values of "instantaneous copolymer composition", $F_{10}\big|_{@M2=5\%wt} = 0.9618$, $F_{10}\big|_{@M2=1\%wt} = 0.9949$, and $F_{10}\big|_{@M2=0.1\%wt} = 0.9992$, showing the sensitivity and reliability of the Monte-Carlo simulations done.

The "right Y-axis" in **Figure 5.3.21** corresponds to the open symbols for time profiles of pendant double bond conversion ($M2_{con.}$). For 0.1%wt crosslinker, the $M2_{con.}$ initially increases with time from 0.1 to 0.3 until about 250 seconds, then it levels off. For 1%wt and 5%wt crosslinker level systems, pendant double bond conversions are less than that of 0.1%wt.

Corresponding to the increase in PDB conversion, in **Figure 5.3.22** one can also see a fluctuating change in total polymer chain number with reaction time (right Y-axis).

This reveals that for the 0.1%wt crosslinker level case, there is some opportunity for some polymer chains co-exist with crosslinked chains in a polymer particle. However, given time, the number of polymer chains approaches unity. At higher levels of divinyl monomer crosslinking is predominant and only a single polymer chain can exist in the polymer particle over the entire polymerization time.

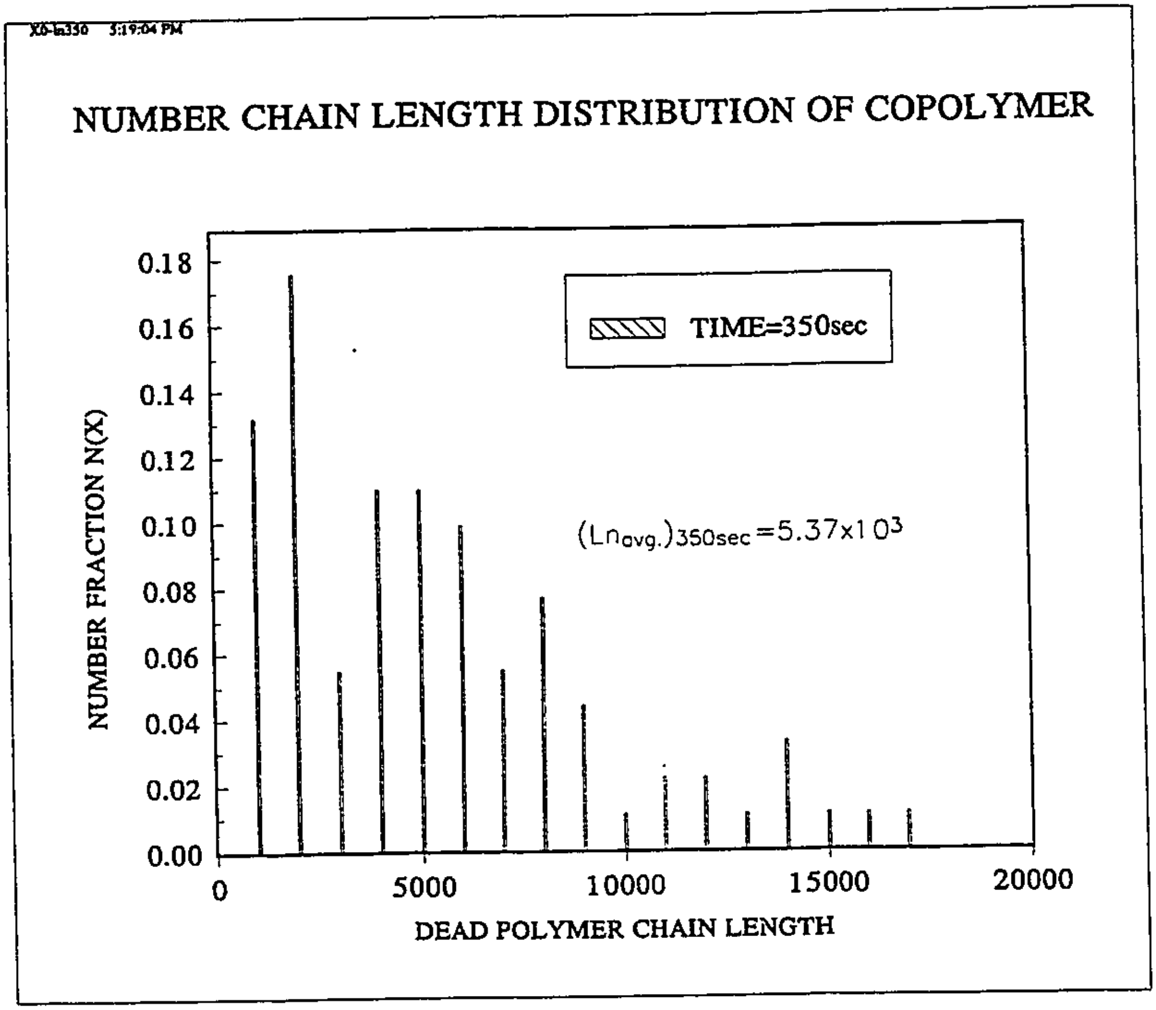

Figure 5.3.18a Results of the Monte-Carlo simulation of number chain length distribution of linear copolymer versus time in a polymer particle during emulsion copolymerization without crosslinking using data X0350 in Table 5.2.

$k_{p11} = 446$ L/mol•s, $k_{p22} = 2\ k_{p11}$, $r_1 = 0.67$, $r_2 = 1.49$, M2=0.1%wt.

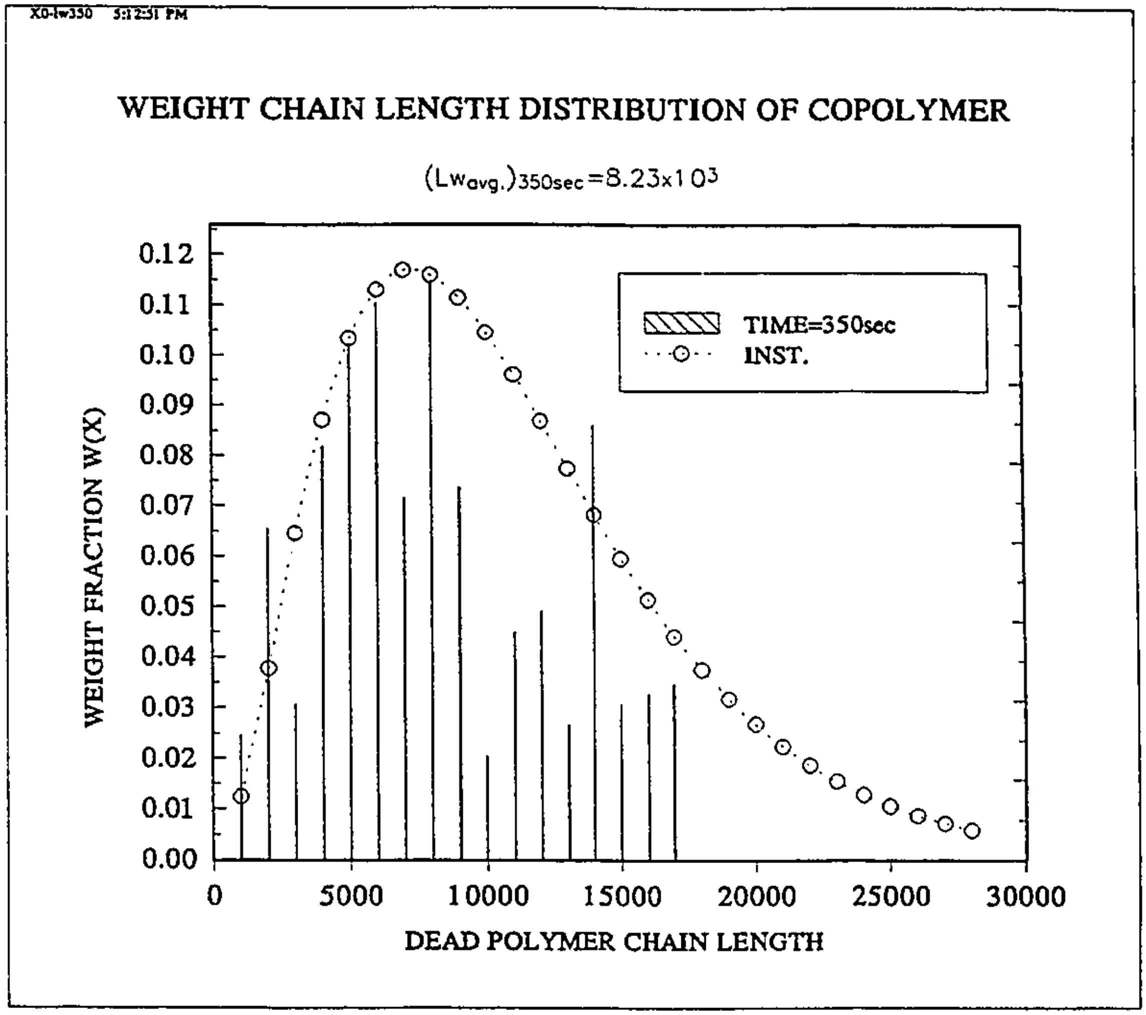

Figure 5.3.18b Results of the Monte-Carlo simulation of weight chain length distribution and the "instantaneous weight chain length distribution" calculation of linear copolymer versus time in a polymer particle during emulsion copolymerization without crosslinking using data X0350 in Table 5.2. $k_{p11} = 446$ L/mol•s, $k_{p22} = 2\ k_{p11}$, $r_1 = 0.67$, $r_2 = 1.49$, M2=0.1%wt. $\beta = 2.75\times10^{-4}$.

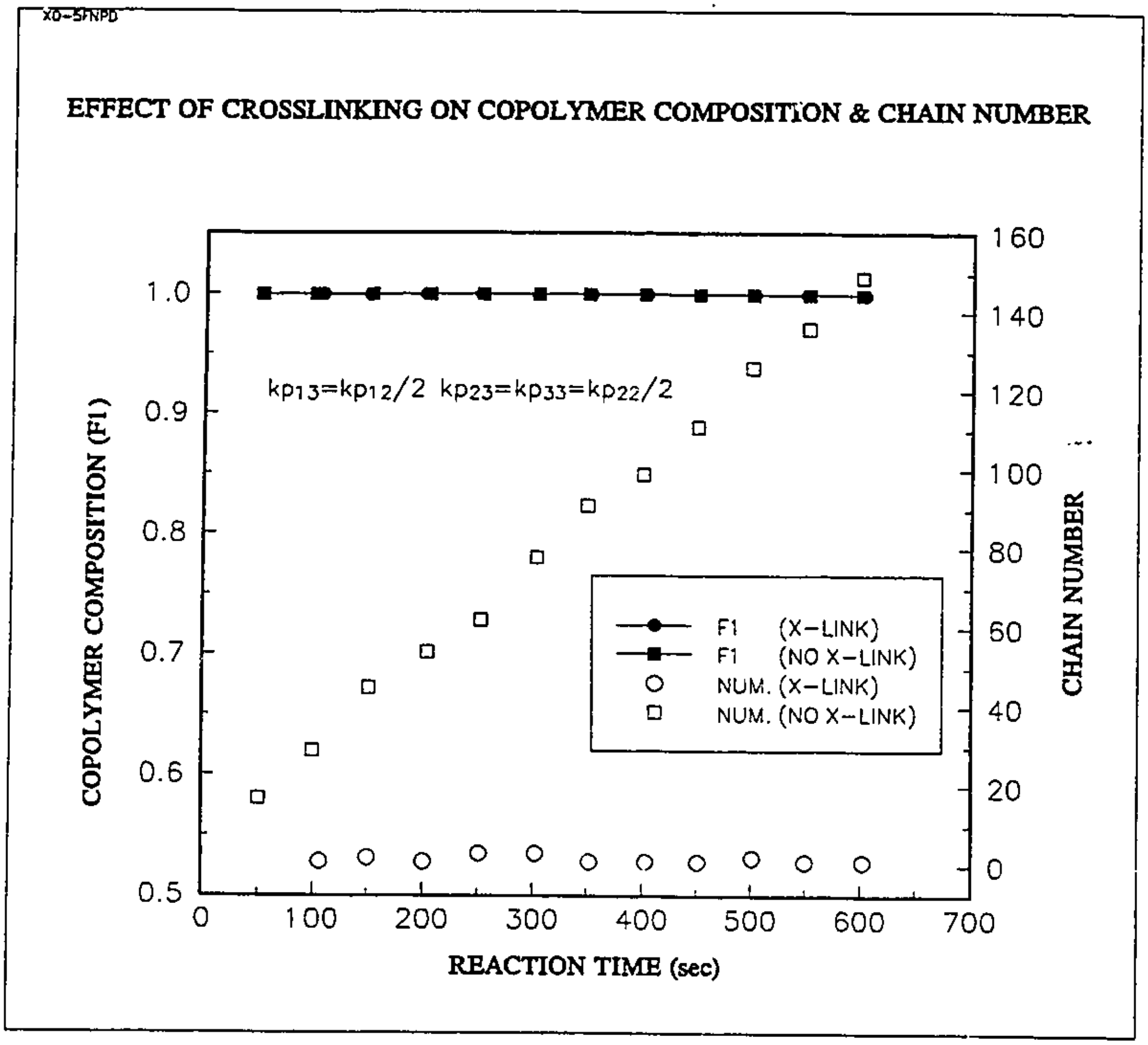

Figure 5.3.19 Effect of crosslinking on calculated time profiles of polymer chain number and composition of copolymer in a polymer particle during emulsion copolymerization (without / with crosslinking). $k_{p11} = 446$ L/mol•s, $k_{p22} = 2\ k_{p11}$, $r_1 = 0.67$, $r_2 = 1.49$, M2 = 0.1%wt.

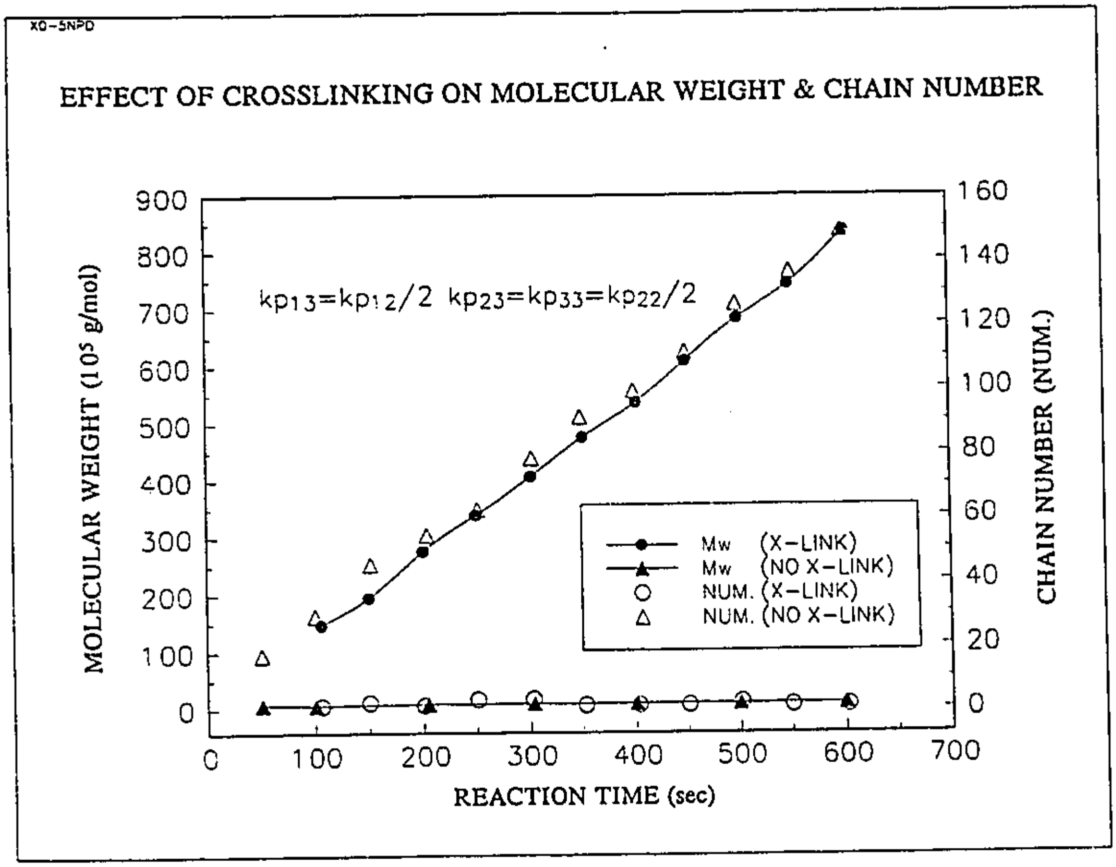

Figure 5.3.20 Effect of crosslinking on calculated time profiles of polymer chain number and molecular weight of copolymer in a polymer particle during emulsion copolymerization (without / with crosslinking). $k_{p11} = 446$ L/mol•s, $k_{p22} = 2\ k_{p11}$, $r_1 = 0.67$, $r_2 = 1.49$, M2=0.1%wt.

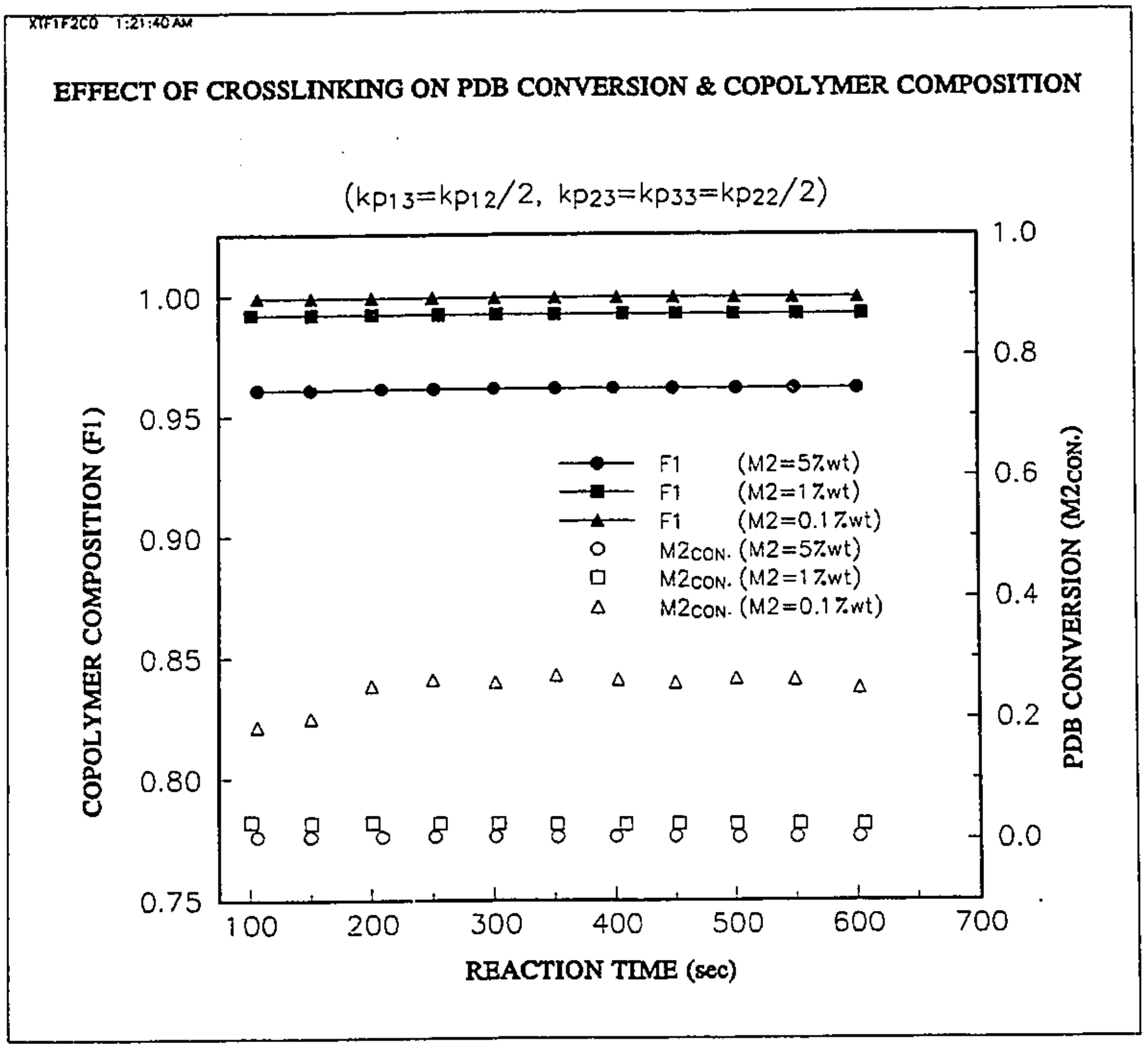

Figure 5.3.21 Effect of crosslinker level on the calculated time profiles of copolymer chain composition and PDB conversion in a polymer particle during emulsion copolymerization with crosslinking. $k_{p11} = 446$ L/mol•s, $k_{p22} = 2\ k_{p11}$, $r_1 = 0.67$, $r_2 = 1.49$.

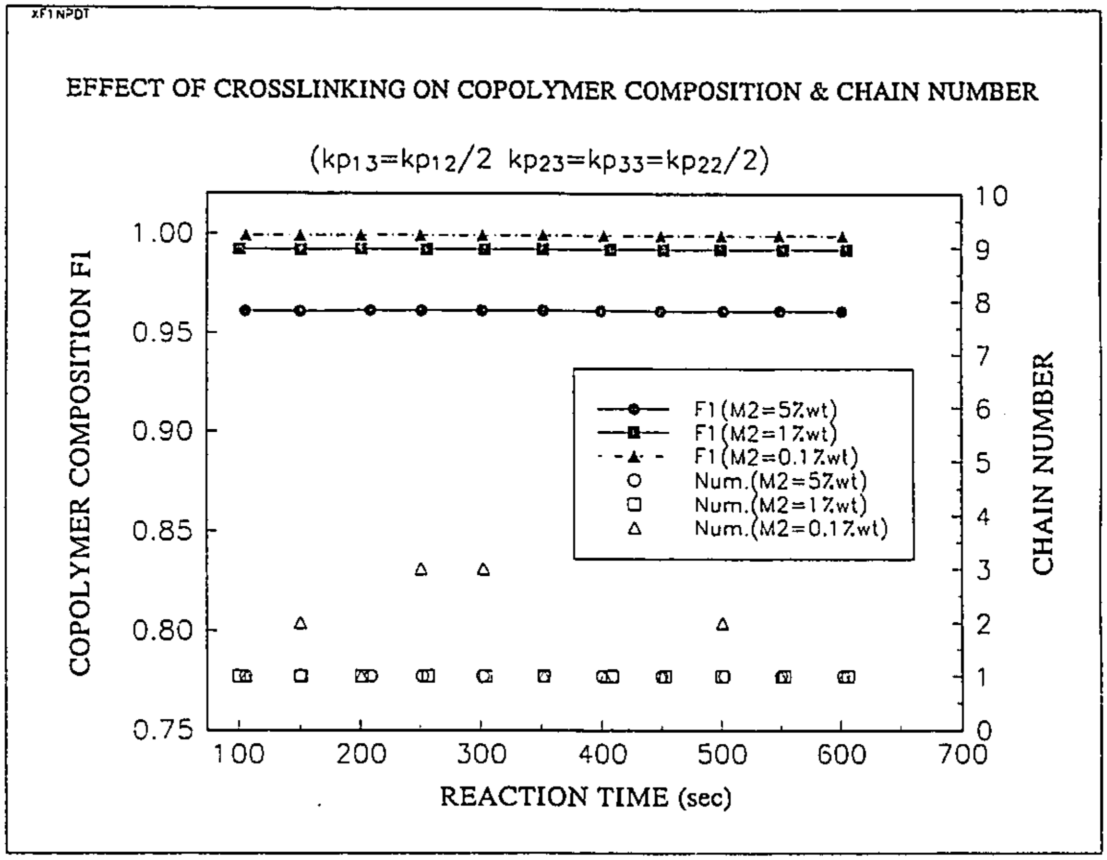

Figure 5.3.22 Effect of crosslinker level on the calculated time profiles of copolymer chain composition and chain number in a polymer particle during emulsion copolymerization with crosslinking. k_{p11} = 446 L/mol•s, $k_{p22} = 2\ k_{p11}$, $r_1 = 0.67$, $r_2 = 1.49$.

5.4 Summary

In this chapter is presented the development of a new general stochastic Monte-Carlo simulation algorithm for emulsion copolymerization. This simulation method was developed to account for polymerization in stage II where the number of polymer particles and the concentrations of monomers are constant.

The Monte-Carlo simulation of chemical reaction system is based on the master equation which describes the stochastic time evolution of this system by answering the following questions: (1) the time interval probability density for one radical entering a particle; (2) the probability for one oligomeric radical to desorb from a particle, (3) the probabilities for specific reaction steps; (4) the probability for the time interval between two successive reaction steps.

After basic testing, the method was applied to homo polymerization with long chain branching and copolymerization with or without crosslinker. Calculated results reflect the polymer properties for these situations, which one would expect. A novel observation is the tendency to maintain a single polymer chain in a polymer particle under crosslinking conditions and thus the formation of a “microgel”.

For the present simulations, the total number of polymer particles is considered as constant (stage II). However, the algorithm could be extended to include nucleation steps (stage I) and changes in monomer concentration (stage III) and covering a host of kinetic event combinations provided that the proper kinetic expressions, constraints and criteria conditions are used.

5.5 References

1 Zhu, S., "Advances in Free Radical Polymerization Kinetics", Ph.D. Thesis, McMaster University, Canada, (1990)

2 Gillespie, D. T. *J. Phys. Chem.* 1977, **81**, 2340

3 Hanusse, P., Blanche, A. *J. Chem. Phys.* 1981, **74**, 6148

4 Cupta, A.M., Hendrickson, R. C. and Macosko, C. W. *J. Chem. Phys.* 1991, **95**, 2097

5 Speckhard, T. A., Miller, J. A. and Cooper, S. *Macromolecules* 1986, **19**, 1558

6 Speckhard, T. A., Homan, J. G., Miller, J. A. and Cooper, S. *Polymer* 1987, **28**, 768

7 Mirabella, F. M. *Jr. Polymer* 1977, **18**, 705

8 Stockmayer, W. H. *J. Chem. Phys.* 1945, **13**, 199

9 O'Driscoll, K. F. *J. Coat. Technol* 1983, **55**, 57

10 Galbraith, M. N., Moad, G., Solomon, D. H. and Spurling, T. H. *Macromolecules* 1987, **20**, 675

11 Aleksandrov, A. P., Genkin, V. N., Kitai, M. S., Smironva, I. M. and Sokolov, V. V. *J. Quantum Electron (Engl. Transl)* 1977, **7**, 547

12 Olaj, O. F., Bitai, I. and Hinkelmann, F. *Makromol. Chem.* 1987, **155**, 177

13 O'Driscoll, K. F. and Kuindersma, M. E. *Makromol. Chem., Theory Smilu.* 1994, **4**, 469

14 Lu, J., Zhang, H. and Yang, Y. *Makromol. Chem., Theory Smilu.* 1993, **2**, 747

15 Tang, A. *"Statistical Tehory of Polymerization Reaction"*, Chinese Academic Press, Beiging, 1985

16 Bamford, C. H., Barb, W. G., Jenkins, A. D. and Onyon, P. F. *"The Kinetics of Vinyl Polymerization By Radical Mechanisms"*, Butterworth, London, 1958

17 Tobita, H. *Macromolecules* 1993, **26**, 836,

18 Tobita, H. *Macromolecules* 1993, **26**, 5427

19 Tobita, H. *Macromolecules* 1994, **27**, 5413

20 Tobita, H., Yamamoto, Y. and Ito, K. *Macromol. Theory Simul.* 1994, **3**, 1033

21 Chiu, Y. Y. and Lee, L. J. *J. Polym. Sci., Part A: Polym. Chem.* 1995, **33**, 257

22 Chiu, Y. Y. and Lee, L. J. *J. Polym. Sci., Part A: Polym. Chem.* 1995, **33**, 269

23 Manneville, P. and Seze, de, in *"Numerical Methods in the Study of Critical Phenomena"*, della Dora I, Demongeot, J. and Lacolle. L eds, Springer, Berlin, 1981

24 Boots, H. and Pandey, R. B. *Polym. Bull.* 1984, **11**, 415

25 Boots, H., Kloosterboer, J., Her, G. van de, and Pandey, R. B. *Br. Polym. J.* 1985, **17**, 219

26 Boots, H. and Dotson, N. *Polym. Commun.* 1988, **29**, 346

27 Tobita, H., Takada, Y. and Nomura, M. *Macromolecules* 1994, **27**, 3804

28 Gillespie, D. T. *J. Computational Phys.* 1976, **22**, 403

29 "Monte Carlo Methods", Volume I, Basic, Kalos, M. H. and Whitlock, P. A. eds, A Wiley-Interscience Publication, HOHN WILEY & SON, 1986

30 Sobol, I. M "The Monte Carlo Method", The University of Chicago Press, 1974

31 Steams, S. D. "A Portable Random Number Generator for Use in Signal Processing," Sandia National Laboratory technical Report, 1981

32 Tobita, H. *J. Polym. Sci., Part B: Polym. Phys.* 1993, **31**, 1363

33 Odian, G. "Principles of Polymerization", second edition, Wiley-Interscience, 1981, pp. 428

34 Li, W-H., Hamielec, A. E. and Crowe, C. M., *Polymer* 1989, **30**, 1513, 1518

APPENDICES:

In this part is shown one program of the Monte-Carlo for the simulation of crosslinking emulsion polymerization of vinyl/divinyl monomers. In order to make the basic simulation algorithm clear, the "BASIC" version is presented with some reminds (REM) to make the program easy to read.

APPENDIX : X-LINKING

```
40    REM    Mon-XK (Propagation,  XLINK,  Termination)
50    REM    CONSIDER COPOLYMERIZATION
60    REM    For combined termination
70    REM    Radical type 1 into particle
80    REM    MONOMER 1 is MMA, MONOMER 2 is EGDMA

100   REM    npt, npr, np
             Number of monomer units on total, polyradical and polymer chain
104   REM    npe1, npe1
             INITIAL MONOMER UNITS IN EACH RADICAL TYPE
106   REM    npd
             TOTAL NUMBER OF DEAD POLYMER CHAINS !!!
110   REM    Vp,
             VOLUME OF one LATEX PARTICLE
120   REM    np,
             NUMBER OF THE MONOMER UNITES ON all POLYMER CHAINS
130   REM    Mw1, Mw2
             MOLECULAR WEIGHT OF MONOMER TYPE one & two (g/mol)
132   REM    Fp1, Fp2
             TOTAL NUMBER OF MONOMER 1 & 2 IN ALL POLYMER CHAIN
```

```
133   REM    Fm1, Fm2
             MOL FRACTION OF MONOMER 1 & 2 IN ONE PARTICLE
134   REM    Mp1 Mp2
             MONOMER CONCENTRATION OF 1 & 2 IN ONE PARTICLE
138   REM    PHI1 PHI2
             MOL FRACTION OF RADICAL TYPE 1 & 2
140   REM    Vc,
             TOTAL VOLUME FRACTION OF POLYMER IN one LATEX
             PARTICLE
150   REM    Xc,
             TOTAL WEIGHT FRACTION OF POLYMER IN one PARTICLE
160   REM    dp,
             DIAMETER OF one LATEX  (micro-meter)
180   REM    DenP1, DenP2
             DENSITY OF POLYMER one & two (g/cmE3)
190   REM    DenM1;  DenM2
             DENSITY OF MONOMER one & two (g/cmE3)
192   REM    DenP,  DenM
             AVERAGE DENSITY OF POLYMER & MONOMER
194   REM    Vpp1, Vpp2
             POLYMER VOLUME OF TOTAL 1 & 2 REPEAT UNITS IN
             PARTICLE
200   REM    kf= A/dp2
             DESORPTION RATE CONSTANT (1/s)
210   REM    ktcij
             COMBINATION TERMINATION RATE CONSTANT OF 1 & 2
             RADICAL IN ONE LATEX (L/mol*s)!!!
212   REM    kpij
             PROPAGATION CONS. OF RADICAL i WITH MONOMER j (L/molxs)
220   REM    Nt,
             TOTAL NUMBER OF PARTICLE IN SYSTEM
230   REM    AveN,
             AVERAGE NUMBER OF RADICALS PER PARTICLE
250   REM    AveT,
             AVERAGE TIME INTERVAL OF one RADICAL ENTERING (s)
260   REM    Rw,
             INITIATION RATE IN THE WATER PHASE
262   REM    Mh1, Mh2,
             MONOMER CON. IN H2O PHASE OF TYPE 1 & 2 (SOLUBILITY)
280   REM    W, ALPHA α IN PAPER
```

```
300 DenP1 = 1.189: DenP2 = 1.2
302 DenM1 = .9374: DenM2 = 1.051
310 RwNt = .5
330 Mw1 = 100: Mw2 = 198

332 kp11 = 446.1667: kp22 = 2.04 * kp11:         REM    From Li (liter/mol*s)
334 Ratio1 = .67: Ratio2 = 1.49
336 kp12 = kp11 / Ratio1: kp21 = kp22 / Ratio2
340 kp13 = 0 * (kp12 / 2) * 1E+15:               REM    (micro3/mol*s)
345 kp23 = 0 * (kp22 / 2) * 1E+15:               REM    From Li
355 PRINT kp11; kp12, kp22; kp21, kp13, kp23


350 Nt = 600
360 ktc11 = 2.066E+21:                           REM    (in micro3/mol*s)
                                                        1.24e9(L/mol*min)
362 ktc12 = ktc11: ktc22 = ktc11: ktc21 = ktc11
370 Nav = 6.02E+23
380 a = 0: npr = 0: npd = 0: npt = 0

382 DIM P(250), pp(250), R1(10), R2(10):          REM    For dead-polymer & Two radicals
385 BONE = 0: XLINK = 0: PXB = 0: NPP = 0:        REM    FOR X-LINKING

400 INPUT "NUMBER OF RADICAL terminal 1  n1%   ?", n1%
402 INPUT "NUMBER OF RADICAL terminal 2  n2%   ?", n2%
404 n% = n1% + n2%

462 FOR I = 1 TO 250
464 P(I) = 0
480 NEXT I

490 FOR J = 1 TO 10
492 R1(J) = 0: R2(J) = 0
496 NEXT J

505 Cfp = 0
510 Cm = 0
520 kfm = Cm * kp
525 kfp = (Cfp * kp) * 1E+15
```

```
530 Mp1 = 6.6:                 REM     Monomer 1 conc. in particle (mol/L) NAPPER
                                       JPS VOL 22, 3225 1984
532 Fm1 = .999495:             REM     MOL FRACTION 1  W1%=.25 W1%=5
                                       F1m=0.0258933 W1%=1
                                       F1m=5.0756268E-3
534 Mp2 = Mp1 * (1 - Fm1) / Fm1
536 Fp10z = Ratio1 * Fm1 ^ 2 + Fm1 * (1 - Fm1)
538 Fp10m = Ratio1 * Fm1 ^ 2 + 2 * Fm1 * (1 - Fm1) + Ratio2 * (1 - Fm1) ^ 2
540 Fp10 = Fp10z / Fp10m
550 Ko = 0: TRA = 0:           REM     THE DESORPTION RATE CONST.
                                       Oligomeric-RADICAL
555 Vc = .58:                  REM     THE VOLUME RATIO OF POLYMER IN
                                       PARTICLE

560 Mh1 = .008: Mh2 = 0
562 Fh1 = Mh1 / (Mh1 + Mh2)
564 Fh2 = 1 - Fh1
566 PRINT "Fh1="; Fh1

580 INPUT "Initial total unites in all radical are npe ?", npe:
                                    REM     For each poly-radical at beginning
582 npe1 = INT(npe * Fp10 + .5):    REM     Initial copolymer composition Mayo equ.
584 npe2 = npe - npe1

590 FOR I = 1 TO n1%:               REM     Get initial radical into particle
592 R1(I) = npe1
593 PRINT R1(I);
594 npr = npr + R1(I)
598 NEXT I

600 FOR J = 1 TO n2%:               REM     Get initial radical into particle
602 R2(J) = npe2
604 npr = npr + R2(J):              REM     Initial monomer unites in all polymer
                                            radicals=npe
605 PRINT R2(J);
606 NEXT J
608 npt = npr + np
609 PRINT "": PRINT "INITIAL npt"; npt, "npe  "; npe
```

```
610 Fp1 = npe1: Fp2 = npe2: F2X = npe2
612 PRINT "F1o =  "; npe1; "F2o =  "; npe2; "Fp10"; Fp10

620 ST = 12
622 TIME = 1:                          REM     Total reaction time cycle(sec)
625 TT = TIME * 50

630 Vpp1 = (Fp1 * Mw1) / (DenP1 * Nav)
632 Vpp2 = (Fp2 * Mw2) / (DenP2 * Nav)
635 vp = ((Vpp1 + Vpp2) / Vc) * 1E+12:  REM     In micro3
645 PRINT "VOLUME "; vp,
650 dp = (6 * vp / 3.14158) ^ (1 / 3): REM     In micro
655 PRINT "DIAMETER "; dp,

660 kf = a / (dp ^ 2):                 REM     (1/s)
670 REM W = (2 * RwNt * vp * Nav) / kt:
                                       REM     Cal. of the average number radial
                                               n particle
680 REM m = (2 * kf * vp * Nav) / kt
690 REM K1 = W + W / m
700 REM AveN = .5 * (SQR(K1 ^ 2 + 2 * K1) - K1) + SQR(.25 + W / 2) - .5
710 AveT = 1 / (RwNt + kf * AveN)

740 RANDOMIZE TIMER
750 RTEN = RND:                        REM     For radical entering
755 IF RTEN = 0 THEN 750 ELSE
760 Ten = LOG(RTEN) * (-AveT):         REM     Ten is real time interval of entry
762 TA = 0:                            REM     Reaction time in one radical entry
770 TRA = TRA + Ten:                   REM     Real simulated time
775 PRINT "Time---   "; TRA
780 IF TRA >= TT THEN GOTO 10000:      REM     To check end
790 PRINT "n1% & n2% "; n1%; n2%; "After entry",

800 IF (n1% + 1) <= 0 THEN n1% = 0: GOTO 860
860 R1(n1% + 1) = 1:                   REM     Create a unit length R1 radical
                                               in particle
870 PRINT "R1("; n1% + 1; ")= "; R1(n1% + 1), "n1% & n2%"; n1% + 1; n2%

1000 GOTO 9000:                        REM     GET Phi1 AND Phi2
1002 IF n% = 0 THEN GOTO 7000 ELSE
```

```
1010 Rp1 = (kp11 * Phi1 + kp21 * Phi2) * Mp1
1012 Rp2 = (kp22 * Phi2 + kp12 * Phi1) * Mp2
1020 ktc = ktc11 * Phi1 ^ 2 + 2 * ktc12 * Phi1 * Phi2 + ktc22 * Phi2 ^ 2
1025 Rt = ktc * (n% - 1) / (vp * Nav)
1030 Rp3 = (kp13 * Phi1 + kp23 * Phi2) * F2X / (vp * Nav)
1040 A0 = Rp1 + Rp2 + Rp3 + Rt

1050 RANDOMIZE TIMER
1055 R2 = RND
1057 IF R2 = 0 THEN 1055 ELSE
1060 Tnext = LOG(1 / R2) / A0
1070 TA = TA + Tnext
1080 IF TA >= Ten THEN GOTO 7000:        REM     START ANOTHER ENTRY
1090 Prp1 = Rp1 / A0:                    REM     Propagation to monomer 1
1100 Prp2 = Rp2 / A0:                    REM     Propagation to monomer 2
1200 Prp3 = Rp3 / A0:                    REM     X-LINKING
2010 Prt = Rt / A0:                      REM     Termination
2015 PT1 = Prp1 + Prp2
2020 PT2 = Prp1 + Prp2 + Prp3

2040 RANDOMIZE TIMER
2050 R3 = RND
2055 IF R3 = 0 THEN 2050 ELSE
2100 IF R3 <= Prp1 GOTO 3200 ELSE 2110:
                                         REM     PROPAGATION WITH 1
2110 IF R3 <= PT1 THEN 4000 ELSE 2130:
                                         REM     4000 PREP WITH 2
2130 IF R3 <= PT2 THEN 5000 ELSE 6000:
2140 REM   5000 XLINK  6000 COM. TERMINATION

3200 RANDOMIZE TIMER:                    REM     GET one radical type to prop. with
                                                  monomer 1
3210 RPhi1 = RND
3215 IF RPhi1 = 0 THEN 3210 ELSE
3220 IF RPhi1 <= Phi1 THEN GOSUB 35000 ELSE GOSUB 36000
3540 GOTO 1000:                          REM     Next reaction step

4000 RANDOMIZE TIMER:                    REM     GET one radical type to prop. with
                                                 monomer 2
```

```
4010 RPhi2 = RND
4015 IF RPhi2 = 0 THEN 4010 ELSE
4020 IF RPhi2 <= Phi1 THEN GOSUB 37000 ELSE GOSUB 38000
4030 GOTO 1000:                          REM     Next reaction step

5000 IF npd = 0 THEN GOTO 1000 ELSE :
                                         REM     Only consider dead polymer
5002 NPP = 0: XBD = 0: BONE = 0: PXB = 0: XRADICAL = 0
5004 PRINT "": PRINT "X-linking !"; "n1% & n2% "; n1%; n2%,
5015 FOR I = 1 TO npd
5020 NPP = NPP + P(I)
5025 NEXT I

5030 RB4 = RND
5040 IF RB4 = 0 THEN 5030 ELSE
5045 REM CHOSE ONE CHAIN
5050 FOR XB = 1 TO npd
5055 PXB = PXB + P(XB) / NPP
5060 IF RB4 <= PXB THEN 5070 ELSE 5095
5070 BONE = P(XB)
5075 XBD = XB
5080 P(XB) = 0
5085 GOTO 5100
5095 NEXT XB

5100 REM CLEAR P(XB)
5110 IF XBD = npd THEN GOTO 5150 ELSE
5120 FOR XB1 = XBD TO npd - 1
5125 P(XB1) = P(XB1 + 1)
5130 P(XB1 + 1) = 0
5140 NEXT XB1
5150 npd = npd - 1

5200 RANDOMIZE TIMER
5210 RPhiX = RND
5215 IF RPhiX = 0 THEN 5210 ELSE
5220 IF RPhiX <= Phi1 THEN GOSUB 57000 ELSE GOSUB 58000
5230 PRINT "B4 POINT IS   "; XLINK, F2X, Fp2, Fp1 / (Fp1 + Fp2); XRADICAL
5500 GOTO 1000
```

```
6000 PRINT "": PRINT "Termination! "
6002 PRINT "n1%-- "; n1%, "n2%-- "; n2%, "n-- "; n%
6010 RANDOMIZE TIMER
6012 R6 = INT(RND * (n% + 1)):          REM     Get one radical
6016 IF R6 = 0 THEN GOTO 6012
6018 RANDOMIZE TIMER
6020 R7 = INT(RND * (n% + 1)):          REM     Get another radical
6025 IF R7 = 0 THEN GOTO 6020
6030 IF R6 = R7 THEN GOTO 6020

6060 IF R6 <= n1% AND R7 <= n1% THEN GOTO 40000 ELSE :
                                        REM     Two in R1
6070 IF R6 <= n1% AND R7 > n1% THEN GOTO 41000 ELSE :
                                        REM     R6 in n1% R7 in n2%
6080 IF R7 <= n1% AND R6 > n1% THEN GOTO 42000 ELSE 43000:
                                        REM     R6 in n2% R7 in n1%

6110 n% = n1% + n2%
6120 IF n% = 0 THEN 7000 ELSE :         REM     NO RADICAL IN PARTICLE
                                                NEED ANOTHER
6200 GOTO 1000

7000 REM Total units in Polymer to get another radical
7045 PRINT "": PRINT "npt before new radical"; npt, Fp1 / npt; Fp10
7046 PRINT "At 7050 LINE  ! Before new entry "
7050 FOR I = 1 TO 10
7052 PRINT R1(I); R2(I),
7054 NEXT I

7070 GOTO 630:                          REM     RE-Calculate Vp

9000 n1% = 0: n2% = 0: Phi1 = 0: Phi2 = 0
9010 FOR Ph1 = 1 TO 10
9020 IF R1(Ph1) = 0 THEN GOTO 9040 ELSE
9030 n1% = n1% + 1
9040 NEXT Ph1

9060 FOR Ph2 = 1 TO 10
9070 IF R2(Ph2) <= 0 THEN GOTO 9090 ELSE
```

```
9080 n2% = n2% + 1
9090 NEXT Ph2
9100 n% = n1% + n2%
9102 IF n% = 0 THEN GOTO 9130 ELSE
9110 Phi1 = (n1%) / n%
9120 Phi2 = 1 - Phi1
9130 GOTO 1002

10000 SOUND (RND * 100 + 57), 15
10006 INPUT "THE NAME OF FILE P$  ", P$
10010 nfile = 1
10020 OPEN "O", #nfile, P$
10030 WRITE #nfile, "Number", "length"
10040 FOR MWP% = 1 TO npd + 5
10050 WRITE #nfile, MWP%, P(MWP%)
10060 NEXT MWP%
10080 WRITE #nfile, "Time", "npt", "vp", "npd", "Fp1", "Fp2", "F2X", "B4"
10085 WRITE #nfile, TRA, npt, vp, npd, Fp1, Fp2, F2X, XLINK
10088 WRITE #nfile, "Radical 1", "Radical 2"
10089 FOR Rw = 1 TO 10
10090 WRITE #nfile, R1(Rw), R2(Rw)
10092 NEXT Rw
10094 CLOSE #nfile
10097 PRINT TRA; npt; vp; npd; Fp1; Fp2; F2X, XLINK

10100 ST = ST - 1
10110 IF ST = 0 THEN 20000 ELSE
10120 TIME = TIME + 1
10130 GOTO 625
20000 END

35000 REM Get one R1 radical to PROPAGATE with monomer 1
35002 RANDOMIZE TIMER
35010 R11 = INT(RND * (n1% + 1))
35020 IF R11 = 0 THEN GOTO 35010
35030 R1(R11) = R1(R11) + 1:
                                    REM     Chosen radical propagate one MONOMER 1
35040 Fp1 = Fp1 + 1
35045 npt = npt + 1
35050 RETURN:                       REM     3540
```

```
36000 REM Get one R2 radical to PROPAGATE with monomer 1
36002 RANDOMIZE TIMER
36010 R21 = INT(RND * (n2% + 1))
36020 IF R21 = 0 THEN GOTO 36010
36030 R2(R21) = R2(R21) + 1:
                                        REM    Chosen R2 radical get one MONOMER 1
36040 R1(n1% + 1) = R2(R21)
36050 R2(R21) = 0
36060 IF R21 >= n2% THEN 36110 ELSE
36070 FOR KR21 = R21 TO n2% - 1
36080 R2(KR21) = R2(KR21 + 1)
36090 R2(KR21 + 1) = 0
36100 NEXT KR21
36110 Fp1 = Fp1 + 1
36115 npt = npt + 1
36120 n1% = n1% + 1
36130 n2% = n2% - 1
36150 RETURN:                           REM    3540

37000 REM Get one radical 1 to PROPAGATE with monomer 2
37002 RANDOMIZE TIMER
37010 R12 = INT(RND * (n1% + 1))
37020 IF R12 = 0 THEN GOTO 37010
37030 R1(R12) = R1(R12) + 1:
                                        REM    Chosen 1 type radical get one MONOMER 2
37040 R2(n2% + 1) = R1(R12)
37050 R1(R12) = 0
37060 IF R12 >= n1% THEN 37110 ELSE
37070 FOR KR12 = R12 TO n1% - 1
37080 R1(KR12) = R1(KR12 + 1)
37090 R1(KR12 + 1) = 0
37100 NEXT KR12
37110 Fp2 = Fp2 + 1
37115 F2X = F2X + 1
37117 npt = npt + 1
37120 n2% = n2% + 1
37130 n1% = n1% - 1
37150 RETURN:                           REM    4030
```

```
38000 REM Get one radical 2 to PROPAGATE with monomer 2
38002 RANDOMIZE TIMER
38010 R22 = INT(RND * (n2% + 1))
38020 IF R22 = 0 THEN GOTO 38010
38030 R2(R22) = R2(R22) + 1:
                                        REM     Chosen radical propagate one MONOMER 1
38040 Fp2 = Fp2 + 1
38045 F2X = F2X + 1
38047 npt = npt + 1
38050 RETURN:                           REM     4030

40000 PRINT " 40000 road!  Both in n1%"
40002 PR6 = R1(R6): PR7 = R1(R7):       REM     Two from R1
40004 GOSUB 50000

40006 IF R6 > R7 THEN 40050 ELSE
40010 RL = R6: RH = R7
40020 GOTO 40100
40050 RL = R7: RH = R6
40100 R1(RL) = 0: R1(RH) = 0
40110 IF RH = n1% THEN GOTO 40160 ELSE

40120 FOR KR1 = RH TO n1% - 1
40130 R1(KR1) = R1(KR1 + 1)
40140 R1(KR1 + 1) = 0
40150 NEXT KR1

40160 FOR KR2 = RL TO n1% - 1
40170 R1(KR2) = R1(KR2 + 1)
40180 R1(KR2 + 1) = 0
40190 NEXT KR2
40200 n1% = n1% - 2
40210 PRINT "Back ", "n1% & n2%"; n1%; n2%
40220 FOR I = 1 TO 10
40230 PRINT R1(I); R2(I),
40235 NEXT
40240 GOTO 6110

41000 PRINT "41000 road !  R6 in n1% R7 in n2%":
                                        REM     R6 IS IN n1% R7 IS IN n2%
```

```
41002 R7 = R7 - n1%
41004 PR6 = R1(R6): PR7 = R2(R7)
41006 GOSUB 50000
41007 R1(R6) = 0
41009 IF R6 >= n1% THEN 41040 ELSE
41010 FOR KR3 = R6 TO n1% - 1
41015 R1(KR3) = R1(KR3 + 1)
41020 R1(KR3 + 1) = 0
41030 NEXT KR3
41040 n1% = n1% - 1

41045 R2(R7) = 0
41047 IF R7 >= n2% THEN 41090 ELSE
41050 FOR KR4 = R7 TO n2% - 1
41060 R2(KR4) = R2(KR4 + 1)
41070 R2(KR4 + 1) = 0
41080 NEXT KR4
41090 n2% = n2% - 1
41100 PRINT " Back", "n1% & n2%"; n1%; n2%
41120 FOR I = i TO 10
41130 PRINT R1(I); R2(I),
41140 NEXT
41150 GOTO 6110

42000 PRINT "42000 ROAD !  R6 in n2% R7 in n1%":
                                        REM      R6 IS IN n2% R7 IS IN n1%
42002 R6 = R6 - n1%
42004 PR6 = R2(R6): PR7 = R1(R7)
42006 GOSUB 50000
42007 R1(R7) = 0
42008 IF R7 >= n1% THEN 42040 ELSE
42009 FOR KR5 = R7 TO n1% - 1
42010 R1(KR5) = R1(KR5 + 1)
42020 R1(KR5 + 1) = 0
42030 NEXT KR5
42040 n1% = n1% - 1

42045 R2(R6) = 0
42047 IF R6 >= n2% THEN 42090 ELSE
42050 FOR KR6 = R6 TO n2% - 1
```

```
42060 R2(KR6) = R2(KR6 + 1)
42070 R2(KR6 + 1) = 0
42080 NEXT KR6
42090 n2% = n2% - 1
42100 PRINT "Back", "n1% & n2%"; n1%; n2%

42220 FOR I = 1 TO 10
42230 PRINT R1(I); R2(I),
42235 NEXT
42240 GOTO 6110

43000 PRINT "43000 ROAD! Both in n2% ":        REM     TWO IN N2%
43002 PR6 = R2(R6): PR7 = R2(R7)
43006 GOSUB 50000
43008 IF R6 > R7 THEN 43090 ELSE
43010 RL = R6: RH = R7
43020 GOTO 43100
43090 RL = R7: RH = R6
43100 R2(RL) = 0: R2(RH) = 0
43110 IF RH = n2% THEN GOTO 40160 ELSE
43120 FOR KR7 = RH TO n2% - 1
43130 R2(KR7) = R2(KR7 + 1)
43140 R2(KR7 + 1) = 0
43150 NEXT KR7
43160 FOR KR8 = RL TO n2% - 1
43170 R2(KR8) = R2(KR8 + 1)
43180 R2(KR8 + 1) = 0
43190 NEXT KR8
43200 n2% = n2% - 2
43210 PRINT "Back ", "n1% & n2%"; n1%; n2%

43220 FOR I = 1 TO 10
43230 PRINT R1(I); R2(I),
43235 NEXT
43240 GOTO 6110

50000 R67 = PR6 + PR7:                    REM     SUB FOR TERMINATION
50010 PRINT PR6; PR7, "R1+R2="; R67,
50050 P(npd + 1) = R67:                   REM     COMBINATION TERMINATION
                                                  ONLY
```

```
50080 npd = npd + 1
50090 PRINT "Dead Polymer # "; npd
50100 RETURN:                           REM     40006, 41006, 42006, 43006

57000 REM Get one radical 1 to react with PDB P(XB)=BONE
57002 RANDOMIZE TIMER
57010 R12 = INT(RND * (n1% + 1))
57020 IF R12 = 0 THEN GOTO 57010

57030 R1(R12) = R1(R12)    BONE
57040 R2(n2% + 1) = R1(R12)
57050 R1(R12) = 0

57060 IF R12 >= n1% THEN 57110 ELSE
57070 FOR KR12 = R12 TO n1% - 1
57080 R1(KR12) = R1(KR12 + 1)
57090 R1(KR12 + 1) = 0
57100 NEXT KR12

57110 XLINK = XLINK + 1:                REM     X-B4 POINT NUMBER
57115 F2X = F2X - 1
57120 XRADICAL = R2(n2% + 1)
57130 n2% = n2% + 1
57140 n1% = n1% - 1

57150 PRINT "Back from 57000 ", "n1%--n2%"; n1%; n2%
57170 RETURN:                           REM     5500

58000 REM Get one radical 2 to react with PDB P(XB)=BONE
58002 RANDOMIZE TIMER
58010 R22 = INT(RND * (n2% + 1))
58020 IF R22 = 0 THEN GOTO 58010
58030 R2(R22) = R2(R22) + BONE
58040 XLINK = XLINK + 1
58045 F2X = F2X - 1
58050 XRADICAL = R2(R22)
58060 PRINT "Back from 58000 ", "n1%--n2%"; n1%; n2%
58070 RETURN:                           REM 5500
```